Design of a Thermal Diffusion Sensor for Noninvasive Assessment of Skin Surface Perfusion and Endothelial Dysfunction

by

Vivian V. Li

S.B., Mechanical Engineering
Massachusetts Institute of Technology, 2006

Submitted to the Harvard-MIT Division of Health Sciences and Technology
in Partial Fulfillment of the Requirements for the Degree of

MASTER OF ENGINEERING IN BIOMEDICAL ENGINEERING

at the

MASSACHUSETTS INSTITUTE OF TECHNOLOGY

June 2008

Signature of Author:_____
Harvard-MIT Division of Health Sciences and Technology
May 22, 2008

Certified by:_____
H. Frederick Bowman, Ph.D.
Senior Academic Administrator
Harvard-MIT Division of Health Sciences and Technology
Thesis Supervisor

Accepted by:_____
Martha L. Gray, Ph.D.
Edward Hood Taplin Professor of Medical and Electrical Engineering
Director, Harvard-MIT Division of Health Sciences and Technology

Design of a Thermal Diffusion Sensor for Noninvasive Assessment of Skin Surface Perfusion and Endothelial Dysfunction

by

Vivian V. Li

Submitted to the Harvard-MIT Division of Health Sciences and Technology on May 22, 2008 in Partial Fulfillment of the Requirements for the Degree of Master of Engineering in Biomedical Engineering

Abstract

The skin microcirculation performs a range of vital functions, such as maintaining nutritional perfusion to the tissues and overall thermoregulation. Not only does impairment to the skin blood supply lead to tissue necrosis and other disease complications, increasing evidence shows that dysfunctional vasoreactivity in the skin microcirculation is associated with multiple disease states, including hypertension, diabetes mellitus, hypercholesterolemia, peripheral vascular disease, and coronary artery disease, and it is one of the earliest indicators of systemic endothelial dysfunction, the precursor to atherosclerotic disease. Endothelial dysfunction is functionally characterized by abnormal vasomotor response to either a pharmacological or flow-mediated stimulus and can be demonstrated in the skin by measuring reperfusion following a period of ischemia, a phenomenon known as post-occlusive reactive hyperemia (PORH).

In my research, I have reviewed the literature regarding endothelial dysfunction and its association with a wide range of cardiovascular risk factors. I have also described the mechanisms thought to link endothelial function in the central vascular beds (i.e. coronary) to that of peripheral conduit vessels and the microcirculation. The knowledge thus gathered confirmed that the microcirculation of the skin is an appropriate site for endothelial function assessment. The ultimate goal of my thesis is to design a noninvasive sensor that is capable of obtaining a quantitative measure of skin perfusion, continuously and in real-time, using the principle of thermal diffusion in perfused tissue.

I performed preliminary noninvasive endothelial function testing with a modified Thermal Diffusion Probe (TDP), which has been previously validated for absolute perfusion measurement in an invasive setting. Based on an initial analysis, I have shown that thermal surface perfusion measurements are feasible and reflect the natural perfusion and temperature fluctuations intrinsic to skin tissue. I also established guidelines for determining quantitative parameters of reactivity from tests of PORH as well as temporal parameters of perfusion variations over time through a spectral analysis of resting blood flow.

After establishing the necessary thermal boundary conditions for obtaining surface perfusion measurements, I embarked on a process of computer-assisted modeling and rapid prototyping of various design iterations on an insulated sensor housing, with subsequent fabrication of first generation noninvasive sensors. As a result of these initial sensor designs, specifications for the sensor housing were created to ensure that the appropriate thermal field would be established at the skin measurement site – an important step as it permits the most accurate determination of tissue thermal properties. Finally, I propose a candidate design for an ideal sensor capable of improving the reproducibility of noninvasive perfusion measurements on skin.

The development of a noninvasive measure of endothelial dysfunction in the skin is of great value in the early identification of individuals at risk for atherosclerotic complications. Furthermore, the nature of such a technique would provide quantitative information on the presence of a disorder, the extent of dysfunction, and the effectiveness of treatment interventions.

Thesis Supervisor: H. Frederick Bowman, Ph.D.
Title: Senior Academic Administrator, Harvard-MIT Division of Health Sciences and Technology

Acknowledgements

The research I have completed and the knowledge I have gained would not have been possible without the support and guidance of my advisor, Fred Bowman. He has been a true advocate for my education and future aspirations, always inspiring me to overcome any frustrations or obstacles encountered along the way.

I am also grateful to Dr. Robert Lees, who provided me with the clinical perspective I needed to understand the implications of my research. His patient-centered outlook has guided my own path between the fields of engineering and medicine.

I wish to thank the entire engineering team at Thermal Technologies and Hemedex. Their endless patience as well as their willingness to share their time and resources has contributed a great deal to my understanding of the thermal diffusion probe and to the preparation of my thesis.

A special thanks goes to my parents, Jan and Tien-Sheng Li, who have supported my personal and educational ambitions all along the way. I am also fortunate to have my wonderful sisters, Jing and Melissa, who have always been there to make me laugh and enjoy life outside of MIT.

I would also like to thank my friends, who inspire me with their enthusiasm and passion every day. In particular, I would like to thank Chewie, whose delight in "making small things look big" aided in the high-magnification photos of certain sensor components; Francisco, for his immense MATLAB expertise; and Charles, whose continual encouragement and editing suggestions have helped me prepare the thesis presented herein.

The funding that made this work possible was provided in part by the Boston Heart Foundation, the Harvard-MIT Division of Health Sciences and Technology, the National Institutes of Health (Grant 5R43DK070408), and Thermal Technologies of Cambridge, MA.

Table of Contents

List of Figures

List of Tables

List of Symbols

Heat Transfer Symbols	
a	Thermistor probe radius calibration constant (cm)
C_1	Zeroth order Steinhart-Hart calibration constant
C_2	First order Steinhart-Hart calibration constant
C_3	Third order Steinhart-Hart calibration constant
c_{bl}	Specific heat of blood (W·s/g·°C)
k	Thermal conductivity (mW/cm·°C)
k_b	Sensor thermal conductivity
k_m	Tissue intrinsic thermal conductivity
P	Power (mW)
$\vec{q}$	Heat flux vector (W/m^2)
$\dot{q}_{bl}$	Volumetric heat exchange between blood and tissue (W/mL)
$\dot{q}_g$	Metabolic volumetric heat exchange (W/ml)
t	Time (s)
ΔT	Volume average sensor temperature rise above baseline (°C)
T_i	Initial baseline tissue temperature (°C)
V	Sensor Volume
$\propto_m$	Tissue intrinsic thermal diffusivity (cm^2/s)
ρ_{bl}	Density of blood (g/mL)
ω	Perfusion (ml/min·100g)
Perfusion and Temperature Response Parameters	
ω_{peak}	Amplitude of post-occlusion peak perfusion
ω_{max}	Maximum increase of perfusion during reactive hyperemia compared to baseline (ω_{peak} - mean baseline perfusion)
$\omega_{\%}$	Percent hyperemic response = $\frac{\omega_{peak} - \text{Mean Baseline Perfusion}}{\text{Mean Baseline Perfusion}} \times 100$
ω_{AUC}	Area under the perfusion curve following release
TTP_ω	Time-to-peak perfusion
V_{mean}	Mean velocity of the post-occlusion hyperemia increase = $\frac{\omega_{peak}}{TTP_\omega}$
T_{NP}	Nadir-to-peak temperature change ($T_{peak} - T_{nadir}$)
T_R	Temperature recovery, defined as $T_{peak} - Ti_{initial}$ (initial pre-occlusion temperature)
$T_{\%}$	Percent temperature rebound = $\frac{T_R}{T_{initial} - T_{nadir}} \times 100$
T_{AUC}	Area under the temperature curve
TTP_T	Time-to-peak temperature

List of Terms and Abbreviations

ACE	Angiotensin Converting Enzyme
Ach	Acetylcholine
AVA	Arteriovenous Anastomoses
CAD or CHD	Coronary Artery Disease or Coronary Heart Disease
CVD	Cardiovascular Disease
DTM	Digital Thermal Monitoring (Endothelix, Inc.)
EDHF	Endothelium-Derived Hyperpolarizing Factor
EDRF	Endothelium-Derived Relaxing Factor (later known as Nitric Oxide, NO)
FBF	Forearm Blood Flow
FCD	Functional Capillary Density
FMD	Flow-Mediated Dilatation
HDL	High-Density Lipoprotein
HF	Heart Failure
LDF	Laser Doppler Flowmetry
LDI	Laser Doppler Imaging
LDL	Low-Density Lipoprotein
MRI	Magnetic Resonance Imaging
NO	Nitric Oxide
NTC	Negative Temperature Coefficient
OPS	Orthogonal Polarization Spectral Imaging
PAD	Peripheral Artery Disease
PAT	Peripheral Arterial Tonometry
PET	Positron Emission Tomography
PORH	Post-Occlusive Reactive Hyperemia
PWA	Pulse Wave Amplitude
RBC	Red Blood Cell
RH	Reactive Hyperemia
RH-PAT	Reactive Hyperemia Peripheral Arterial Tonometry (Itamar Medical)
RTD	Resistance Temperature Detector
SMC	Smooth Muscle Cell
TDP	Thermal Diffusion Probe (Hemedex, Inc.)
VOP	Venous Occlusion Plethysmography

Chapter 1. Introduction

1.1 Motivation

The microcirculation of tissues and organs is a vital component of the body's cardiovascular network. Blood flow at this level is generally known as perfusion and is comprised of the smallest blood vessels in the body. In addition to regulating the blood flow to individual organs, perfusion is responsible for a number of critical functions including oxygen delivery, carbon dioxide and waste product removal, targeted transport of substances (e.g. blood cells, platelets, hormones), thermoregulation, and blood volume distribution. The efficiency of the circulatory system is demonstrated by the careful balance of blood flow between vital organs (e.g. heart, brain) and peripheral tissues (e.g. skin). This balance is maintained by local as well as global mechanisms which ensure that perfusion matches tissue metabolic and functional needs.

An important local regulator of tissue blood flow is the vascular endothelium, which lines the interior walls of blood vessels. Although the endothelium has many functional roles, the term "endothelial function" generally refers to the ability of the endothelium to release compounds that induce relaxation of the smooth muscle cells within the vascular wall. Endothelial dysfunction is thus defined as an impairment of endothelium-dependent vasodilatation due to an imbalance in the bioavailability of endothelium-derived vasodilators or vasoconstrictors. Additional elaborations on current scientific understanding of endothelial dysfunction have characterized this state as being prone to atherogenesis through a combination of proinflammatory, proliferative, and procoagulatory states [1]. Current evidence shows that endothelial dysfunction is an early marker of atherosclerosis and is implicated in an entire spectrum of cardiovascular diseases.

While most studies have focused on studying endothelial dysfunction in either the coronary or brachial arteries, the microcirculation has also been shown to display functional abnormalities. These abnormalities have typically been regarded as a secondary phenomenon in pathological disease states. However, the development of methods to evaluate the microcirculation have challenged this assumption with evidence that microvascular dysfunction plays a key role in the pathogenesis and pathophysiology of a large range of diseases. A significant association has been shown to exist between microvascular dysfunction and diseases such as hypertension, diabetes mellitus, coronary artery disease (CAD), atherosclerosis, and peripheral arterial disease (PAD). Just as endothelial dysfunction in coronary arteries has been shown to precede the physical presence of atherosclerosis [2], impaired microvascular reactivity may actually precede disorders of the systemic circulation.

Interest in this area has established a vast field of research and development aimed at evaluating microvascular perfusion *in vivo*. Often, the most reliable, quantitative methods are invasive, involve complicated procedures, do not permit continuous data collection, and are relatively expensive. As a result, there is a strong demand for a routine, noninvasive method for assessing

absolute perfusion in appropriate and accessible tissues, particularly in the skin. Not only would such a method hold great potential clinical value in the early identification of patients at risk for cardiovascular complications, but it would also permit noninvasive assessment of wound healing ability, diabetic skin complications, tissue graft perfusion following reconstructive surgery, extent of ischemia and multiple other disorders of the skin perfusion. Other applications include shock monitoring in critical care settings and the development of a microcirculatory index to assess the impact of drugs, diet, or lifestyle changes. Perfusion in the skin is thus positioned to play a pivotal role in clinical diagnosis, prognosis, and treatment of major systemic disorders as well as in research of the microcirculation.

1.2 Objectives of Research

Early identification of the preclinical signs of atherosclerosis is a necessary target for technical innovation in noninvasive diagnostics as well as patient risk management. The development of a sensitive screening tool to detect endothelial dysfunction early in a person's life has the potential to identify pre-symptomatic individuals at a high risk of atherosclerotic complications. Considering the substantial medical resources dedicated to cardiovascular complications (heart disease, diabetes, stroke, etc.), early diagnosis shifts the burden of acute care towards the vital implementation of primary preventive strategies. Ideally, a test of endothelial function should be inexpensive, noninvasive, safe, repeatable, reproducible, and clearly standardized between different laboratories [3]. Although several methods for evaluating endothelial function exist, no technique meets all the above criteria.

Endothelial dysfunction has been established as a systemic disorder that manifests in the coronary arteries, peripheral conduit arteries, and the peripheral microvasculature. Due to its superficial location and extensive vascularity, the skin microcirculation is an appropriate vascular bed for assessing relevant defects in vascular reactivity, functional capillary density, and tissue blood perfusion. Skin perfusion measurement, in particular, is a field of research with a wide range of clinically important applications. A diverse body of literature addresses the methods of measuring the individual aspects of skin blood flow (capillary morphology, red blood cell velocity, O_2 concentration, etc.). However, nearly all have fallen short of developing a noninvasive technique that delivers an absolute measure of the blood flow in the skin. The ideal device for measuring superficial tissue perfusion has been previously defined for reconstructive surgery applications [4, 5]. Generally, such a technique would be able to provide reliable, sensitive, and continuous data in real-time so that rapid changes in blood flow could be detected. It would be able to track blood flow in a variety of tissues and the monitoring system would be simple to use, safe, inexpensive and portable. The blood flow sensor itself would be noninvasive, not only for patient comfort and safety in routine clinical use, but also to eliminate the effects of tissue trauma on perfusion.

A clinical method of monitoring perfusion has been developed for invasive applications which enables determination of absolute blood flow values based on the physiological heat transfer properties of perfused tissue [6]. This technique has demonstrated significant potential for obtaining precise, continuous, and real-time assessments of absolute tissue blood flow invasively, as it must be inserted into (and completely surrounded by) soft tissue. The Thermal Diffusion Probe (TDP) developed by Bowman, et al. has been validated and successfully used for monitoring perfusion following human liver transplantation [7] as well as for monitoring cerebral blood flow in patients with traumatic brain injury [8]. It has also been used to determine the viability of prefabricated skin flaps used for reconstructive surgery [5]. While this device possesses the desired characteristics of continuous measurement of absolute perfusion, the invasive nature of its design limits its applicability in many desired areas. However, the thermal model of the TDP could theoretically be adapted to the geometry of surface perfusion measurements.

The concepts behind the TDP operation are based on thermal models of the interaction between tissue and blood flow. These two components account for the dominant modes of heat transfer in living tissue such that a tissue's thermal conductivity and thermal diffusivity govern how heat is distributed over time. A mathematical model can simplify the complex thermal interactions between conduction, perfusion, and metabolism in vascularized tissue, despite considerable anisotropy and non-homogeneity. The advantage of such a model lies in the ability to calculate a value for blood flow based on empirically determined thermal properties. This thesis addresses the design of a thermal sensor that can monitor perfusion in skin using heat as an inert diffusible tracer. The noninvasive sensor is based on the invasive TDP, which has proven to be sensitive to skin blood flow when applied to the tissue surface with an appropriate contact geometry and pressure. Because of its low cost and non-invasiveness, thermal diffusion may be an ideal method for assessing endothelial function by measuring reactive hyperemia responsiveness. Further improvements on such a design would be a significant realization of the need for a safe and widely applicable method of measuring tissue blood flow.

To begin, I will address the multiple, interconnected elements that must be considered for the development of a truly noninvasive skin surface perfusion sensor, with particular focus on the assessment of endothelial dysfunction. Such an understanding requires a reverence for the physiological structure and regulation of skin blood flow that has made previous attempts in this field so difficult to interpret.

I will devote a great deal of attention to the systemic mechanisms of endothelial dysfunction as it relates to the inherent physiological relationship between various vascular beds in the body. Descriptions of the alternative techniques for assessing endothelial dysfunction are provided to establish a foundation for the methodology as well as a discussion of the challenges that confront peripheral vascular measurements. From the accumulated knowledge of vasoreactivity testing, I hope one can appreciate the breadth of previously documented findings for studies within the peripheral circulation. Additionally, appropriate design parameters which relate to device

operation, cost, complexity, clinical applicability, and functional constraints of user and patient interaction can also be gauged from the alternative technologies available.

I will also discuss the methods that have been developed within the field of noninvasive tissue perfusion measurement, with a focus on thermal modalities. Particular attention is given to thermal diffusion methods and the heat transfer modeling that enables quantification of absolute blood flow values as these form the foundation for my noninvasive thermal sensor design.

I will present the preliminary observations from a noninvasive application of the Thermal Diffusion Probe for functional reactive hyperemia measurements on the digital skin of human subjects. These observations have led to a significant understanding of the challenges inherent to skin perfusion measurement and the design specifications that must be met to ensure optimal sensor reliability. The perfusion measurements obtained from these initial experiments are used to establish suitable parameters to serve as indicators of vascular reactivity and endothelial function.

Finally, I will present the design and configuration of a potential sensor housing that addresses many of the weaknesses in the preliminary sensor measurements. Key efforts will be made regarding selection of appropriate materials and geometries, analysis of the issues associated with heat transfer between a surface sensor and the human skin, and appropriate specifications to implement this within a clinical setting.

Improvements on the methods for determining peripheral blood flow and vascular reactivity may ultimately contribute to an improved method for assessing cardiovascular risk. Additionally, it is possible to gain a deeper understanding of the control of skin perfusion with respect to endothelial function and the role of local vasomotion.

Chapter 2. Skin Microvascular Physiology

As the largest organ of the human body, skin takes on a remarkable range of functions and adaptive mechanisms. It serves as a defensive barrier from environmental stresses and is an active participant in the body's immune system. Skin also gathers sensory information from the environment and responds to sensations of touch, pain, heat, and cold. Owing to its position on the surface of the body and its extensive vascularization, the skin is also a site of active temperature regulation. The structure of skin is uniquely arranged for its multiple roles and is comprised of three distinct layers: the epidermis, dermis, and underlying subcutaneous tissue. The outermost epidermis is avascular stratified epithelium varying in thickness over the body from 75 to 150 μm, except on the palms and soles where it is between 400 and 600 μm thick. The dermis also varies in thickness depending on location – from 4 mm on the back to 2.5 mm on the thigh to 1.25 mm on the palm [9]. This layer is structurally divided into a superficial region adjacent to the epidermis called the papillary region and a deep thicker area known as the reticular region, and it contains the blood vessels, nerves, and specialized cells and structures such as hair follicles and sweat glands. The subcutaneous tissue is the underlying layer of fat and connective tissue that contains larger blood vessels and nerves. These features contain the relevant configuration of blood vessels that are often targeted in microvascular assessments of the skin. To understand the skin microcirculation within the larger context of the circulatory system (in health and disease), a description of the major vascular components and regulatory mechanisms is provided.

2.1 Organization of the Microcirculation

Although the skin is the largest and perhaps the most accessible organ for study on the human body, scientific knowledge about the structure and organization of the cutaneous circulation has only been developed in the past three decades. Since then, Irwin Braverman [10] has written extensively on the organization of the vascular network of human skin. Rather than existing as a randomly anastomosing network lacking stratification, the skin microcirculation is highly organized, with two horizontal plexuses: the upper, which lies 1-1.5 mm below the epidermis with ascending arterial and descending venous limbs (capillary loops) to supply each papilla, and the lower, which is at the junction between the dermis and the underlying subcutaneous tissue. The lower (reticular) plexus is formed by perforating vessels from the underlying muscles and subcutaneous fat (subcutis) and gives rise to arterioles and venules that directly connect with the upper horizontal (subpapillary) plexus, as well as lateral tributaries that supply the hair bulbs and sweat glands. These two major networks are contained in the papillary dermis 1 to 2 mm below the epidermal surface and make up most of the microvasculature. Figure 2.1 depicts the layers of skin with the corresponding vascular plexuses within each layer.

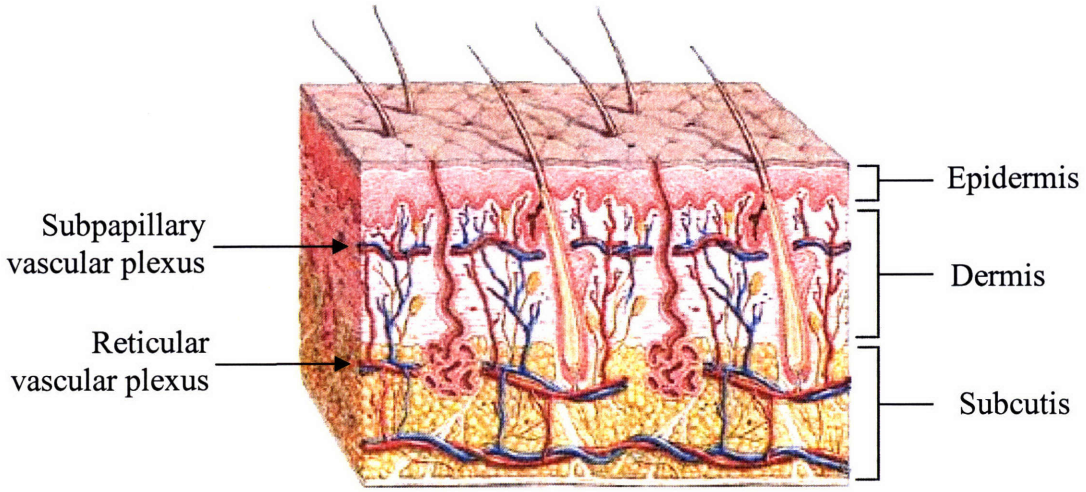

Figure 2.1 Layers of skin with microvascular ultrastructure

There are two types of vessels which regulate the terminal blood supply to the skin. The most numerous are arterioles composed of smooth muscle, which supply capillary beds and are innervated with sympathetic constrictor fibers. They provide nutrient flow to the skin. Veins draining these vascular beds comprise large venous networks which provide a large surface area for heat exchange with the environment. This vascular network is described in more detail in Sections 2.1.1 to 2.1.3.

The second type of vessel is found in certain skin regions and is composed almost exclusively of smooth muscle. These vessels, known as arteriovenous anastomoses (AVA), are located in the subcutaneous plexuses and provide a direct connection between arteries and the venous networks, bypassing the capillary networks. AVA are especially abundant in exposed areas of skin with a high surface area to volume ratio, including the pads and nail beds of toes and fingers, palms, soles of the feet, lips, nose and ears [11] and are important for thermoregulation. They have a relatively large diameter, on average 35 μm (20—70 μm) as compared to capillaries (5—10 μm) and are richly (and exclusively) supplied with sympathetic nerve fibers [12]. When they open, large amounts of blood can pass. Activation of sympathetic nerves leads to active vasoconstriction, and decrease in sympathetic activity leads to passive vasodilatation. In a moderately warm environment the AVA are open. In a slightly cold environment, the AVA are almost closed. Since the capillaries provide the nutritional requirements of the skin, with the effective capillary area controlled by pre-capillary sphincters, AVA are capable of controlling capillary blood flow by diverting large volumes of blood through low-resistance pathways. This type of blood flow is termed non-nutritional flow, or shunt flow.

2.1.1 Arteries & Arterioles

The walls of all arteries are made up of an outer layer of connective tissue, the adventitia; a middle layer of smooth muscle, the media; and an inner layer, the intima, made up of the endothelium and underlying connective tissue. The walls of the aorta and other arteries of large

diameter contain a relatively large amount of elastic tissue, primarily located in the inner and external elastic laminas. They are stretched during systole and recoil on the blood during diastole. The walls of the arterioles contain less elastic tissue but much more smooth muscle. In the skin, arterioles appear with venules in the deep vascular plexus and average 17 to 26 μm in diameter. The arterioles in skin have two layers of smooth muscle cells: the cells of the inner layer are longitudinally oriented while the cells of the outer layer form a spiral [10]. These vessels are capable of augmenting microvascular resistance and blood flow distribution in the skin through dynamic fluctuations in diameter, resulting in blood flow oscillations. The arterioles are the major site of the resistance to blood flow, and small changes in their caliber cause large changes in the total peripheral resistance.

2.1.2 Capillaries

Capillaries are small exchange vessels that are fed by terminal arterioles. The openings of the capillaries are surrounded by precapillary sphincters, which are supplied by sympathetic fibers from the autonomic nervous system. These fibers maintain a certain basal tone in the sphincters. In the skin, capillaries have an inner diameter of 4-6 μm. When the sphincters are dilated, the diameter of the capillaries is just sufficient to permit red blood cells to squeeze through in "single file." The state of contraction of precapillary sphincters determines the number of perfused capillaries. Compared to capillaries in other parts of the body in which the vascular wall is usually only 0.1 μm thick, capillaries in the skin have relatively thick walls, measuring 2-3 μm [13].

While capillaries lack smooth muscle cells, their walls contain pericytes outside of the endothelial cells. Pericytes are thinner than smooth muscle cells, have fewer myofilaments, and lack dense bodies. These cells have long processes that wrap around the vessels. They contain the contractile proteins necessary for cellular contraction and release a wide variety of vasoactive agents. Pericytes also synthesize and release constituents of the basement membrane and extracellular matrix. One of their physiologic functions appears to be regulation of flow through the junctions between endothelial cells, particularly in the presence of inflammation.

The capillary loop is an important structure in the microcirculation of the skin and supplies the only nutritional perfusion available to the epidermis. In some cases a capillary loop can be up to 100 μm from the epidermal cells which it supplies. It arises from the terminal arteriole in the superficial horizontal plexus and is composed of an ascending limb, a hairpin turn, and a descending limb that returns to the superficial horizontal plexus and connects with the postcapillary venule. Each dermal papilla is supplied by a single capillary loop which is the primary site of nutrient and oxygen exchange. Generally, a single capillary loop supplies 0.04-0.27 mm^2 of the skin surface [14]. Compared to most other tissues, capillary density is relatively low in skin, ranging from 10 to 70 capillaries/mm^2. At different skin sites, there are no differences in the ultrastructure of the capillary loops; only density varies.

2.1.3 Venules & Veins

The descending capillary loop feeds into the postcapillary venules, which make up the majority of vessels in the papillary dermis. The internal diameter enlarges from 8 μm (at venous capillaries) to 26 μm and the walls of the venules are only slightly thicker than those of the capillaries. Blood then passes through the small venules and into systemic veins of increasing size. Veins have relatively little smooth muscle or elastic tissue and thus are easily distended. In contrast to small arteries and arterioles, which are resistance vessels, venules and veins function as capacitance vessels. Pressures within the venous system are low, ranging from 20 mmHg at the venular ends of capillaries to about 0 mmHg at the entrance to the vena cava. Due to these properties, the venous system normally contains about 2/3 of the total blood volume, and acts as a blood reservoir for the body.

2.2 Levels of Blood Flow Regulation

The blood vessels are a closed system of vessels that carry blood from the heart to the tissues and back to the heart. Figure 2.2 contains a schematic of the various types of vessels in the circulatory system and their organization in the circulatory network. The resistance to flow depends mostly on the diameter of the vessels of the microcirculation, principally the arterioles. The blood flow to each tissue is regulated by local chemical and general neural and humoral mechanisms that dilate or constrict the vessels of the tissue. A parallel arrangement permits wide variations in regional blood flow without changing total systemic flow. In humans and other mammals, multiple cardiovascular regulatory mechanisms have evolved. These mechanisms increase the blood supply to active tissues and increase or decrease heat loss from the body by redistributing the blood. In the face of challenges such as hemorrhage, blood flow is maintained at near constant values in the heart and brain. When the challenge is severe, flow to these vital organs is maintained at the expense of the circulation to the rest of the body.

At rest, about 67% of the circulating blood volume is in the systemic veins and venules. Five percent is in the heart cavities, and 12% is in the low-pressure pulmonary circulation. Only 11% is in the aorta, arteries, and arterioles, and 5% in the capillaries [15]. Although only 5% of the circulating blood is in the capillaries, this portion is the most vital component of the blood volume because it is across the systemic capillary walls that O_2 and nutrients enter the interstitial fluid and CO_2 and waste products enter the bloodstream. The nutrient exchange across the capillary walls is essential to the survival of the tissues. Thus, the larger vessels of the body can be viewed as distinct conduits to and from the heart and peripheral organs whereas the microcirculatory vessels are embedded within an organ to enhance communication between the tissue and the vessels.

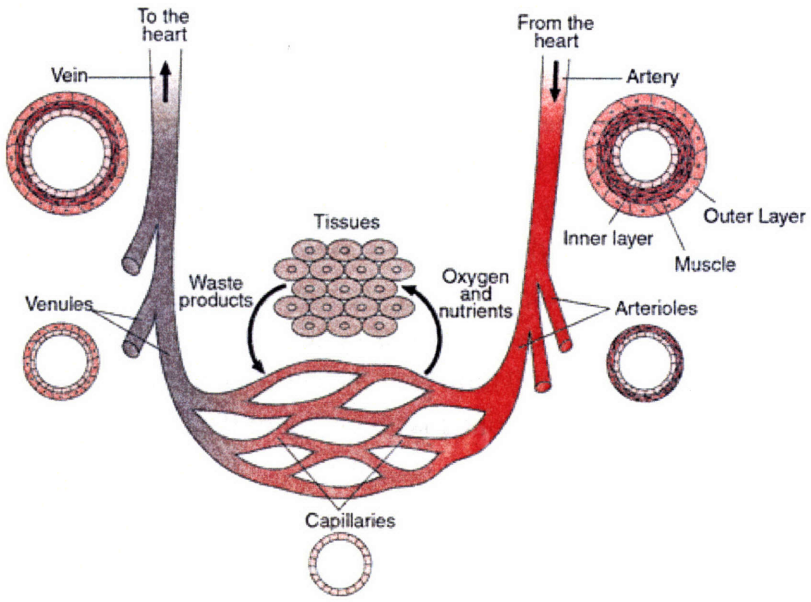

Figure 2.2 Vessels of the circulatory system. Blood travels from the heart in arteries, which branch into smaller and smaller vessels, eventually becoming arterioles. Arterioles connect with still smaller blood vessels called capillaries. Through the thin walls of the capillaries, oxygen and nutrients pass from blood into tissues, and waste products pass from tissues into blood. From the capillaries, blood passes into venules, and then into veins to return to the heart.

The vascular endothelium modulates smooth muscle tone by releasing several vasoactive substances. The critical role of the endothelium in regulating vasodilator tone was first described by Furchgott and Zawadzki in 1980 [16]. They demonstrated that the rabbit aorta dilates in response to the application of acetylcholine only in the presence of intact endothelium, confirming the existence of an endothelium-derived vasodilator. The principal endothelium-derived relaxing factor (EDRF) was later confirmed to be nitric oxide (NO) [17, 18], and numerous subsequent studies have explored the multiple vascular functions of this simple, diatomic molecule, confirming its role as a central signal transducer and essential antiatherogenic molecule. It is released during basal conditions in response to chemical stimuli, such as acetylcholine (ACh), and in response to mechanical stimuli, such as shear stress.

Endothelial cells also generate several other vasoactive mediators, including the vasodilator molecules prostacyclin and endothelium-derived hyperpolarizing factor (EDHF), and the vasoconstrictor agents endothelin-1, angiotensin II, superoxide anions, and vasoconstrictor prostanoids. The development of an imbalance in the release of vasoconstrictor and vasodilator agents from the endothelium leads to an impairment of endothelium-dependent vasodilatation, which represents the hallmark of endothelial dysfunction [19]. In parallel with the vasomotor changes, activated dysfunctional endothelial cells also acquire a vascular phenotype that establishes a local environment favoring the initiation and progression of atherosclerosis [20]. This area of blood flow regulation will be addressed more thoroughly with regard to endothelial dysfunction in Section 3.1.

2.3 Skin Blood Flow: Roles in Tissue Nutrition and Thermoregulation

The skin is both a protective barrier and an important thermoregulatory organ. As a result, it has an extensive and well-developed microcirculation. Human skin microcirculation serves three main functions, namely skin tissue nutrition, heat exchange for thermoregulation, and blood flow redistribution during stress. While the oxygen and nutrient requirements of the skin are small and thus little blood flow is necessary to sustain nutritional perfusion, the skin is the primary means of maintaining body temperature. To meet these needs, skin blood flow can vary between less than 1 ml/min per 100 g of tissue to a maximal flow of 150 to 200 ml/min·100g during times of severe heat stress (up to 60% of total cardiac output) [21]. In a thermoneutral environment, skin blood flow ranges between 10 and 20 ml/min·100g [22]. This impressive range of possible circulatory states is achieved through a balance of neural and local control mechanisms that precisely modulate the vasomotor tone and vascular resistance of the peripheral microcirculation. In particular, thermoregulatory control is largely mediated through reflex neural control of skin blood flow.

Skin blood flow is controlled by two branches of the sympathetic nervous system: a noradrenergic vasoconstrictor system and an active vasodilator system, which is less well-understood. While both types of nerves innervate all areas of non-acral skin (trunk, leg, forearm, etc.), areas of acral skin (lips, ears, nose, palmar/plantar surface of hands and feet) are innervated only by sympathetic vasoconstrictor nerves [21]. In thermoneutral environments, the vasoconstrictor system is tonically active such that withdrawal of the impulses to these nerve fibers allows blood vessels to dilate. This allows for a "neutral" or "vasomotor" zone of thermoregulation where the skin responds to subtle changes in the environment by fine-tuning heat loss solely via adjustments in sympathetic tone [23]. In skin areas outside of acral regions, an active sympathetic vasodilation system exists which is inactive in thermoneutral environments, but is activated during increases in internal temperature. Therefore, as core body temperature begins to rise (such as during exercise or environmental heat exposure), the initial increase in skin blood flow is mediated by release of vasoconstrictor tone. However, upon reaching a specific threshold, sweating and reflex active vasodilatation are initiated in tandem, stimulating the co-release of acetylcholine (ACh) and an associated yet-unknown vasodilator from sympathetic cholinergic nerves [21]. The active vasodilator system is responsible for 80%-90% of the large increases in skin blood flow during heat stress, which can reach levels as high as 6-8 L/min.

As was discussed in Section 2.1, numerous arteriovenous anastomoses (AVA) exist in acral skin. These thick-walled, low-resistance conduits are richly innervated by sympathetic vasoconstrictor nerves and allow high rates of shunt flow between arterioles and venules. Therefore, in acral areas, opening or closing of these AVA can cause substantial changes in the blood volume that passes through the skin. Sympathetic input to AVA is controlled from hypothalamic temperature regulation centers, while cutaneous arterioles are primarily controlled by neural activity, with local metabolic control secondary.

The periodic oscillations recorded in cutaneous blood flow reflect both vasomotion and flow motion and have been quantified by spectral analysis of the laser Doppler perfusion signal [24]. Vasomotion is defined as the rhythmic changes in the diameter of small blood vessels and is produced by contraction and relaxation of the muscular components in their walls. An important component of vasomotion in skin includes the myogenic activity of terminal arterioles as well as endogenous endothelial activity, such that not all skin microvascular units are open and perfused at any moment in time. Flow motion results from the motion of the blood cells and their interaction with the vessel walls and is dependent on the different vasomotor control mechanisms. The characteristic oscillation frequencies present in skin flow motion include a cardiac component (~1 Hz in a resting, healthy subject) and respiratory component (~0.3 Hz), which demonstrate the dependence of peripheral blood flow on the pressure difference generated by the heart and lung pumps. There are also contributions from intrinsic myogenic activity of the vessel wall (0.1 Hz) and neurogenic activity of the local sympathetic nerves (0.03 Hz) [25]. An oscillation with a period of around 1 min (~0.01 Hz) has been suggested as being endothelium-dependent and may reflect either periodic release of NO or the rhythmic response to NO of an oscillator in vascular smooth muscle cells [26].

2.4 Reactive Hyperemia

If arterial inflow to a vascular bed is stopped temporarily, perfusion within that bed decreases to zero. Upon release of the occlusion, the blood flow immediately exceeds the average flow before occlusion and then gradually returns to the baseline level. This increase in flow is called reactive hyperemia. The peak flow and duration of the reactive hyperemia are relatively proportional to the duration of the occlusion within certain limits. If the extremity is exercised during the occlusion period, reactive hyperemia is increased. These suggest a locally mediated mechanism, either metabolic or otherwise, in the regulation of tissue blood flow.

Post-occlusive skin reactive hyperemia has been primarily defined in laser Doppler flowmetry studies of skin perfusion flux and refers to the increase in skin blood flow above baseline levels following the release of a brief arterial occlusion. It is also called post-ischemic hyperemia. It can be characterized by an initial peak in flux (perfusion) that occurs within a few seconds of removal of the occlusion, and a sustained hyperemia. Four major factors have been proposed to be involved in the hyperemic response: metabolic vasodilators, endothelial vasodilators, the myogenic response and sensory nerves. The post-ischemic peak flow reflects the sudden increase of the blood flow in the skin microvessels after removal of the occlusion and can be considered an indicator of the increased shear stress on the microvascular wall. The more prolonged hyperemic phase reflects the metabolic debt repayment to the tissue [27] and can be considered as an indicator of successive tissue reperfusion.

Unlike flow-mediated dilatation, reactive hyperemia is a complex response that depends on the local production of non-endothelium-dependent vasodilators which dilate tissue microvessels to accelerate the delivery of oxygen following a period of ischemia [28]. Endothelium-derived

nitric oxide plays a role in reactive hyperemia as well [29, 30]. Despite the similarities in procedure and vascular regions, it is now thought that reactive hyperemia proceeds through different mechanisms compared to conduit artery flow-mediated dilatation (FMD). This topic will be addressed more fully in Section 3.2.

2.5 Skin Microcirculation in Health and Disease

The microcirculation is of interest because it is where fine control of blood supply takes place, and tissue ischemia is dependent on microvascular flow in many circumstances. During circulatory failure (e.g. hypovolemic shock), blood flow is diverted from the less important tissues (skin, subcutaneous fat, muscle, large intestine) to vital organs (heart, brain, kidneys). Thus monitoring perfusion in the less vital tissues such as skin could be an early clinical marker of critical tissue hypoperfusion. Indeed, the assessment of perfusion in peripheral tissues is more easily obtainable using noninvasive monitoring techniques, thus facilitating earlier recognition of abnormalities. The skin can provide a good platform for this, and in diabetes, for example, measurable changes in the skin have been found to pre-date the symptoms of microvascular disease in other organs by many years [31]. In the dermal microcirculation, endothelial function may be assessed noninvasively using several methods, although no one technique is entirely satisfactory. Nevertheless, this vascular bed is highly suitable for assessment of the endothelium, and is particularly convenient.

By posing the dermal microcirculation as a way to interrogate overall vascular health, it is important to recognize that cutaneous blood flow is a dynamically fluctuating biological variable which possesses substantial spatial heterogeneity. Its magnitude and regulation is modulated through many external and internal parameters by virtue of its central role in thermoregulation and tissue perfusion. Microcirculatory flow adjusts as a result of variations in blood gas concentration, hormones, and physical factors like temperature and pressure. It is also carefully controlled by the autonomous nervous system. Such signals increase or decrease the microvascular perfusion by stimulating the endothelium to release substances leading to vasoconstriction or vasodilatation of the upstream arterioles. Characterizing these systemic regulators of blood flow also impacts current understanding of perfusion. Several important clinical goals arise from these local and global relationships. Not only is the status of a patient's generalized microvasculature important, but direct associations must be determined to provide information as it relates to underlying pathophysiology.

Chapter 3. Endothelial Dysfunction & Methods of Assessment

3.1 Pathophysiology of Endothelial Dysfunction

The normal endothelium plays a key role in the local regulation of vascular tone by producing and secreting substances within a region of the vascular bed. To maintain vascular homeostasis, healthy endothelial cells perform a variety of functions [32] (Figure 3.1):

- Promote vasodilation
- Antioxidant effects
- Anti-inflammatory effects
- Inhibition of leukocyte adhesion and migration
- Inhibition of smooth muscle cell (SMC) proliferation and migration
- Inhibition of platelet aggregation and adhesion
- Anticoagulant effects
- Profibrinolytic effects

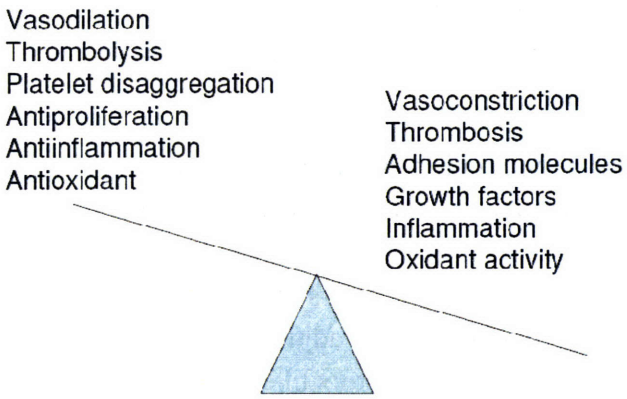

Figure 3.1 Regulatory functions of the endothelium. Healthy endothelium protects the vessels from atherosclerosis. Dysfunctional endothelium possesses proatherogenic properties, shifting the balance towards vasoconstriction, thrombosis, inflammation, and ultimately atherogenesis. [33]

Normal endothelial cells promote an antiatherogenic vessel phenotype and are capable of maintaining a delicate balance between local and systemic stimuli. However, when endothelial cells lose this ability, the resulting imbalance leads to a state of endothelial "activation," which is characterized by abnormal vasomotor function in addition to a proinflammatory, proliferative, and prothrombotic state that favors the initiation and progression of atherosclerosis [1]. Although the precise mechanisms that cause endothelial dysfunction are not fully understood, it is thought to be a multifactorial process involving mechanical or biochemical damage to endothelial cells and the loss of appropriate response to certain stimuli. One possible mechanism relates to the increased production of reactive oxygen species, such as superoxide, which have been shown to reduce endothelial nitric oxide availability via multiple pathways [34]. Furthermore, cardiovascular risk factors are known to activate a number of pro-oxidative genes in the vascular

wall. In fact, increased vascular superoxide production has been demonstrated in all major conditions predisposing to atherosclerosis [35].

Endothelial dysfunction is most effectively defined by the diminished production or bioavailability of vasodilators (e..g. nitric oxide, or NO) or an increase in endothelium-derived contracting factors, leading to impaired endothelium-dependent vasodilatation [36]. This can be assessed functionally by a measure of abnormal vasoreactivity (response to pharmacological or physiological stimulation). However, it is the positive feedback loop in which inflammatory factors promote monocyte and T-cell adhesion, foam cell formation, extracellular matrix digestion, and vascular smooth muscle migration and proliferation that ultimately leads to atherosclerotic plaque formation. This can include multiple mechanisms, such as up-regulation of adhesion molecules, increased chemokine secretion and leukocyte adherence, increased cell permeability, enhanced low-density lipoprotein (LDL) oxidation, platelet activation, cytokine elaboration, and vascular smooth muscle cell proliferation and migration [33]. The host defense response is triggered, allowing the endothelium to be invaded by lipids and leukocytes and inciting an inflammatory response within the vessel wall. Fatty streaks appear and develop into plaques that are susceptible to rupture with subsequent thrombogenesis and vascular occlusion [33].

Given the relationship between endothelial dysfunction and atherosclerosis, it is likely that the status of an individual's endothelial function reflects their susceptibility to develop atherosclerotic disease and may thus serve as a marker of an unfavorable cardiovascular prognosis. Both novel and conventional cardiovascular risk factors are associated with abnormal endothelial function and may influence the bioavailability of endothelial NO or lead to a state of endothelial activation. For example, hypertension, chronic heart failure, diabetes, hypercholesterolemia, smoking, aging, and a family history of premature atherosclerotic disease are all associated with impaired endothelium-mediated vasodilatation. Table 3.1 summarizes many of the established and recent conditions that have been associated with endothelial dysfunction.

Furthermore, many interventions that are known to limit cardiovascular risk have been shown to restore endothelial function. Thus, endothelial dysfunction is a reversible disorder, and strategies aimed at reducing cardiovascular risk factors, such as cholesterol lowering [37], antihypertensive therapy [38], smoking cessation [39], estrogen replacement therapy in postmenopausal women [40], supplementation with folic acid [41], and physical exercise [42] also translate into an improvement in endothelial health, further supporting the association between risk factors and endothelial dysfunction. Moreover, the observation that several pharmacological interventions that improve endothelial function are associated with a decrease in cardiovascular events independent of risk factor modification supports the concept that cardiovascular risk factors share a common pathway that leads to endothelial dysfunction, such as oxidative stress. A Medline search reveals that several hundred articles are published every year on the role of

different therapeutic interventions aimed at influencing endothelial function. It is clear that evaluation of endothelial function in humans is of great clinical relevance.

Table 3.1 Factors associated with endothelial dysfunction in the literature and investigated therapies that improve endothelial dysfunction

Factors related to endothelial dysfunction	References	Factors improving endothelial function	References
Age	[43-46]	Angiotensin-converting enzyme inhibitors	[38, 47, 48]
Male sex	[43]	Hormone-replacement	[40, 49, 50]
Smoking	[3, 39, 51, 52]	Smoking cessation	[39, 53]
Passive Smoking	[54, 55]	Exercise	[42, 56-58]
Diabetes mellitus: Types 1 and 2	[59-62]	L-Arginine	[53, 63]
Hyperglycemia	[64]	Calcium channel blockers	[65, 66]
Family History of CAD	[67, 68]	Statin therapy	[69-74]
Hypertension	[52, 75-77]	LDL apheresis	[78]
High cholesterol	[79-82]	Antioxidants	[83-85]
Low HDL	[67, 86]	Homocysteine lowering	[87, 88]
Obesity	[89, 90]	Weight loss	[91]
Heart failure	[92-94]	Omega-3 Fatty Acids	[95]
Hyperhomocysteinemia	[96, 97]	Aspirin	[98]
End-Stage Renal Disease	[99, 100]		
Elevated C-reactive protein	[101]		
Chronic Systemic inflammation	[102]		

Given the endothelium's unique position as both the mechanical and biological barrier between blood and the vascular wall, endothelial function represents an integrated index of overall cardiovascular risk factors and local factors (e.g. shear stress), genetic predisposition, and yet-unknown factors (protective and harmful) that confer individual susceptibility to developing atherosclerotic disease as well as predisposition to the subsequent acute complications (Figure 3.2). Indeed, some investigators consider endothelial dysfunction to be the "risk of risk factors" [32]. Therefore, the status of endothelial function offers unparalleled potential for improved risk stratification, as well as the possibility of targeted therapies and prognosis.

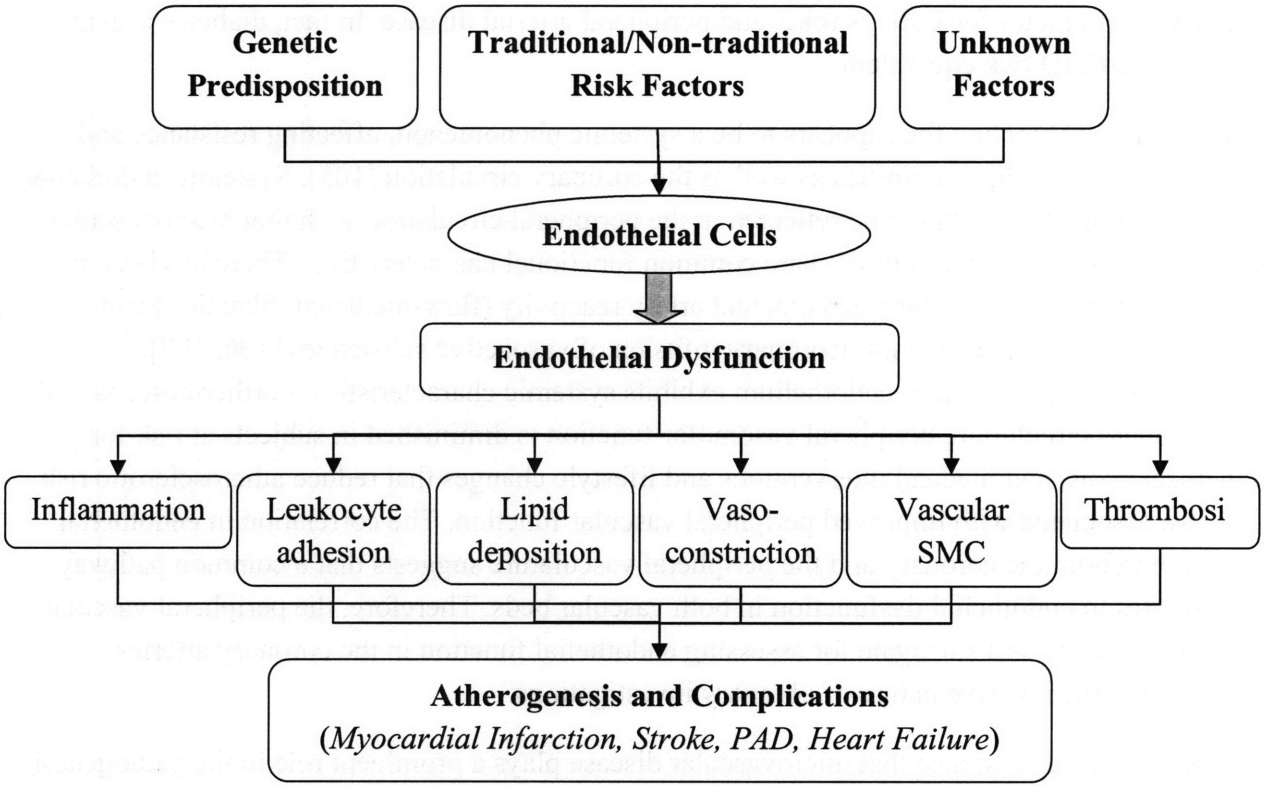

Figure 3.2 Endothelial dysfunction as an index of overall cardiovascular risk

3.2 Systemic Impact of Endothelial Dysfunction and Atherosclerosis

Because atherosclerosis is a generalized macrovascular disease, lesions in one vascular territory predict disease in other arterial regions. This systemic nature was documented by the Framingham study which showed that patients first presenting with myocardial infarction, cerebral vascular accident, heart failure, or peripheral vascular insufficiency would, in the following 10 years, manifest disease in another vascular territory in proportions varying from 16% to 50%, both for men and women [104]. Similar risk factors are present among patients with coronary, peripheral, and carotid atherosclerosis. Of particular importance is evidence that disease in noncoronary arteries is a powerful predictor of coronary heart disease (CHD) mortality. Aortic, peripheral, and carotid artery diseases have been termed "Coronary Heart Disease Equivalents" because the level of CHD risk and CHD event rates associated with these conditions is approximately equivalent to the level of risk seen in stable CHD. That is, the rate of CHD events in persons with atherosclerotic vascular disease in other territories is similar to event rates in patients with known CHD. Additionally, macro- and micro-vascular disease are the principle causes of morbidity and mortality in patients with diabetes mellitus, which is, by itself,

a powerful predictor for CHD, stroke, and peripheral arterial disease. In fact, diabetes is also known as a CHD risk equivalent.

Endothelial dysfunction thus appears to be a systemic phenomenon, affecting resistance and conduit vessels in the extremities as well as the coronary circulation [105]. Systemic endothelial dysfunction is often found to be reflected in the peripheral circulation such that macrovascular and microvascular abnormalities share common functional characteristics. There has been a demonstrated correlation between brachial artery reactivity (flow-mediated dilatation) and coronary artery response to intracoronary infusion of vasoactive substances [106, 107], suggesting that the vascular endothelium exhibits systemic characteristics. Furthermore, as with the coronary circulation, peripheral vasomotor function is diminished in subjects at risk for atherosclerosis, and medical interventions and lifestyle changes that reduce atherosclerotic risk are also associated with improved peripheral vascular function. The correlation in endothelial function in both the coronary and the peripheral vasculature suggests that a common pathway contributes to endothelial dysfunction in both vascular beds. Therefore, the peripheral vascular bed may be used as a surrogate for assessing endothelial function in the coronary arteries, minimizing the invasive nature of coronary investigations.

There is growing evidence that microvascular disease plays a prominent role in the pathogenesis of vascular diseases and mortality [108]. There is also increasing evidence that coronary microvascular dysfunction may be one underlying mechanism in patients with symptoms and signs of myocardial ischemia without angiographically detectable coronary artery disease, and even in asymptomatic patients with cardiovascular risk factors [109, 110]. Microvascular processes, primarily in the coronary microcirculation, have also been implicated in left ventricular dysfunction and subsequent heart failure, particularly in people with diabetes and hypertension, as well as in patients with dilated or hypertrophic cardiomyopathy. However, the majority of these studies have been cross-sectional and have focused on small samples of highly selected symptomatic patients. In addition, since the coronary circulation cannot be visualized in vivo and methods to assess the coronary microcirculation are invasive and applicable only in experimental settings, what is known about microvascular mechanisms in the pathogenesis of congestive heart failure has been derived indirectly from studies of functional parameters such as myocardial blood flow and coronary flow reserve.

Several studies have suggested that microcirculation in the skin resembles the microcirculation in other tissues and could be used to mirror the state of the microcirculation in other vascular beds to gauge overall cardiovascular health. Furthermore, the skin is highly vascular and an easily accessible model of the microcirculation. Therefore, skin microcirculation offers an opportunity to noninvasively explore the relation of systemic microvascular dysfunction to cardiovascular disease and its risk factors [111].

For example, in individuals with hypertension, microvascular defects can be demonstrated in heart, skeletal muscle and skin. Similarly, an association of diabetes and insulin resistance with

microvascular function has been reported in heart, skeletal muscle and skin tissue [112]. Not only have the metabolic and vascular effects of insulin been demonstrated in skin [113, 114], several studies have demonstrated that impaired microvascular reactivity in the skin are associated with elevated blood pressure and insulin resistance [111, 115-118]. Impairment of post-ischemic reactive hyperemia as measured by laser Doppler signal in forearm skin has also been associated with increased heart disease risk according to the Framingham risk score [119]. These studies suggest that microvascular function in the skin resembles microvascular function in other tissues, particularly with regard to functional deficits related to disease. Additional support comes from studies demonstrating that impaired responses of the skin microcirculation may be reversed after cholesterol-lowering therapy [70, 120, 121]. These findings suggest that microvascular function in skin may be a valid model for the study of the relationships between cardiovascular risk factors and vascular function. What's more, individuals at an increased risk for cardiovascular disease can be characterized by impaired microvascular function in skin.

It is nevertheless important to note that the relationship between the commonly assessed brachial FMD does not clearly correspond to the magnitude of skin reactive hyperemia [122, 123], and there seems to be uncertainty regarding the relationship between conduit artery function and downstream peripheral perfusion. While some investigators have found a correlation between the two [123, 124], others have shown no correlation between conduit artery reactivity (FMD) and microvascular vasomotion (LDF perfusion) [122, 125]. In one such study showing no correlation, it was found that laser Doppler-derived indices during reactive hyperemia were actually more specific for diagnosis of coronary artery disease than measurement of brachial FMD [122]. Thus, further research must investigate the possibility of different vasodilatory mechanisms or factors that would account for this lack of correlation between conduit vessels and the cutaneous microcirculation.

A notable finding in the vasodilatory mechanism of skin microvascular reactivity has revealed that different mechanisms of endothelium-dependent responses vary among different vascular beds. It was established that brachial artery reactivity is principally mediated through endothelium-dependent release of nitric oxide [126]. However, reactivity of skin microvessels has been demonstrated to be largely nitric oxide-independent [127], although it has also been shown to play a role [29, 30]. Instead, skin reactive hyperemia appears to be principally regulated by endothelial release of prostaglandins (vasodilators) [71] as well as endothelium-independent factors induced by ischemia such as adenosine, pH, pO_2, and myogenic control [125]. This is an important consideration when interpreting data from different techniques employing tests of reactive hyperemia as skin perfusion reactivity may or may not be an endothelium-dependent response.

Kullo *et al.* [52] suggest that reactive hyperemia is primarily a microvascular response to transient ischemia and involves the local release of ischemia-induced vasodilator substances from resistance vessels, although a portion of the hyperemic response may be endothelium-dependent. FMD, on the other hand, is mainly dependent on the release of the vasodilator NO

from the conduit artery endothelium. Their relationship can be most understood when considering a test of reactive hyperemia: In healthy endothelium, an occlusion of the conduit artery induces release of vasodilators from the microvasculature. When occlusion is released, the reduced microvascular resistance results in increased conduit artery and flow, causing shear stress to the endothelium and culminating in vasodilatation of the conduit artery mainly via nitric oxide.

Thus, reactive hyperemia and FMD, although interrelated, may represent different vascular phenotypes, and these two measures may provide additive rather than redundant information about vascular alterations in tests of endothelial dysfunction. It appears that both microvascular and conduit artery function are independently impaired in the presence of coexisting CV risk factors, and different mechanisms may be involved in the development of microvascular versus conduit artery dysfunction. In a recent prospective study by Huang *et al.* [128], investigators acknowledged the different mechanisms underlying each stimulus and showed that both flow-mediated dilatation and reactive hyperemia were significant predictors of cardiovascular risk. Furthermore, a lower hyperemic flow velocity (a measure of microvascular function) predicted cardiovascular events in a high risk group of patients with peripheral arterial disease referred for surgery.

3.3 Techniques for the Assessment of Endothelial Dysfunction

Endothelial dysfunction is the loss or reduction of the endothelium's capacity to defend against proatherogenic factors. It is evaluated by assessing the reactivity of the endothelium, either directly or indirectly.

3.3.1 Intracoronary Studies

The first experiments to evaluate endothelium-dependent vasodilatation were performed by invasive catheterization of atherosclerotic epicardial coronary arteries in 1986 [129]. Drugs that induced NO release were injected, such as acetylcholine, metacholine, papaverine, P substance, etc., and the percentage of vasodilatation was measured. Ludmer *et al.* [129] found that injecting acetylcholine in normal coronary arteries produced endothelium-dependent vasodilatation, whereas in coronary arteries with moderate or severe atherosclerotic lesions a paradoxical vasoconstriction was obtained, indicating that endothelial dysfunction was present. The paradoxical vasoconstriction is due to stimulation of the muscarinic receptors of the smooth muscle cells by direct acetylcholine action. It was also found that after injecting nitroglycerine, an NO donor and direct smooth muscle dilator, there was always vasodilatation (endothelium-independent). This preserved response to the direct smooth muscle vasodilator further suggests disturbances of endothelial origin. Using the same method, Vita *et al.* [130] found that the amount of coronary vasodilatation obtained by acetylcholine diminished inversely with the increase of total cholesterol or LDL-cholesterol levels. They also observed that the presence of

multiple cardiovascular risk factors was associated with a greater constrictor response to acetylcholine, evidencing the additive effects on endothelial dysfunction.

Noninvasive assessment of coronary endothelial function is also possible through Doppler echocardiography, positron emission tomography (PET) and phase-constrast magnetic resonance imaging (MRI). However, the invasive assessment of coronary endothelial function by quantitative coronary angiography and coronary Doppler flow measurements, in conjunction with intracoronary infusions of endothelium-dependent vasodilators, such as acetylcholine, is considered the "gold standard" for endothelial function testing.

To measure endothelial dysfunction in peripheral vascular beds, less invasive techniques have been developed, such as strain-gauge forearm plethysmography and high-resolution ultrasound to measure flow-mediated endothelium-dependent vasodilatation of the brachial artery during reactive hyperemia. These techniques are based on the previously discussed view that endothelial dysfunction is not confined to the coronary arteries but rather represents a systemic disorder that also affects peripheral vascular beds, including both conduit arteries and small resistance vessels in the extremities.

3.3.2 Strain-Gauge Venous Occlusion Plethysmography (VOP)

Studies seeking a noninvasive way to investigate endothelial dysfunction have focused on reactivity of peripheral resistance arteries using forearm plethysmography. This technique, known as venous occlusion plethysmography (VOP), is an established method of measuring total blood flow and vascular resistance in either the upper or lower limb with a strain gauge that has been tied around the limb of interest. With this technique, measurements in the forearm vascular bed have demonstrated the significance of microvascular resistance artery endothelial dysfunction in essential hypertension [75-77, 131, 132], diabetes [133], dyslipidemia [81], heart failure [134, 135], coronary artery disease [136], and smoking [137]. Most of these investigations were semi-invasive since they demonstrated endothelial function by drug infusions into the brachial artery.

The basic methodology of forearm venous occlusion plethysmography involves an interruption in venous return from the forearm by inflating a cuff, placed around the upper arm, to well above venous pressure but below diastolic pressure (30-40 mmHg). Arterial inflow is unaltered and causes forearm volume to increase over time, until the venous pressure overcomes the occluding pressure. Typically, the cuff is inflated for intervals of 10 seconds, followed by 5 seconds of deflation to allow for venous emptying, resulting in linear increases in forearm volume over time, which are proportional to the arterial inflow [138] (Figure 3.3). Hand blood flow is excluded from measurement due to its high level of temperature-dependence (arteriovenous anastomoses) and nonlinear contribution to the measurement [139]. It is standard practice to inflate a smaller cuff around the wrist to a suprasystolic pressure about 60 seconds before starting measurement. Since the hand becomes ischemic, measurement periods are limited, but periods of up to 13 minutes have been employed safely [140].

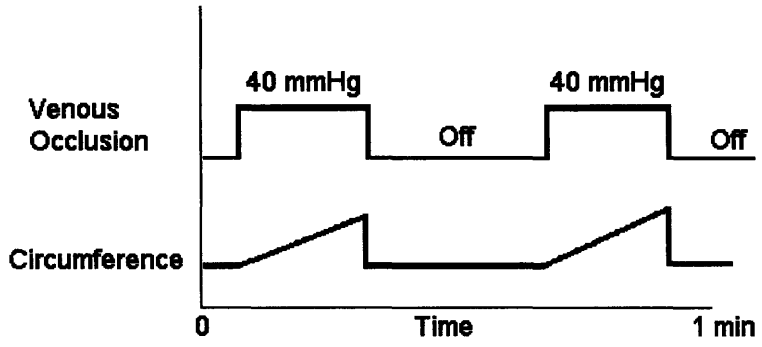

Figure 3.3 Venous Occlusion Plethysmography (VOP) measures the changes in blood volume within a limb during short periods of venous occlusion.

Changes in limb volume during forearm blood flow (FBF) measurements are assessed by a plethysmograph. Calibrated mercury-in-silastic strain gauges (or indium-gallium gauges) are placed around the widest part of the forearm. When the forearm volume changes, a corresponding change in the circumference of the arm occurs, thereby altering the strain gauge length and the electrical resistance of the gauge. Thus, changes in limb volume are directly related to changes in gauge resistance, providing a measure of blood flow to the enclosed volume of the forearm, assuming a cylindrical shape [141]. This is usually expressed as ml per 100 ml of forearm volume per minute. Technical advances in this method include computer control and the use of an electro-mechanical sensor with automated calibration instead of the conventional strain gauge.

Venous occlusion plethysmography can also be used to observe flow changes following a period of ischemia, such as with post-occlusion reactive hyperemia. In this test, an arterial cuff is placed proximal to the venous occlusion cuff and plethysmograph. After establishing a baseline flow, the arterial occlusion cuff is inflated to a suprasystolic pressure for 3-5 minutes and the resulting flow following release of the cuff is recorded.

Although VOP is a widely-used method of measuring forearm blood flow, it is technically challenging, especially during reactive hyperemia. It has been most useful when coupled with intra-arterial drug infusion, which, due to its invasive nature, has limited its application and reliability. For example, this technique is not appropriate for applications that require investigators to distinguish between skin and muscle blood flow, which account for roughly 30% and 70% of resting blood flow in the forearm [139]. Also, VOP provides only discontinuous measurements, taken every 10-15 seconds. However, the data obtained from studies measuring FBF support the concept of measuring flow, or flow and shear rate-dependent parameters during the hyperemic response, to investigate the integrity of endothelium-dependent vascular reactivity.

3.3.3 Brachial Artery Ultrasound Measurement of Endothelium-Dependent Flow-Mediated Dilatation (FMD)

In 1992, Celermajer *et al.* [67] evaluated flow-mediated vasodilatation (FMD) of the brachial artery, an endothelium-dependent function, by high-resolution ultrasound imaging. In this study, investigators found evidence of endothelial dysfunction, characterized by diminished FMD, in individuals at risk for atherosclerosis. Also known as the reactive hyperemia test, this technique is now widely used in basic science and clinical research. Because of the ease with which it can be done and its reliability, endothelium-dependent FMD is considered to be the gold standard in noninvasive endothelial function assessment [33]. Figure 3.4 displays typical ultrasound measurements taken on the brachial artery during a test of reactive hyperemia.

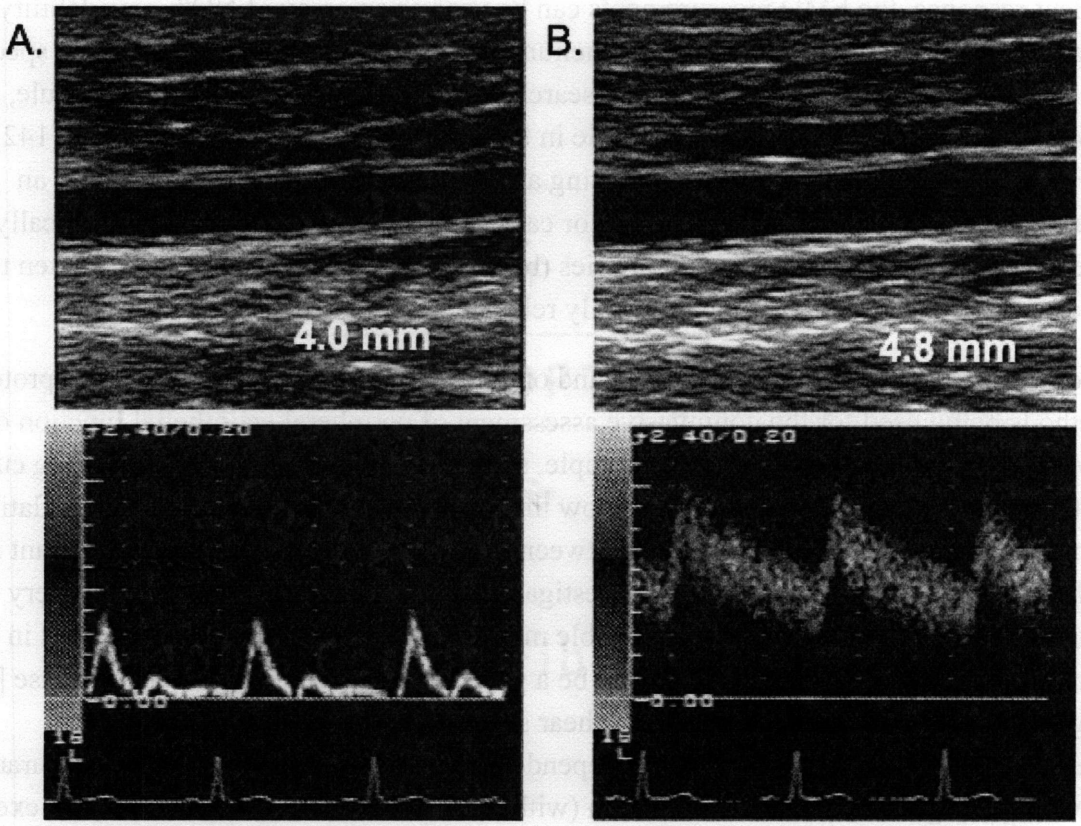

Figure 3.4 Brachial artery ultrasonography and endothelial function testing. Brachial artery ultrasonography has been used to evaluate endothelial function noninvasively by measuring vascular reactivity to increases in flow-induced shear stress, a NO-mediated event. This method has been shown to correlate with coronary vasodilator responses. (A) Baseline brachial artery ultrasound image (top) with corresponding flow velocities (bottom). (B) Reactive hyperemia induces flow-mediated vasodilatation of the brachial artery (top) that is accompanied by increased flow velocities in the artery (bottom).

In a typical FMD measurement, forearm or hand ischemia is induced and maintained for 5 minutes by interrupting arterial blood supply with a blood pressure cuff inflated to suprasystolic pressure. When the pressure is released, reactive hyperemia occurs caused by dilation of the distal microvasculature. The reactive hyperemic response can be characterized by two distinct phases: a maximal, or peak, response that occurs within a few seconds after removal of the

occlusion and a more prolonged total hyperemic period that is thought to represent the blood flow debt repayment. This capacity of blood vessels to respond to physical and chemical stimuli in the lumen confers the ability to self-regulate tone and to adjust blood flow and distribution in response to changes in the local environment. Many blood vessels respond to an increase in flow, or more precisely shear stress, by dilating (lowering the vascular resistance). This phenomenon is designated FMD and is thought to be principally mediated by endothelium-derived nitric oxide (NO).

Theory suggests that shear stress and alterations in hydrostatic pressure during reactive hyperemia result in the local release of NO with subsequent vasodilatation that can be imaged and quantitated by ultrasound. By creating a shear stress stimulus that produces an NO-dependent response, the FMD measurements can be used as an assay of NO bioavailability (a combination of NO production by the endothelium and destruction by reactive oxygen species). In this case, NO is of particular interest to researchers as it is an antiatherogenic molecule, and a reduction in its bioavailability may play a role in the pathogenesis of vascular disease [142]. A small FMD response is interpreted as indicating a low NO bioavailability and possibly an associated increased risk of vascular disease or cardiac events. In humans FMD is typically assessed in the large peripheral conduit arteries (brachial, radial and femoral) and is often taken to represent the response in the more clinically relevant coronary circulation [106].

Despite widespread use in clinical research and ongoing attempts to standardize FMD protocol, the methods being used for the noninvasive assessment of peripheral endothelial function differ greatly between laboratories [143]. For example, some investigators place the occluding cuff above the elbow, whereas others place it below the elbow [144]. The time after cuff deflation when measurements are taken also varies between laboratories [145]. These are important areas of further standardization, especially for investigators who hope to evaluate conduit artery endothelial function in a consistent and reliable manner. Under specific flow conditions in the brachial artery, dilatation has been shown to be a primarily NO-dependent FMD response [126] although later evidence reveals that certain shear stress stimulus profiles (e.g. sustained hyperemia) elicit mechanisms primarily independent of NO [80]. Different occlusion durations, cuff positions, degrees of ischemic dilatation (with the addition of an ischemic forearm exercise) or areas of the circulation examined (upper versus lower limb) result in distinct shear stress profiles created upon occlusion release [144]. This suggests that there are multiple mechanisms involved in FMD and that the mechanisms involved in any given response are highly sensitive to the nature of the stimulus imposed (stimulus-response specificity).

Unfortunately, current studies frequently do not address the conditions that are required to evoke a reliable NO-dependent FMD response. The high cost of an ultrasound imaging device and the need for a skilled operator further limit the technique's utility in a clinical setting. Finally, there is considerable operator dependence in several aspects of how the test is performed and the results can have up to 25% day-to-day variability [19]. Therefore, this tool is limited in clinical

utility until standard methodology is developed that will provide more consistency for longitudinal follow-up and allow comparisons of data from various laboratories.

Despite the disadvantages posed by lack of standardization, brachial FMD measurement is one of the few noninvasive techniques that can measure peripheral endothelial dysfunction, even in subjects as young as 5 years of age [68]. This technique is attractive because it is safe and allows repeated measurements. Furthermore, brachial artery reactivity has been shown to accurately reflect coronary reactivity and therefore can be used as a surrogate marker of coronary endothelial function [106]. This observation is based on the principle that endothelial dysfunction actually precedes clinical manifestations of coronary artery disease and is thus a better prognostic indicator of events than coronary lesions themselves. In contrast, other modalities are more invasive and largely provide information about the presence and severity of fixed anatomic disease, which may be less relevant to the pathogenesis of events. FMD is associated with several risk factors and can be improved by the correction of many classic risk factors such as hypercholesterolemia and arterial hypertension [143].

3.4 Current Methods for Noninvasive Evaluation of the Microcirculation

The ability to evaluate the microvascular structure and function is important for an understanding of pathophysiological processes in multiple disease states. A range of techniques are available or emerging for investigating different aspects of the microcirculation in humans. Techniques such as orthogonal polarization spectral imaging allow visualization at the level of single microvessels. Venous occlusion plethysmography can be used to measure regional blood flow in organs and limbs, and laser Doppler flowmetry to measure red blood cell flux in small areas of tissue. A variety of thermal methods have been proposed as well and are discussed in Section 3.5.

3.4.1 Laser Doppler Flowmetry

Laser Doppler flowmetry (LDF) is a noninvasive, continuous measure of microcirculatory blood flow and has been used to measure microcirculatory blood flow in many tissues including neural, muscle, skin, bone, and intestine. The principle of this measurement is the Doppler shift, or the frequency change that light undergoes when reflected by moving objects – in this case: red blood cells (Figure 3.5). A sample volume of the tissue under observation is illuminated with monochromatic laser light from a probe. When the tissue is illuminated, only 3–7% is reflected. The remaining 93–97% of the light is either absorbed by various structures or undergoes scattering due to interactions with static and moving cells [146]. Photons scattered on blood cells are frequency-shifted (Doppler effect) proportional to the speed of the moving cells. Another optical fiber collects the backscattered light from the tissue and returns it to the monitor. After the signal is amplified and analyzed, LDF produces an analog output signal that is proportional to the number of blood cells multiplied by the mean velocity of these cells, or the blood cell perfusion (flux).

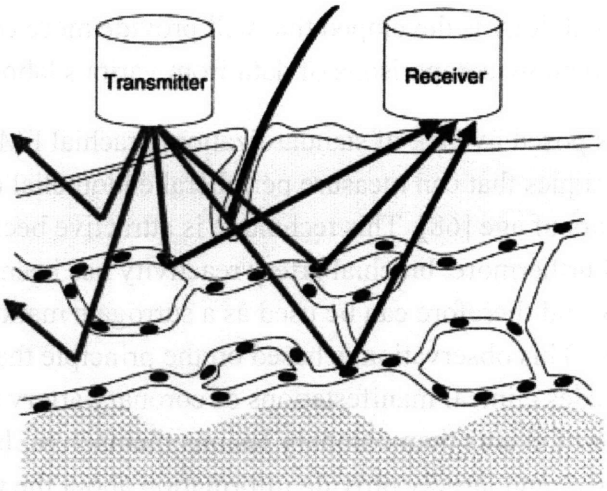

Figure 3.5 Basic operating principles of laser Doppler flowmetry (LDF). Laser light is directed at an area of tissue where it is reflected and scattered by red blood cells within the tissue, resulting in frequency-shifted light which is detected and received by a photodetector.

As a noninvasive measure of peripheral blood flow, LDF is often designed with a fiber optic probe separation of 500 μm between the transmitting and receiving fibers. When applied to the skin, this results in a penetration depth of about 1.0-1.5 mm and an interrogated volume of approximately 1 mm^3 [10]. Therefore, it can be assumed that flow is measured in arterioles, venules, arteriovenous anastomoses, and, to a much smaller extent, nutritional capillaries (about 5%). Indeed, evidence suggests that the dominant part of the LDF signal is generated by movement of blood cells in the subpapillary vascular bed of the skin while only a small portion is due to motion of blood cells in the nutritional capillaries [147]. However, the relative distribution of blood between non-nutritional, subpapillary vascular beds and nutritional papillary capillaries in the skin differs markedly across skin regions, making interpretation of results difficult in some cases. The measuring depth and volume of LDF on skin is also influenced by multiple factors, e.g. the amount of blood and the composition of skin, and decreases in sensitivity in relation to the depth in the dermis.

LDF has been applied to obtain information on the functional state of the skin microcirculation during either reactive hyperemia following ischemia or the noninvasive local application of acetylcholine or sodium nitroprusside in several conditions. An impairment in reactive hyperemia has been observed in patients with multiple disorders, including diabetes mellitus [31, 60, 113, 115, 116, 148], essential hypertension [149, 150], coronary artery disease [122], hypercholesterolemia [71], peripheral arterial occlusive disease [151], end-stage renal disease [99], and sepsis [152]. A typical LDF result from studies comparing healthy subjects and patients with endothelial dysfunction is shown in Figure 3.6. Spectral analysis of the cutaneous perfusion signal is also useful for the evaluation of characteristic oscillation frequencies (i.e. flowmotion) corresponding to influences from the heart beat, respiration, the intrinsic myogenic activity of the vascular smooth muscle, the neurogenic activity of the vessel wall, and the vascular endothelium [153]. These have been demonstrated to be dependent on arteriolar diameter oscillations, i.e.

vasomotion, which is a critical factor in the optimal distribution of blood flow in the skin microcirculation [154]. Due to the finely controlled nature of skin blood flow, researchers have begun using LDF to investigate skin flowmotion in response to vasoactive drugs and in certain vascular diseases, including diabetes, hypertension, and peripheral arterial occlusive disease [24].

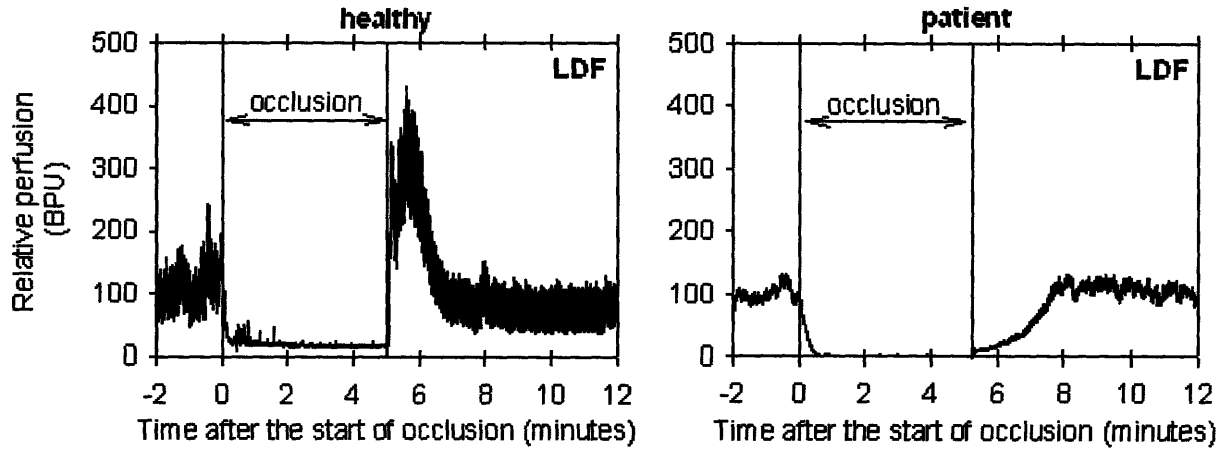

Figure 3.6 Representative LDF measurement during test of Post-Occlusive Reactive Hyperemia (PORH): Comparison of a healthy subject and a subject with endothelial dysfunction.

A major limitation of the reproducibility and cross-study comparisons involving LDF is its significant site-specificity that can lead to considerable spatial and temporal variations. The spatial heterogeneity of skin lowers the reproducibility of the desired perfusion index since skin blood flow signal varies markedly depending on probe position. Considering the heterogeneity of the skin vasculature, studies comparing multiple LDF measurements must make measurements at identical sites under identical environmental conditions. Moreover, the device only examines a superficial layer of dermis in a small, yet undefined volume of tissue and may require several measurement sites for an accurate representation of tissue perfusion. Finally, no current laser Doppler instrument can present absolute perfusion values (e.g., ml/min per 100 g tissue) and measurements are expressed as perfusion units, which are arbitrary and related to a pre-defined electrical signal, which is often set by individual device manufacturers. Thus, LDF measurements are only valid on a relative scale with respect to the specific patient and tissue of interest.

A recent advance in the field is that of laser Doppler imaging (LDI), a non-contact device that generates two-dimensional maps of perfusion based on the same principles of LDF [155]. With systematic scanning of a defined region, this technique allows an estimate of the temporal and spatial heterogeneity of skin blood flow. However, the resulting signal is still expressed in relative units and the quality of validation is limited to a small number of studies.

3.4.2 Orthogonal Polarization Spectral (OPS) Imaging

Orthogonal polarization spectral (OPS) imaging is a noninvasive technique that uses reflected light to produce real-time images of the microcirculation on the surface of solid organs and through mucous membranes [156]. Of the possible tissue beds, the sublingual mucosa has been most extensively studied [157, 158]. Visualizing the microcirculation allows investigators to detect microvascular pathologies and quantify perfusion in the microcirculation. In contrast to studies using laser Doppler or plethysmography to investigate global microvascular blood flow, OPS imaging allows assessment of the heterogeneity of the local microcirculation.

In OPS imaging, polarized light in one plane is directed towards the tissue of interest by a set of lenses. As the light reaches the tissue, the depolarized light is reflected back through the lenses to a second polarizer, or analyzer, oriented orthogonal to the first polarizer. If a wavelength within the hemoglobin absorption spectrum (e.g. 548 nm) is chosen, small blood vessels containing red and white blood cells can be clearly seen. The vessel walls themselves are not visualized directly and their imaging depends, therefore, on the presence of red blood cells. By definition, only vessels containing red blood cells will be visualized, providing a measure of perfusion in the analyzed tissue. The technology has been incorporated into a small hand-held video-microscope which can be used in both research and clinical settings [156]. OPS can assess tissue perfusion using the functional capillary density (FCD), defined as the length of red blood cell (RBC)-perfused capillaries per observation area (measured as cm/cm^2). The speed of blood flow can be estimated by software used to analyze dynamic capillaroscopy, although the current technical limit for blood flow velocity determination is approximately 20 mm/s [159].

Functional capillary density is a direct measure of the state of nutritive perfusion to the tissue and is an indirect measure of oxygen delivery. The prior use of sublingual tissues with OPS provides information about the dynamics of microcirculatory blood flow, and has been studied as a monitor of perfusion during the clinical treatment of circulatory shock [160]. However, alterations in the sublingual microcirculation may not be representative of blood flow in other microvascular beds. Noting the need for the OPS technique in dermatologic investigations, Lupi *et al.* [161] reviewed the prospects of OPS imaging in assessment of microcirculation in the skin, stating that the technique is promising in the study of vasculitis, chronic venous insufficiency, and skin tumors. OPS measurements have also been validated against intravital fluorescence microscopy in experimental models of skin wound healing [162].

However, there are limitations of the technique that restrict its usefulness in studies involving the skin. In particular, OPS imaging is influenced by the amount of melanin at the dermal-epidermal junction, making visualization difficult in individuals with a large amount of melanin in their skin. The variability of skin thickness also complicates measurement as image resolution is good for tissue depths of approximately 300 μm [163], although penetration of up to 3 mm has been reported [161]. Moreover, to be a useful monitor of perfusion, the obtained images must be interpreted uniformly and quantification of microcirculatory flow must be reproducible. Due to

the inherent heterogeneity of the microcirculation and technical requirements of OPS imaging, a temporal assessment of tissue perfusion is difficult to interpret based on momentary images of individually perfused vessels. Furthermore, analysis of microcirculatory parameters are semi-quantitative and can only be performed 'off-line'.

3.4.3 Peripheral Arterial Tonometry (PAT)

The peripheral arterial tonometry (PAT) technique is very similar to arterial applanation tonometry used to measure the radial artery pressure waveform [164], although with PAT, the goal is to use the arterial waveform to derive the pulse wave amplitude (PWA). The technology involves a finger plethysmographic device that allows the isolated detection of pulsatile arterial volume changes. A proprietary PAT device (Figure 3.7), made by Itamar Medical Ltd., Caesarea, Israel, consists of a pneumatic finger probe which covers the distal phalanx of the finger and allows the application of a constant and evenly distributed near-diastolic counterpressure within the entire probe. This increases sensitivity by unloading arterial wall tension and prevents venous blood pooling and blood stasis, which could induce venoarteriolar reflex vasoconstriction [165]. Pulsatile volume changes of the fingertip are sensed by a pressure transducer and transferred to a personal computer where the signal is filtered, amplified, displayed, and stored. The RH-PAT (reactive hyperemia peripheral arterial tonometry) technique has been developed specifically for evaluation of endothelial function and permits the noninvasive assessment of peripheral vascular reactivity by measuring digital pulse volume at rest and during reactive hyperemia.

Figure 3.7 RH-PAT finger plethysmographic device developed by Itamar Medical

Used originally to measure peripheral vasoconstriction during REM sleep [166], this technology has since been found to demonstrate impaired digital hyperemic response corresponding to coronary artery disease. Based on the technique of measuring endothelial function through NO-mediated vasodilatation, a study carried out by Bonetti *et al.* [167] examined PWA changes following brachial artery occlusion with a blood pressure cuff. The extent of reactive hyperemia was calculated as an RH-PAT index, defined as the ratio of the average amplitude of the PWA over a 1-min time interval beginning after exactly 60 seconds of reactive hyperemia divided by the average PWA for the 210 second-period before cuff inflation (baseline). The RH-PAT device

was tested on 94 consecutive patients who were referred for coronary angiography. The average RH-PAT index was lowered in individuals with known coronary artery disease and demonstrated a correlation with coronary artery response to acetylcholine (see Figure 3.8).

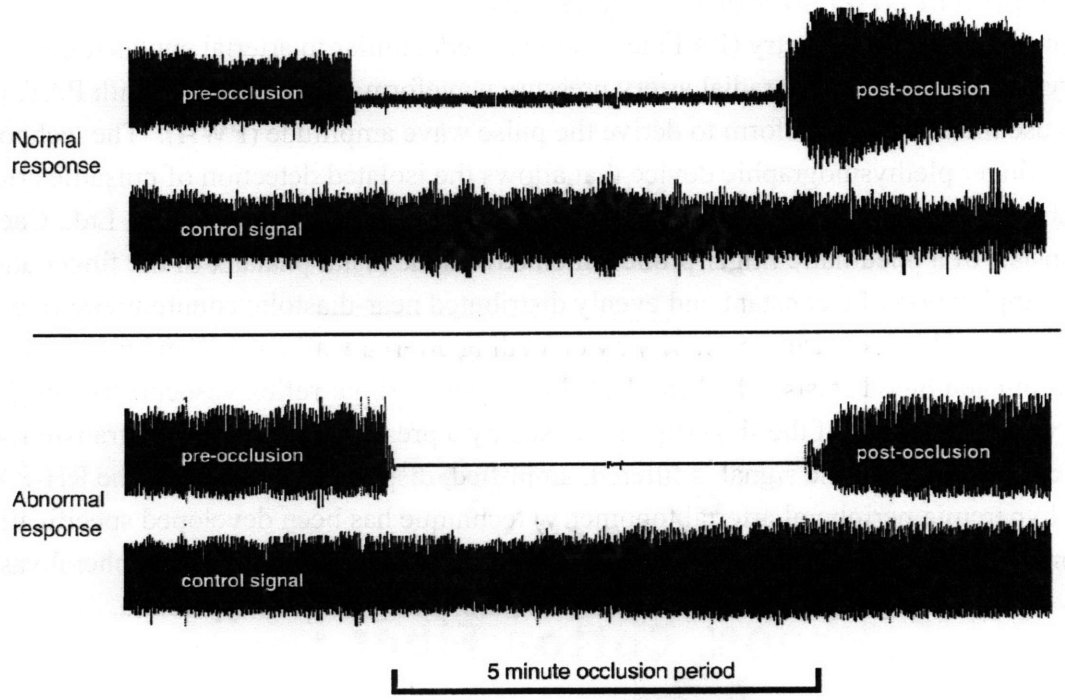

Figure 3.8 Representative RH-PAT signal recorded in subjects with normal and abnormal reactive hyperemic responses. Normal response is characterized by a distinct increase in the signal amplitude after cuff release compared with baseline. [167]

In another study conducted by Kuvin *et al.* [165], it was found that a lower RH-PAT index (here, called PAT hyperemia ratio), was related to factors known to affect endothelial function, such as hypertension, hyperlipidemia, and tobacco use. The investigators also demonstrated endothelial behavior similar to that of flow-mediated vasodilatation of the brachial artery such that the PAT hyperemia ratio was reduced in subjects with impaired endothelial function represented by low FMD and was higher in subjects with greater brachial artery FMD responses consistent with more preserved endothelial function. These studies confirm that a reduction in digital PWA reactivity coexists with evidence of endothelial dysfunction in coronary and brachial arteries of individuals with atherosclerosis or its risk factors.

Blood flow in the fingertip can vary by a great amount due to the overwhelming presence of arteriovenous anastomoses, which are primarily regulated by the sympathetic nervous system. Prior investigations have shown that nitric oxide plays a minimal role in controlling resting digital blood flow [168, 169]. This poses questions regarding the validity of evaluating digital endothelial dysfunction since decreased nitric oxide bioavailability is a defining characteristic of endothelial dysfunction and cardiovascular disease. Nohria *et al.* [170] have demonstrated that

nitric oxide is the principle mediator in modulating digital vascular function in response to a reactive hyperemia flow stimulus. In their study, there was a significant reduction in digital PWA response during reactive hyperemia when nitric oxide production was inhibited by the nitric oxide synthase inhibitor, N^G-nitro-L-arginine methyl ester (L-NAME). In agreement with the prior investigations, inhibition of nitric oxide synthase did not alter baseline digital PWA. The results from Nohria *et al.* establish a central role for nitric oxide in digital reactive hyperemia. It is reasonable to conclude that measurement in the fingertip provides a simple and noninvasive method of assessing nitric oxide bioavailability and endothelial function, despite its relative absence during resting blood flow.

The FDA-cleared PAT technology can be applied to measure obstructive sleep apnea as well as endothelial dysfunction. The RH-PAT method for measuring endothelial dysfunction is integrated into the Endo-PAT2000 system and is marketed as a noninvasive tool with the potential to identify patients during the early stages of cardiovascular disease with a simple test based on digital reactive hyperemia [171]. Further research must be done to explore the possibility of applying such a screening index in the general population and to investigate whether the RH-PAT index augments conventional risk scores.

3.5 Current Methods of Noninvasive Assessment: Thermal Methods

The qualitative and indirect assessment of temperature and coloration in the skin is intrinsically linked to tissue perfusion within the microcirculation. For example, a person with a flushed appearance experiences warmth and a reddish color appears in the face and skin. A physician will often note the healthy state of a patient's skin as being "warm and well perfused" while a patient experiencing shock from low blood volume often has skin that is cold, clammy, and pale. Many different methods have been developed to investigate skin perfusion based on thermal principles. The following discussion will focus on those which have applied temperature-based approaches to evaluate perfusion or to assess clinical signs of cardiovascular disease or circulatory distress. The history of thermal techniques for the measurement of local tissue perfusion is reviewed extensively by many researchers, including Bowman *et al.* [172], Eberhart *et al.* [173], Bowman [174], and Chato [175]. This section will address the thermal methods that have been applied in a noninvasive way to assess microvascular perfusion of the skin.

3.5.1 Skin Surface Temperature Gradients

The digital skin surface temperature and core-digit temperature gradients have been proposed for the monitoring of peripheral perfusion in a variety of clinical situations. Since toe temperature was initially studied as an indicator of the severity of circulatory shock [176], body temperature gradients have been used in the monitoring of postoperative care to assess changes in intravascular volume [177], weaning of cardiopulmonary bypass to assess the adequacy of rewarming [178], and active core cooling to detect thermoregulatory vasoconstriction [179]. The principle of core-to-peripheral temperature gradients is based on the transfer of heat from the

body core to the skin, which is controlled by the degree of peripheral vasoconstriction. During vasoconstriction the temperature of the skin falls and the heat conduction from the core decreases. As a result, the core temperature rises and the core-to-peripheral temperature gradient increases. A gradient of 3–7°C normally occurs in patients with stable hemodynamics [180].

The forearm-to-fingertip skin temperature gradient has also been used as an index of peripheral perfusion. Studies have compared the skin surface temperature gradients to total finger blood flow measured with venous-occlusion volume plethysmography and laser Doppler flowmetry, with favorable results [181, 182]. The preferred use of peripheral skin temperature gradients over a core-to-peripheral temperature gradient is based on its usefulness in non-steady state conditions, such as in patients undergoing surgery. Since the forearm skin site is exposed to the same ambient temperature as the fingertip, both are similarly affected by environmental temperature fluctuations, producing little influence in the gradient. This parameter has been proposed as an inexpensive and easy-to-use measure of thermoregulatory peripheral vasoconstriction, particularly in anesthetized patients undergoing surgery [183].

A number of studies have examined the correlation between core-to-peripheral temperature gradients and global hemodynamic variables in hypovolemic, septic and cardiogenic shock, although these have produced conflicting results [180]. A primary source of the discrepancy between a measured body temperature gradient and global hemodynamic parameters in an operating room could be related to an unstable environment, as skin temperature depends on ambient temperature. Another reason may be that global hemodynamic parameters may not be sensitive enough to reflect changes in peripheral blood flow in critically ill patients. Although the forearm-to-fingertip skin temperature gradient offers a validated alternative approach, its use in these conditions has not yet been defined. Nevertheless, it has proven to be a reliable method of evaluating peripheral vascular responses compared to other standard measurements such as finger volume plethysmography and laser Doppler flowmetry.

3.5.2 Thermal Clearance

The thermal clearance technique is based on the theory first described in 1933 by Gibbs [184] in which the rate at which heat is carried away from a source is dependent on conduction through the tissue and local blood perfusion. The first surface-mounted thermal clearance probe using three thermocouples in series was proposed in 1956 by Hensel and Bender [185] and was subsequently improved by the work of Kuiper and van de Staak [186]. Their probe consists of two concentric copper discs separated by a small, known distance that is placed in contact with the skin. The temperature difference between the central heated disc and the unheated, concentric annulus is measured by thermocouples and related to rate of removal of heat from the center of the probe by the blood flow in the skin at that location. When blood flow is high, the heat is dissipated at a greater rate and the temperature difference is low. When blood flow is low, heat dissipation is reduced and the temperature difference between the rings is increased. The

effective thermal conductivity that is determined contains a convection component related to the skin blood flow.

Improvements and modifications to the method have been explored by many researchers with varying degrees of success [187-192]. The method has been used by many investigators in studies to assess its relationship to other measures of perfusion, such as laser Doppler flowmetry and volume plethysmography [193-195] and has been investigated for use in pathological states, such as Raynaud's disease and burns [196, 197]. Nevertheless, it is ultimately limited as a qualitative measure of skin blood flow [195, 198]. Furthermore, its value as a measure of nutrient perfusion in the skin (originally advocated by Holti and Mitchell [191]) has since been proven to be unrealistic in certain locations (e.g. fingers) due to its depth discrimination, which includes flow through arteriovenous anastomoses [199]. This is comparable to the tissue penetration of LDF.

Efforts to gain quantitative measurements of skin blood flow have been investigated. Jaszczak and Serjsen [200] and Midttun *et al.* [201] employed a "heat-washout" method for quantifying blood flow. With this technique, heat is modeled as a diffusible indicator using the principle of Kety's local indicator washout method [202]. After measuring the baseline skin temperature, the temperature of an insulated heater is raised between 2-10°C above baseline values. Once steady-state temperature is reached after 3-5 minutes, the heat is turned off and the temperature decay to baseline is monitored. Flow is calculated afterwards using Kety's principles. Midttun *et al.* compared the calculated perfusion with xenon clearance and found a high degree of correlation between the two, although they did experience conductive heat losses to the air via the probe and the tissue.

3.5.2.A Surface Thermistors

Thermistors have also been used to monitor skin temperature by measuring their temperature-dependent changes in electrical resistance. For negative temperature coefficient (NTC) thermistors, electrical resistance decreases as skin temperature increases. Furthermore, thermistors are capable of generating heat when a current is applied. These characteristics have made it useful in assessing thermal clearance in the skin in a variety of ways. However, none have been successful in accurately tracking and quantifying quickly fluctuating perfusion in absolute units and in real time. The developments presented in this particular area lay the groundwork for the current noninvasive probe design of focus.

In 1979, Patera *et al.* [203] designed a technique of measuring perfusion using a flake thermistor placed on the surface of a tissue. They applied a sinusoidal heat flux and measured the phase shift between the applied signal and the corresponding tissue surface temperature response. For a given applied frequency, this phase shift was a function of perfusion and the intrinsic conductivity of the tissue. Additionally, the method was independent of the temperature of the probe or tissue. However, the phase shift was very small for normal levels of perfusion, making measurement difficult. Furthermore, the accuracy of the calculated perfusion decreases with

increasing driver frequency such that dynamic perfusion fluctuations above approximately 0.1 Hz are lost. As a result, the method is inappropriate for studies of vasomotion. Since Patera *et al.* first proposed a sinusoidal heating technique, Anderson and Burnside [204] have applied the concept of sinusoidal heating of the skin using ultrasound to calculate perfusion from the phase-shifted temperature response. Liu *et al.* [205] have also improved upon the original heating algorithms to establish a similar method with a more strict theoretical foundation.

Castellana *et al.* [206] developed a surface thermal probe consisting of a platinum flake thermistor with an insulating foam support. The thermistor rests on the surface of a tissue and is heated to a fixed temperature while the power to maintain that temperature elevation is measured. The steady-state response of the probe to flow changes is then related to perfusion by a theoretical analysis of the bio-heat transfer equation, which the investigators solved using a Fourier series method. In 1984, Walsh [207] designed a noninvasive probe consisting of two flake thermistors, achieving good sensitivity to changes in perfusion. He also created an analytical one-dimensional model of the noninvasive probe which indicated that the dimensions of the surface probe were more appropriate for a spherical model, rather than a model of the probe as an infinite slab. Patel *et al.* [208] investigated the use of a spherical surface thermistor embedded in an insulator and applied to an isolated, perfused rat liver apparatus. The thermistor's response to perfusion was modeled with a simplified bio-heat equation in which effective thermal conductivity is a linear function of perfusion. Although they demonstrated probe sensitivity to changes in perfusion, the investigators experienced significant errors caused by baseline temperature drift and poor probe-tissue contact.

Noninvasive thermal probes have had limited success with respect to perfusion measurement. There is often difficulty in measuring the actual heat flux going into the tissue due to losses to the ambient air. Many researchers have also encountered problems with the probe-tissue interface, as there is both an issue of thermal contact resistance and of capillary collapse with applied pressure.

3.5.3 Convective Perfusion Bioprobe

Another effort to measure skin perfusion noninvasively has been pursued by researchers at Virginia Tech. Based on the original work of Michener *et al.* [209] and later, Fouquet *et al.* [210], the "bioprobe" consists of a heat flux sensor and surface thermocouple that is placed in contact with surface tissue, while the opposite side is cooled, rather than heated. Cooling of the tissue generates heat flux through the probe. Cooling was original accomplished by water channels, but O'Reilly *et al.* [211] improved upon the probe design by using pressurized air jets. An analytical thermal model was developed to relate the measured heat flux and temperature of tissue to obtain a value for perfusion as well as probe contact resistance through parameter estimation techniques, where the measured heat flux is compared to an estimate predicted by the model in order to solve for the perfusion term in the bio-heat equation.

Further probe and parameter estimation development has been described by the work of Robinson [212], Scott *et al.* [213], Cardinali [214], Mudalier [215] and others. A thorough history of the Virginia Tech Bioprobe is provided in Mudalier's 2007 PhD dissertation [215]. While the method has been shown to be sensitive to changes in blood perfusion in a canine skin flap model, isolated rat liver system, exposed rat kidney system, and perfused phantom tissue system, the model has not been independently validated for measurement of absolute blood flow. Furthermore, variations in skin temperature, motion artifacts and fluctuating air temperature disturb the measurement and confound the analytical perfusion extraction. It is also greatly limited by the post-measurement processing necessary to estimate perfusion, resulting in a clinically unacceptable situation.

3.5.4 Digital Thermal Monitoring (DTM)

In 2003 and 2004, researchers at the University of Texas explored a temperature-based technique for measuring endothelial dysfunction [216, 217]. Their initial analysis of the method is based on temperature changes in the skin of the distal palmar pad of the finger and various locations along the forearm following vascular occlusion and release with an arm blood pressure cuff. Using thermistors attached to the finger and forearm with foam tape, the investigators determined the linear rate of temperature fall during a 5 minute pressure cuff occlusion and rate of temperature rise following release. The percentage increase in the rate of rise compared to the rate of fall was also considered [216]. From their studies, it was established that the distal finger temperature was most responsive to a proximal blood flow occlusion. They also determined that the rate of rise was significantly higher than the rate of fall in temperature [217]. A test of reproducibility in one subject demonstrated a significant variability in the calculated ratio and the percentage increase [216]. The studies were performed on subjects with little health history available and no conclusions were drawn regarding its reliability in detecting endothelial dysfunction.

A device-based method of measuring endothelial dysfunction using finger temperature monitoring has been developed by researchers at the University of Texas Houston Health Science Center and the Texas Heart Institute and is marketed by a Houston-based company, Endothelix, which was formed in December of 2003. The VENDYS® device is a proprietary technology which monitors temperature changes at the fingertip as a marker of endothelial dysfunction, a method called Digital Thermal Monitoring (DTM). The test is conducted by placing resistance temperature detector (RTD) probes on the palmar skin of the distal index fingers of both arms. After a period of temperature stabilization, a pressure cuff is then inflated around one arm to 50 mmHg above systolic blood pressure for two to five minutes. Fingertip temperature usually drops one to two degrees during this period. When the cuff is deflated, the reactive hyperemia is detected as a rise in fingertip temperature. The probes continuously monitor the temperature changes and feed data to software for analysis. It is proposed that the temperature overshoot and area "under the curve" during occlusion and release reflects the state of normal or abnormal vascular reactivity (Figure 3.9). Temperature that struggles to reach

baseline indicates an impaired endothelium, while patients with normal endothelial function overshoot the baseline temperature before settling.

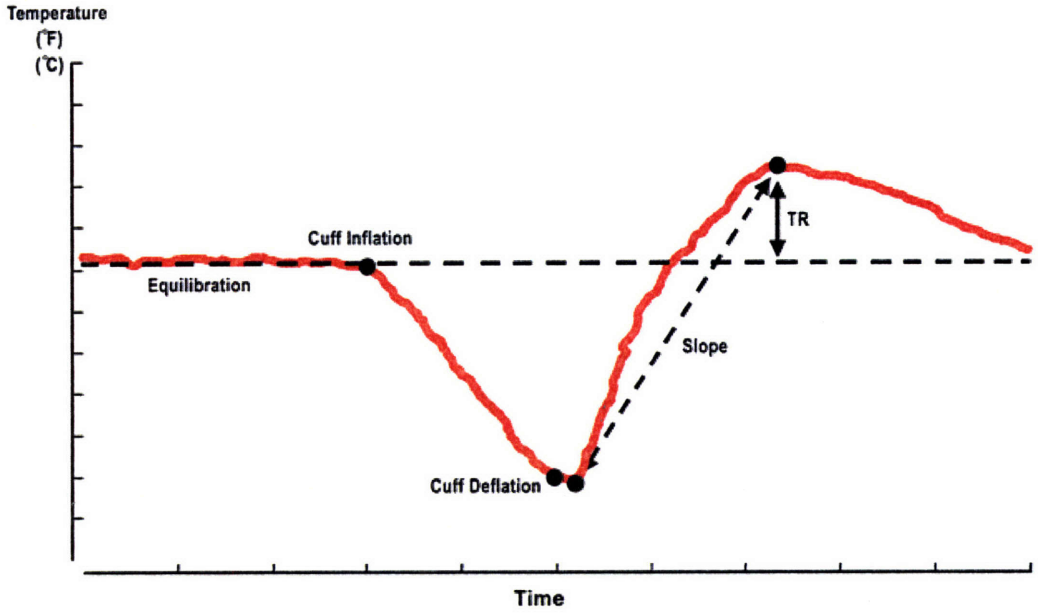

Figure 3.9 Parameters of Digital Thermal Monitoring (DTM) test of endothelial dysfunction [218].

Endothelix gained FDA approval of the VENDYS® technology in 2007 and it is now available in a cart model and portable briefcase model (Figure 3.10). Over the past few years, several clinical studies have been performed by investigators from the Harbor-UCLA Medical Center and Lenox Hill Hospital of New York. Due to the relatively recent development of the DTM technology, there is little published clinical information available in peer-reviewed journals. However, abstracts and posters from scientific meetings available on the Endothelix website [218] indicate that the VENDYS® index of endothelial dysfunction obtained by the DTM technique is correlated with traditional cardiovascular risk factor scores (Framingham Risk Score) [219, 220], coronary calcium score [220], as well as presence of metabolic syndrome and diabetes [221]. Measured parameters have included temperature rebound (TR), slope of recovery, percent of temperature rebound (compared to initial pre-occlusion temperature), and area under the temperature curve (AUC).

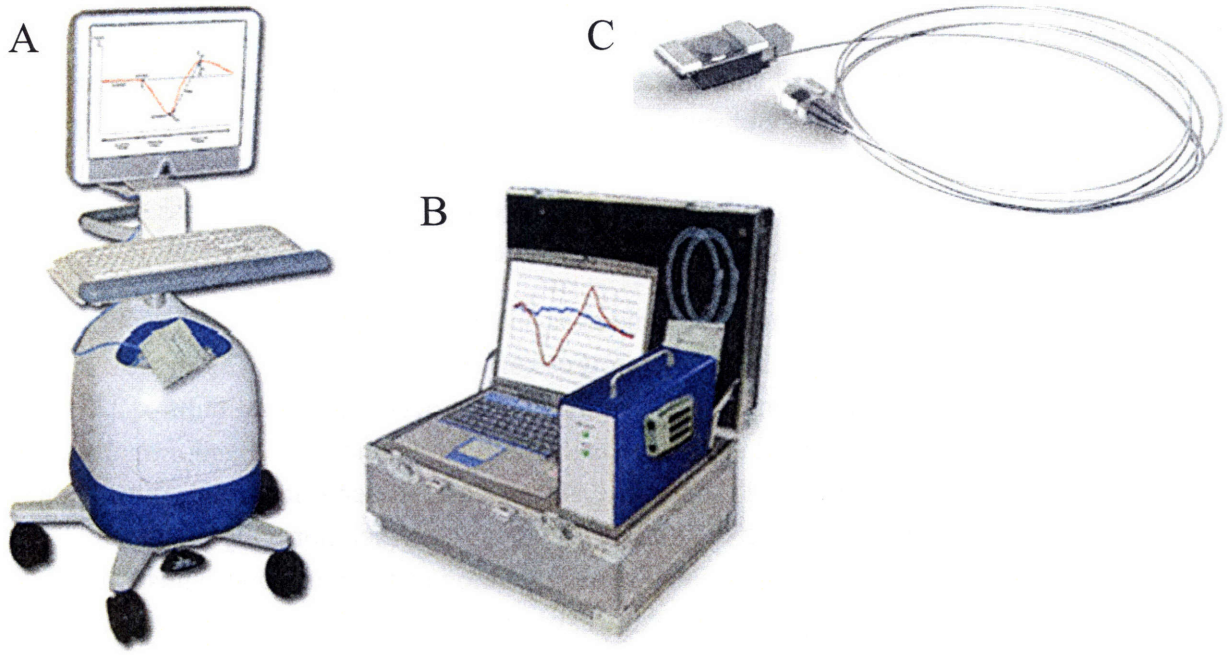

Figure 3.10 VENDYS® technology. The DTM system is available in a cart model (A) and a briefcase model (B). The DTM temperature probe (C) can be used to monitor temperature in 15 separate locations although only 2 are required for the test.

A study of reproducibility was reported in an Endothelix white paper for short-term (1 day) and long-term (3 months) variability of DTM measurements [222]. The results for AUC and TR presented coefficients of variation between 8.9% and 11.5% for short-term measurements and between 8.25% and 16.5% for long-term measurements. The investigators claim this is within acceptable limits of reproducibility. However, it is noted that these results were obtained in a controlled research environment in which participants were measured after an overnight fast and after each had rested 30 minutes in a supine position in a dimmed, temperature-controlled room. These conditions are not always possible for routine clinical use and it remains to be determined how reproducible DTM is in a typical operating environment.

Compared to peripheral arterial tonometry (PAT) technology and other methods of noninvasive assessment, the VENDYS® DTM technique of evaluating endothelial function is proposed as being a more rapid and operator-independent form of endothelial testing and provides simultaneous data output. With this technology, the founders of Endothelix hope to provide a noninvasive, non-imaging, low-cost tool for detection of endothelial dysfunction in routine clinical practice.

3.6 Clinical Implications of Noninvasive Endothelial Function Assessment

Atherosclerosis is the leading cause of mortality in the Western hemisphere and is widely recognized as a systemic vascular disorder with complications in the coronary arteries, carotid arteries, and peripheral circulation. Substantial resources have been devoted to the investigation and treatment for such complications, but the ultimate goal lies in being able to prevent the development of the basic disease or at least to identify those patients who are at risk for an acute event, such as a heart attack or stroke, and to intervene before damage occurs.

Endothelial dysfunction is increasingly recognized as a key early step in the development of atherosclerosis and is also involved in plaque progression and the occurrence of atherosclerotic complications, such as myocardial infarction, angina, sudden death, and heart failure [223]. Atherosclerosis affects essentially all arterial beds including the thoracic and abdominal aorta, coronary arteries, carotid arteries, and the peripheral, renal and mesenteric arteries. Endothelial dysfunction is defined by a loss of self-regulating mechanisms which normally prevent coagulation and inflammation, and promote proper regulation of vascular tone. Thus, the assessment and treatment during the preclinical stages of atherosclerosis requires quantitative measurements of both functional (i.e. flow-mediated vasodilatation) and structural abnormalities (e.g. atherosclerotic plaque).

3.6.1 Epidemiology

Cardiovascular diseases are the single largest killer of both men and women in the United States. According to statistics compiled by the American Heart Association, CVD was determined as the underlying cause of death in 36.3% of all deaths in 2004 [224]. CVD claims about as many lives as the next four leading causes of death (cancer, chronic lower respiratory disease, accidents and diabetes mellitus) combined. An estimated one in three adults have at least one form of CVD. Many unexpected cardiac deaths occur without prior recognition of cardiac disease.

The category of cardiovascular disease includes:

- High blood pressure
- Coronary heart disease (CHD)
- Heart failure (HF)
- Cerebrovascular disease (stroke)
- Peripheral arterial disease (PAD)
- Atherosclerosis and other diseases of arteries, arterioles, and capillaries

Several important factors will serve to accelerate the rate of cardiovascular disease and its complications in the coming years:

- Aging of the population
- Increase in the prevalence of obesity and type II diabetes with their related complications of hypertension, hyperlipidemia, and atherosclerotic vascular disease.

- An alarming increase in unattended risk factors in the younger population (obesity, lack of physical inactivity, poor dietary habits, early onset type II diabetes, teenage smoking)

The estimated cost of cardiovascular diseases (direct and indirect) in the United States for 2008 is estimated at $448.5 billion. This figure includes health expenditures (direct costs) as well as lost productivity resulting from morbidity and mortality (indirect costs). For comparison, in 2007 the estimated cost of all cancers combined was $219 billion [224].

3.6.2 Risk Assessment

Despite several available risk assessment approaches, a substantial gap remains in the detection of asymptomatic individuals who ultimately develop cardiovascular complications. Ideally, a screening test to aid in further risk stratification would [225]:

a) identify high- and low-risk groups more accurately (e.g., low proportion of false negative and false positives).
b) enhance the identification of high-risk individuals.
c) result in a favorable impact on disease outcomes.
d) be relatively free of risk.
e) be cost-effective when compared to the current screening modalities.
f) educate the public concerning atherosclerosis and vascular disease risk.

Vascular disease prevention is most cost-effective in high-risk patients, but the strategy of identifying patients with elevated levels of risk factors is problematic because traditional risk factors (e.g. cholesterol, blood pressure, smoking, etc.) predict only half of vascular events. The goal of cardiovascular disease (CVD) screening is to accurately determine risk early in the natural history of disease, before an individual is considered high-risk. An objective measure of atherosclerotic burden would also aid clinical and research-oriented applications beyond risk stratification, including evaluation of patient response to interventions and identification of novel genetic, cellular and molecular determinants of risk. This has motivated numerous investigators to develop new biomarkers and diagnostic modalities that could help narrow the gap left by traditional risk assessment.

3.6.2 Primary Prevention

Early detection of endothelial dysfunction and subsequent lifestyle modifications could greatly increase survival from cardiovascular complications and reduce CAD risk. Numerous factors contribute to reducing cardiovascular risk, including exercise, dietary modifications, blood pressure reduction, and smoking cessation. Also shown to be associated with improved endothelial function are interventions such as antioxidant therapy, lipid-lowering therapy, ACE inhibitors, hormone replacement therapy, drug therapy to increase insulin sensitivity in diabetics, etc (Table 3.1).

In addition to early detection, the effectiveness of therapeutic intervention or lifestyle changes can be tracked over time, providing quantitative measures in achieving certain goals of treatment. For example, measuring carotid plaque area by ultrasound has been presented as a way to evaluate and track severity of cardiovascular burden [226]. Measuring plaque as a continuous variable appears to be more powerful than simply detecting the presence or absence of plaque at extracoronary sites or counting the number of sites involved. Regression of plaque is also used as the therapeutic goal so that follow-up measurements of plaque can determine whether therapy is successful. In practice, showing patients the pictures and measurements of their plaque progression often seems to help motivate them to implement lifestyle changes such as smoking cessation and dietary change. Moreover, plaque regression validates and encourages persistence with successful lifestyle changes [226]. Since it is currently common for many people to track their blood pressure as an index of current health, it is not hard to imagine other noninvasive indices, such as endothelial function, entering into mainstream comprehension with the development of cheap, diagnostic instruments. Table 3.2 summarizes the potential clinical value of endothelial function testing.

Table 3.2 Endothelial function assessment in standard clinical practice. Table adapted from [103].

Clinical significance of endothelial function assessment
Endothelial function integrates the influences of numerous risk factors (hereditary, environmental, lifestyle-related)
Endothelial dysfunction precedes morphological changes in vascular systemic and clinical manifestations of cardiovascular disease – indicating a need for early and effective prevention
Endothelial dysfunction is reversible by healthy lifestyle change or medical therapy
Noninvasive assessment of endothelial dysfunction provides independent prognostic information in various cardiovascular conditions

Chapter 4. Heat Transfer Mechanisms and Tissue Perfusion

The theoretical advantage of thermal perfusion measurement lies in the ability to quantitatively assess absolute blood flow values with a mathematical model of the heat transfer interactions in perfused tissue. To accomplish this, an effective thermal conductivity is determined experimentally which describes the ability of the tissue to conduct heat by both conduction and convection (blood flow). This integrated measure of tissue conductivity simplifies the complex vascular geometries inherent in living tissue. Thermal methods have long been investigated for use as a clinical measurement of tissue perfusion. The attraction to such a method lies in its potential for meeting the high clinical standards of simplicity, patient safety, applicability across all vascular beds, and measurement speed, accuracy, and reproducibility. Few other methods are able to meet all of these clinical requirements.

4.1 Heat Transfer Principles

The relevant modes of heat transfer that occur in living tissue include tissue conduction, metabolic heat generation, storage of thermal energy, convection by microvascular perfusion, and energy absorbed from external sources [227]. Individual contributions from each of these mechanisms leads to a dynamic thermal system – one which is highly complex, heterogeneous in its structure and composition, and capable of maintaining equilibrium on a local and a global scale. Moreover, the skin surface provides an interface between the heat transfer mechanisms of the body and those of the environment. While heat within the body is transferred mainly through conduction and convection, heat transfer in ambient surroundings occurs by conduction, convection, radiation, and evaporation.

Conductive heat flow is governed by Fourier's Law, which relates the time rate of heat transfer, q, to the temperature gradient at the point of interest, ∇T with the equation

$$\overrightarrow{q_c} = -k\nabla T$$

Here, $\vec{q}$ is the heat flux vector (W/m^2) normal to the direction of heat flow, and the negative sign ensures heat flow occurs in the direction of decreasing temperature. The proportionality constant, k, is defined as the intrinsic thermal conductivity, and it is this material property that determines the ability of a material to transfer thermal energy in the steady state. Thermal conductivity may be defined as heat flow density per unit of time for a certain temperature difference and, in biological materials, is often measured in mW/cm·°C.

In a transient state, the conduction heat transfer is described by another Fourier equation:

$$\nabla^2 \mathrm{T} = \frac{1}{\propto}\frac{\partial \mathrm{T}}{\partial \mathrm{t}}$$

which is the partial differential equation that describes the time-dependent temperature distribution within a material. The thermal diffusivity, $\propto$, determines the rate at which heat

diffuses through the body and is dependent on the material's thermal conductivity, density, ρ, and specific heat, c, according to the relationship,

$$\propto = \frac{k}{\rho c}$$

Thus, thermal diffusivity is the material property that measures the ability of a thermally perturbed system to return to steady-state conditions [172]. In biologically active materials, there are complex interactions between tissue conduction, perfusion, and metabolism that contribute to heat transfer processes. To gain an analytical understanding of these processes and derive relevant tissue thermal properties, a mathematical idealization of the physiological circumstances is commonly employed.

The effective thermal conductivity of perfused tissue depends on two modes of heat transfer: conduction and convection. Heat conduction depends on the nature of the tissue and generally remains constant, while heat transfer due to convection depends primarily on blood flow. The three primary conductive components of living tissue are proteins, lipids, and water [228]. The thermal conductivity of both proteins and lipids is approximately 1.8 mW/ cm·°C. Water's conductivity is much higher at about 6.23 mW/cm·°C. Thus, in the absence of blood flow, the thermal conductivity of a tissue depends largely on its water content.

4.2 Thermal Model of Bio-Heat Transfer

The heat transfer interaction between blood in the vascular network and tissue has been a closely studied interaction, as it is critical to many natural physiological processes in the body. However, to model the heat transfer processes is both an intricate and exceedingly difficult undertaking. Tissues in the body are anisotropic and inhomogeneous, while the complex and irregular organization of the vascular system is further complicated by blood flow that varies greatly over time in diverse organs and tissue throughout the body[172]. The most common analytical approach taken to study bio-heat transfer mechanisms is to model the physical or physiological situation in terms of a mathematical idealization that accounts for individual heat transfer effects in the biological system. In terms of perfusion, this often involves accounting for the thermal interaction between microvascular blood flow and the perfused tissue.

The experimental work of Pennes in 1948 [229] led to the development of a bio-heat equation that described the effects of metabolism and blood perfusion on the energy balance within tissue. It was assumed that the capillary bed was the major site of heat exchange between the tissue and blood due its considerable surface area. Therefore, the volumetric rate of heat exchange between blood and tissue, $\dot{q}_{bl}$ (in W/mL), is a function of the volumetric perfusion rate, ω, measured in grams of blood per mL of tissue per second.

$$\dot{q}_{bl} = \omega c_{bl}(T_a - T_m)$$

Here, c_{bl} is the specific heat of blood, T_a is the arterial temperature, and T_m is the tissue medium temperature. It is also assumed that thermal equilibration occurs in the capillary bed such that blood enters the capillaries at the temperature of arterial blood and enters the venous circulation at the temperature of the surrounding tissue. No energy transfer occurs before or after the blood enters the capillaries. Chen and Holmes [230] and Chato [231] have since demonstrated that significant thermal equilibration between blood and perfused tissue occurs prior to reaching the capillaries, between the terminal arterial branches and the precapillary arterioles. However, the Pennes equation still appears valid if larger, "thermally significant" vessels are evaluated separately [227].

Considering a control volume of tissue, we see that the cumulative rate of change of thermal energy stored in the control volume depends on the sum of local heat transfer contributions

$$\begin{bmatrix} rate\ of \\ energy\ storage \end{bmatrix} = \begin{bmatrix} net\ rate\ of \\ energy\ gain \end{bmatrix} + \begin{bmatrix} rate\ of \\ energy\ generation \end{bmatrix}$$

The change in internal thermal energy is directly related to the ability of the tissue medium to store heat by raising its temperature

$$\begin{bmatrix} rate\ of \\ energy\ storage \end{bmatrix} = \frac{\partial}{\partial t}(\rho c T)_m = \rho_m c_m \frac{\partial T_m}{\partial t}$$

Summing the individual heat transfer contributions of transient heat conduction, convection due to perfusion, and energy generated due to tissue metabolism, we have the familiar Pennes bio-heat equation:

$$\rho_m c_m \frac{\partial T_m}{\partial t} = k_m \nabla^2 T_m + \omega c_{bl}(T_a - T_m) + \dot{q}_g$$

There are notable simplifications in the Pennes model, which describes the temperature field in a homogenous biological medium with isotropic thermal properties. The heat balance assumes that local heat generation is a nondirectional property and that blood flow is nondirectional at the capillary level. Additionally, all convective heat exchange occurs in the capillary system, an assumption which is only valid for blood vessels of terminal arterial branches and smaller vessels.

Alternative bio-heat transfer models have been proposed to account for over-simplification in the model proposed by Pennes. All involve a more complex analytical approach and reduced generality for perfusion measurement applications. Seeing as the current Thermal Diffusion Probe follows from the Pennes model, these will not be addressed here. For further background, an in-depth review of the literature on mathematical modeling of bio-heat transfer is presented by Charney [232].

4.3 History of Thermal Tissue Perfusion Measurements

Thermal methods for measurement of tissue perfusion have been pursued by many investigators for over 70 years. The most common approach involves the principle of thermal clearance in which blood flow is derived from the rate of removal of thermal energy from a heated area of underlying tissue. Gibbs [184] was among the first to propose an approximate method for the estimation of perfusion based on heat clearance with a "thermoelectric blood flow recorder." A brief history of the thermal perfusion measurement research performed before 1970 by Von Rein; Hensel, Betz, and Bender; Grayson; and Perl and Hirsch is given by Walsh [207]. Since these initial contributions to the field, significant advances have been made in both instrumentation and developing analytical solutions from more complete equations that describe the tissue energy balance.

The conceptual foundation for most modern techniques of thermal property measurement consists of a system where a heat source that also acts as a temperature sensor is introduced into the specimen and the thermal conductivity is determined based on the transient temperature measurements. Variations on this technique are the heated thermocouple [233-236], or the thermistor probe [237-239]. The embedded thermistor probe technique first used by Chato [238] modeled the probe as a lumped thermal mass and solved the heat diffusion equation in the surrounding medium. The inaccuracies in this technique were later addressed by the improvements to the thermal model by Balasubramaniam and Bowman [237], in which a pair of coupled heat diffusion equations were developed for the interior of the thermistor and the surrounding tissue medium, thus accounting for the thermal gradients within the probe by modeling it as a distributed thermal mass. Using the Pennes bio-heat equation, they were then able to model the effect of perfusion on tissue heat transfer [240]. By determining the power required to maintain a controlled probe temperature increment above the tissue temperature, it was possible to calculate perfusion from the solution to the steady-state perfusion model for the probe and surrounding tissue.

A major contribution towards measurement of absolute blood flow was made by Valvano *et al.* [239]. Using a spherical thermistor embedded at the tip of a flexible catheter, Valvano formulated the closed-form, transient solution for a heated probe in perfused tissue, which led to an algorithm for extracting perfusion from both the steady-state and transient models. Using this probe alongside a radioactive microsphere technique in an *ex vivo* rat liver model, Valvano showed that absolute perfusion could be measured with an accuracy of about 10% over the perfusion range of 60 to 200 ml/min·100g.

After substantial development and testing of the thermistor probe technique, Bowman and colleagues created a commercial device for minimally invasive measurements of tissue thermal properties and perfusion. The Thermal Diffusion Probe has been progressively refined over the past three decades and has been validated against XeCT, Doppler flowmetry, H_2 clearance, and the radioactive microsphere technique [8, 241-243]. It has also been applied clinically in brain

surgery [8], reconstructive surgery [5], transplantation [7, 242], and other fields of medicine desiring a continuous monitor of absolute blood flow in small volumes of tissue (30-100 μL). After obtaining FDA regulatory approval in 2002, the Bowman Perfusion Monitor, developed by Hemedex, Inc., has introduced the invasive TDP into clinical settings for routine perfusion monitoring in real-time and absolute units.

Another transient technique for quantifying perfusion has been presented as an alternative to the step temperature rise model. The Temperature Pulse Decay (TPD) method is a transient thermal technique based on the introduction of a brief pulse of heat from a point source and the subsequent perfusion-dependent temperature decay. First reported by Chen and Holmes [244], this analytical method relates the measured temperature decay following a short, computer-controlled heat pulse through a small thermistor bead to a theoretical temperature decay, which is also based on the Pennes bio-heat equation [245]. The limitations of this technique restricted its further development, as the small heating element was only able to interrogate a small volume of tissue. The TPD method was further hampered by an unacceptably low sensitivity to perfusion changes.

The ability to measure living tissue thermal properties has been both a challenge and an active area of intense research. Living tissues depart from ideal engineering geometries, compositions and boundary conditions. Furthermore, they must be studied in vivo to obtain accurate measurements, as tissue thermal properties greatly depend on blood flow and water content. Generally, the measurement of tissue thermal properties is performed via insertion of a thermal probe into the biological specimen, often causing significant disturbance in the normal physiological state of the tissue. In living organisms, this may cause obvious pain and discomfort. Drawing on the knowledge gained from this extensive field of research, I will present my investigation into developing a noninvasive thermal technique for measuring thermal conductivity, diffusivity, and local blood perfusion in the skin in Chapters 5 and 6.

Chapter 5. Noninvasive Application of the TDP Probe

5.1 The Invasive Perfusion Probe: Design and Operation

5.1.1 Design

In contrast to the original thermal perfusion probe design by Balasubramaniam and Bowman [237], the minimally invasive thermal diffusion probe (TDP) consists of two thermistors: a distal, "heat" thermistor; and a proximal, "sense" thermistor (Figure 5.1). The addition of the sense thermistor allows the quantification of perfusion using the thermal technique in tissues where the temperature is varying over wide ranges. The two thermistors are contained at the end of a flexible catheter that can be inserted into the perfused tissue of interest. The probe is connected to an electronic monitor by an umbilical cord, where the data collection, storage, processing, and display is controlled by an on-board microprocessor.

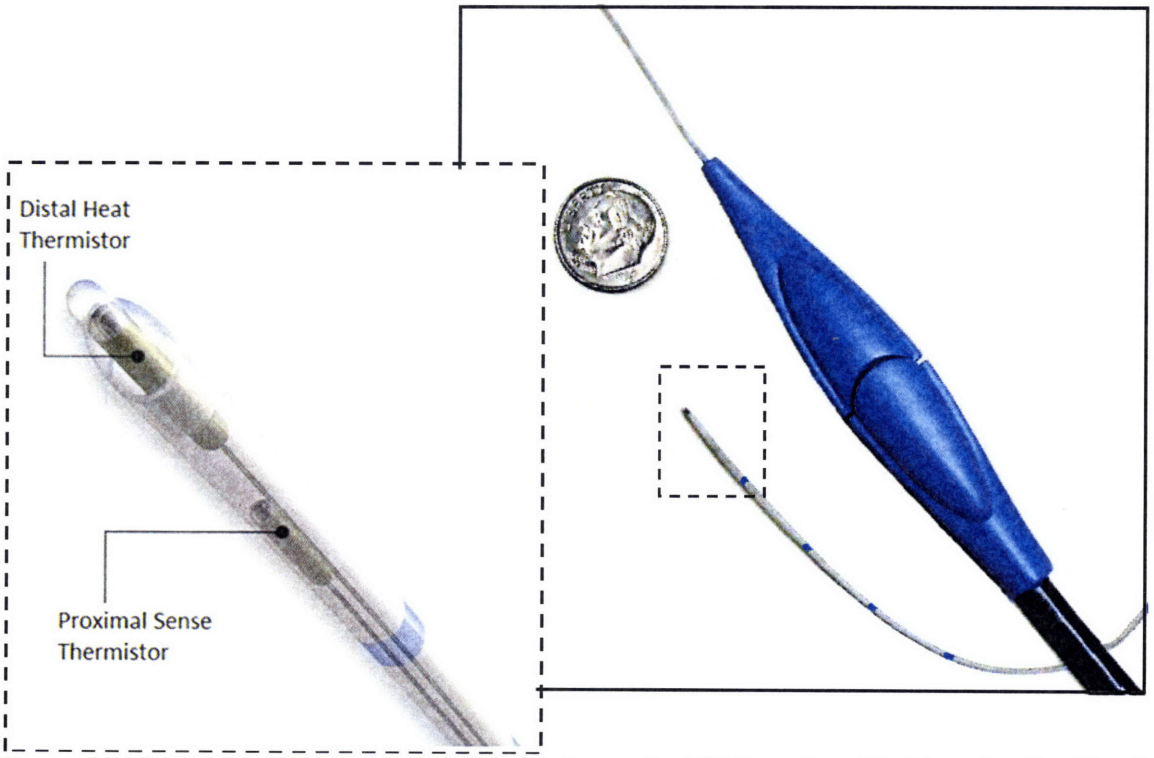

Figure 5.1 The minimally invasive thermal diffusion probe (TDP) produced by Hemedex, Inc. [246]

To measure perfusion, the probe must measure a stable baseline (initial) tissue temperature, T_i. The distal thermistor is then self-heated to a constant temperature slightly above the tissue baseline temperature – usually an increment of about 2°C. The difference between the volume-averaged probe temperature and T_i is defined as ΔT_b (Figure 5.2). While the ΔT_b is established almost instantaneously within the thermistor, the power, P, required to establish and maintain

this temperature takes a very large initial value and then falls over time to a steady state value. The proximal thermistor is located outside of the heated field and passively monitors tissue baseline temperature, compensating for transient temperature fluctuations. The power dissipated in the distal thermistor by resistive heating is related to the tissue's ability to carry thermal energy by both thermal conduction within the tissue ($\overrightarrow{q_c}$) and by thermal convection due to local perfusion blood flow ($\dot{q}_{bl}$). With this information, the probe-tissue heat transfer equations can be solved continuously to provide real-time perfusion data.

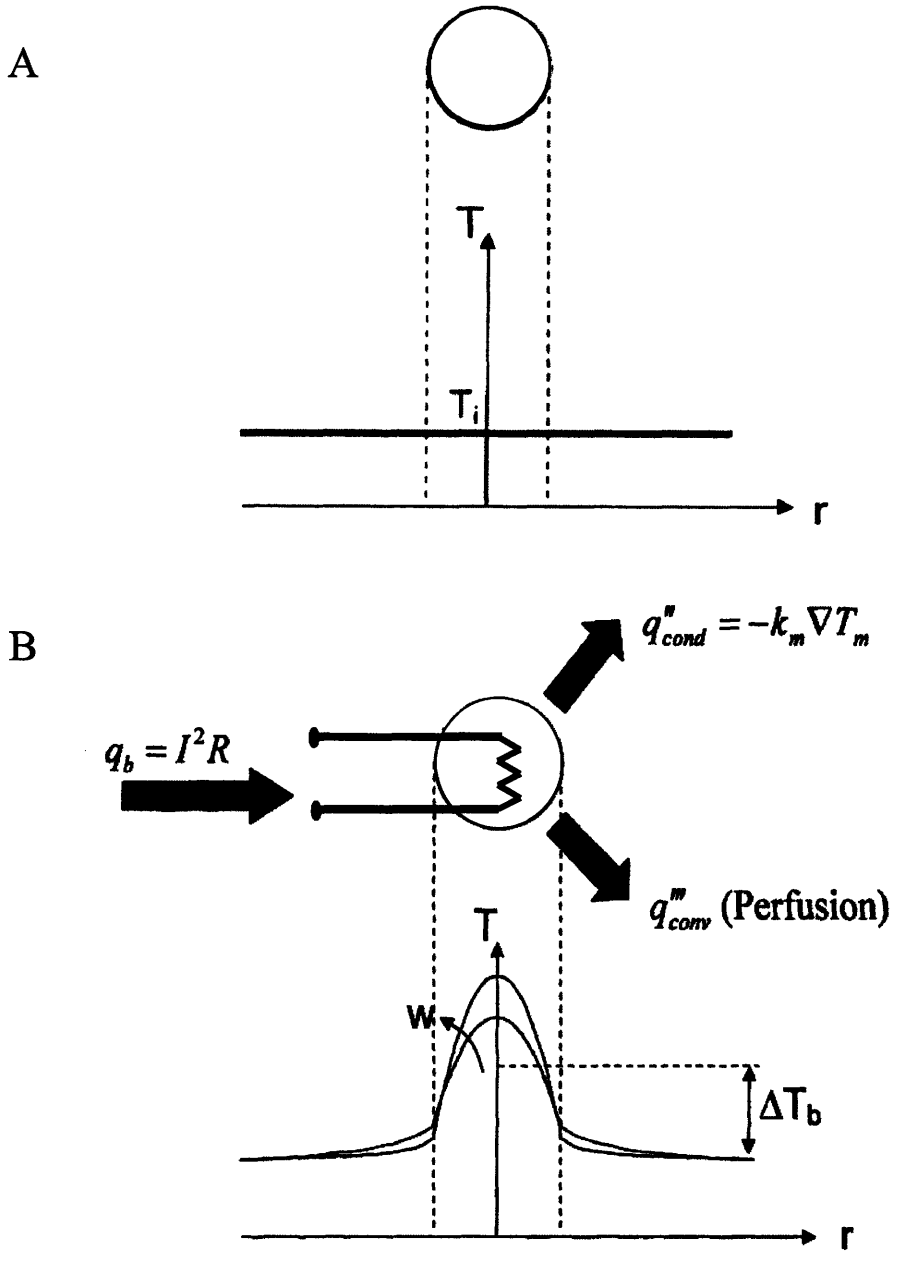

Figure 5.2 Temperature profile of the thermistor probe and tissue before and after heating. (A) Before heating. (B) After heating, at two different levels of perfusion. k_m= tissue thermal conductivity; I= current; R=thermistor probe resistance

The thermal interaction between the perfusion sensor and tissue is described by a coupled set of partial differential equations such that the thermal response of the sensor is described by the heat diffusion equation and the response of the tissue is described by the bio-heat transfer equation. . The solution for the temperature distribution in the heat thermistor and in the affected tissue is necessary to extract perfusion and is derived from the following coupled, differential equations:

$$\frac{1}{\alpha_m}\frac{\partial T_m}{\partial t} = \nabla^2 T_m - \frac{\omega \rho_{bl} c_{bl}}{k_m} T_m \text{ in the tissue}$$

and

$$\frac{1}{\alpha_b}\frac{\partial T_b}{\partial t} = \nabla^2 T_b - \frac{1}{k_b}\frac{P}{V} \text{ in the probe}$$

Here, T_m is the temperature elevation of tissue medium above the baseline; k_m is the tissue intrinsic thermal conductivity; $\alpha_m$is the tissue intrinsic thermal diffusivity; ω is the local perfusion rate; ρ_{bl} is the blood density; c_{bl} is the blood specific heat; T_b is the temperature elevation in the sensor; α_b is the sensor thermal diffusivity; k_b is the sensor thermal conductivity; P is power dissipation and V is the sensor volume. The last term in the probe heat diffusion equation represents the volumetric heat generation in the probe by resistive heating. Metabolic heat generation is implicit in this model as a heat source which maintains the baseline temperature.

The solution for the time-dependent probe-tissue temperature response in the presence of perfusion was solved for by Valvano *et al.* [239] using a term-by-term Laplace transform, converting the second-order system of partial differential equations into a second-order system of ordinary differential equations. The heated thermistor is modeled as a uniformly heated sphere, with perfect thermal contact between the probe and the tissue. It is assumed that power is uniformly distributed throughout the thermistor bead to maintain constant mean volumetric temperature. The boundary conditions require that temperature everywhere is bounded, continuity of temperature and heat flux is maintained at the tissue-thermistor interface and that temperature elevation approaches zero at infinity.

In the case of the spherical invasive sensor operated in constant mean temperature mode, the model solution for probe power dissipation, P, as a function of the perfusion and intrinsic properties is:

$$\frac{P}{4\pi a k_m \Delta T} = \frac{1}{\frac{k_m}{5k_b} + \frac{1}{1+\lambda a}}\left[1 + \frac{\frac{a}{\sqrt{\pi \alpha_m}} f(t)}{\frac{k_m}{5k_b} + 1 + \lambda a}\right]$$

where

$$f(t) = \frac{e^{-\lambda^2 \propto_m t}}{\sqrt{t}} - \sqrt{\pi\lambda^2 \propto_m} \operatorname{erfc}\left(\lambda a \sqrt{\frac{\propto_m t}{a^2}}\right)$$

and

$$\lambda = \sqrt{\frac{\omega \rho_{bl} c_{bl}}{k_m}}$$

Here, a is the thermistor radius and ΔT is the sensor mean temperature rise above the baseline. In the absence of a way to calculate tissue intrinsic conductivity in the presence of perfusion, the intrinsic conductivity and the convective effects of perfusion can be determined in a no-flow situation. However, this is not practical in clinical environments.

To account for any deviations from the model, the sensor thermal conductivity (k_b) and the sensor radius (a) are calibrated as constants for each individual sensor using measurements made in media with known thermal properties. The monitor collects data on the power dissipated (P) and the mean sensor temperature rise above baseline (ΔT). Therefore, the unknown variables are the tissue intrinsic thermal conductivity (k_m), the tissue thermal diffusivity ($\propto_m$) and the tissue perfusion (ω). A significant advantage of the TDP method is the lack of a no-flow calibration requirement to determine k_m. Instead, a series of algorithms are employed to extract the conductive tissue properties from the initial rate of propagation of the thermal field as a function of P and ΔT [239]. This component is separated from the total heat transfer to determine the thermal convection component. With this method, perfusion, ω, is not explicitly solved for, but rather is solved in an iterative fashion.

5.1.2 Calibration

A thermistor is a temperature dependent resistor. Those used for thermal property measurements have a negative temperature coefficient of resistance, indicating that their resistance will decrease when their temperature is increased. Being resistive devices, a thermistor will also heat when a current is passed through it. Both phenomena are exploited in the thermistor based method for thermal property measurement. The thermistor is used both as a temperature sensor and as a point heating source.

The calibration of a thermistor probe is a two-step process. The first step involves characterizing the resistance-temperature relationship, while the second step defines the heat transfer properties of the thermistor.

R-T Curve

The relationship between temperature and resistance is non-linear and is usually described by the empirical Steinhart-Hart equation:

$$\frac{1}{T} = C_1 + C_2 \ln R + C_3 (\ln R)^3$$

where T is the absolute temperature in Kelvin and R is the thermistor resistance in ohms. The terms C_1, C_2, and C_3 are empirically determined calibration coefficients. Thus, an experimental set of data relating temperature and resistance in each thermistor is fit with a regression curve to determine the calibration coefficients. The TDP thermistor probes are calibrated for temperature following assembly using a platinum-resistance thermometer (from 25°C to 46°C). Using the Steinhart-Hart relation, thermistors in the TDP are routinely calibrated to a resolution of 0.001°C.

Heat Transfer Properties: k_b and a

The thermal conductivity and geometry of the thermistors must also be determined to accurately model the heat transfer process. For a thermistor, the thermal conductivity (k_b) and the sensor radius (a) are both determined by calibration in media of known thermal conductivities which approximate the range of conductivities in biological tissue. Repeated, simulated perfusion measurements are made within each media. This calibration is conducted in a constant temperature bath and accounts for the sensor-to-sensor variability in resistance at a certain temperature.

To allow for parallel production of the Thermal Diffusion Probes in appropriate quantities, the calibration procedure is conducted in a semi-automatic, batch-wise process. Calibration values are specific to individual probes. These are written to an EEPROM (Electronically Eraseable Programmable Read-Only Memory) contained within the probe connector. The memory chip also identifies each probe with a unique serial number that is associated with its calibration data.

5.2 Adapting Invasive Probe for Noninvasive Measurement

5.2.1 Sensor Placement

Previous informal studies have shown that the skin of the fingertip is an appropriate location for measurement of perfusion and vasomotor activity with the thermal probe [247]. The palmar side of the hand was used for most investigations and testing confirmed that the distal phalanx of the finger (digit) exhibits a higher degree of signal detection (see Figure 5.3). This area of the finger also has a high capillary density. It is also reasonable to choose the most distal part of the digit, as it is very sensitive to changes in global blood flow distribution. For measurement of reactive hyperemia, the digit is also an appropriate location since the sensor must be placed on the skin surface distal to a blood pressure cuff challenge of the upper arm. Alternative methods for noninvasive determination of endothelial dysfunction have often chosen to measure indices of finger perfusion during reactive hyperemia. These include the previously discussed methods for determining reactivity of finger blood flow by measuring peripheral arterial tone or digital temperature.

Other practical considerations also influence the optimal placement of the thermal sensor. Surfaces with fewer sweat glands are preferred since sweating can lead to artifacts caused by evaporative cooling. Sweating can also progressively change the thermal conductivity during a measurement period, which leads to perfusion artifacts. The sensor attachment site must not be artificially warmed or cooled by other parts of the body, objects, or external influences. These include changes due to temperature variations not resulting from vasoconstriction or vasodilation, such as room temperature fluctuations, air currents, change in sensor location or contact, etc. Due to the small thermal mass of the fingertip, special care must be taken to keep environmental conditions constant and reduce movement or temperature variations.

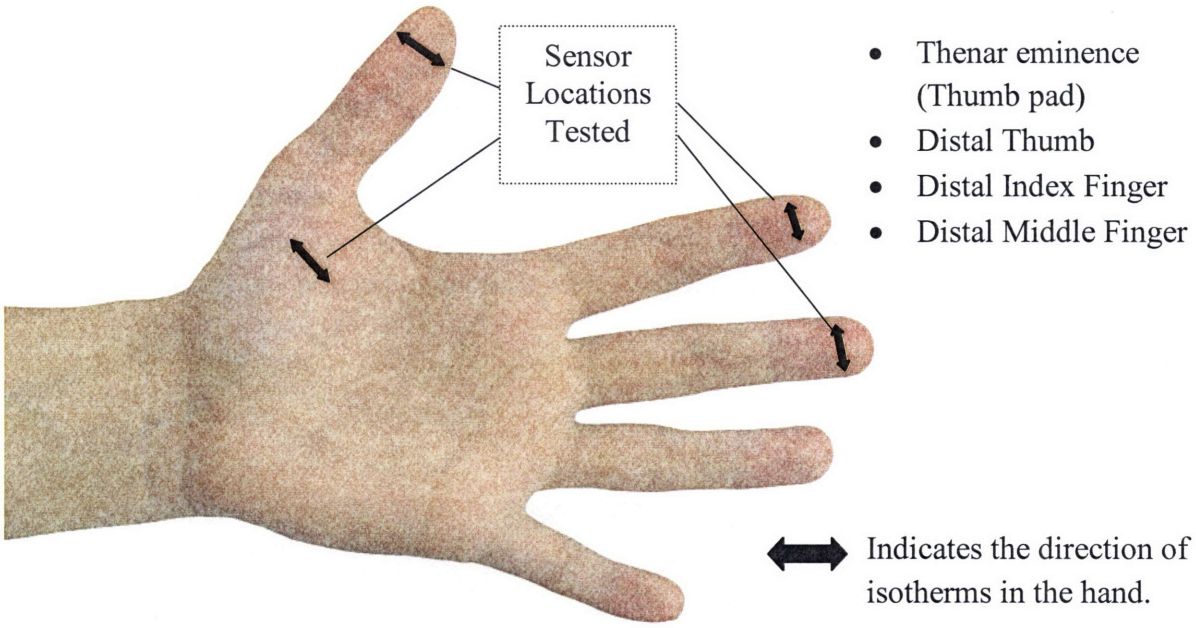

Figure 5.3 Noninvasive sensor measurement locations on palmar face of hand

5.2.2 Sensor-Tissue Surface Geometry

The invasive thermistor probes are designed and calibrated for use in a 4π geometry in which the tissue medium completely surrounds the spherical probe. When applied to surface measurements on skin tissue, the probe (or sensor) takes on a hemispherical, 2π contact surface geometry with the tissue. Therefore, it is reasonable to suspect that the heat transfer properties of the probe for surface measurements differ from those for invasive measurements. It also becomes important to ensure that the same amount of surface area is exposed to tissue for heat transfer to maintain consistent measurement environment conditions. For all surface measurements, a thick foam tape was used to cover the thermistors and create an adiabatic environment (see Figure 5.4).

5.2.3 Contact Pressure

To achieve the appropriate thermal interface which ensures good thermal communication, a suitable contact pressure must be applied to the sensor. However, significant changes in the perfusion of skin occur when this pressure exceeds the sum of the tissue's biomechanical compressive strength and the pressure for capillary collapse. Preliminary testing by G. Martin at Thermal Technologies, where the current Bowman Perfusion Monitor technology was developed, has addressed the issue of appropriate contact pressure in skin.

To define the requirements for the sensor-tissue interface, an invasive TDP was placed in contact with the forearm skin of a volunteer. Relative perfusion was measured as a function of the applied sensor pressure based on various weights placed over a defined sensor contact area. Relative perfusion changes were also assessed with progressive displacement of a sensor into the skin tissue, starting from the skin surface. The results showed that contact pressures greater than about 0.5 mmHg result in significant decreases in relative perfusion. A sensor displacement greater than 1.5 mm from the skin surface also results in a progressive drop in (relative) perfusion. Martin noted that a peak in the relative perfusion was found with a sensor displacement of approximately 0.6 mm, which may represent the sensor contact conditions most suitable to optimize the balance between adequate thermal communication and uncompromised perfusion.

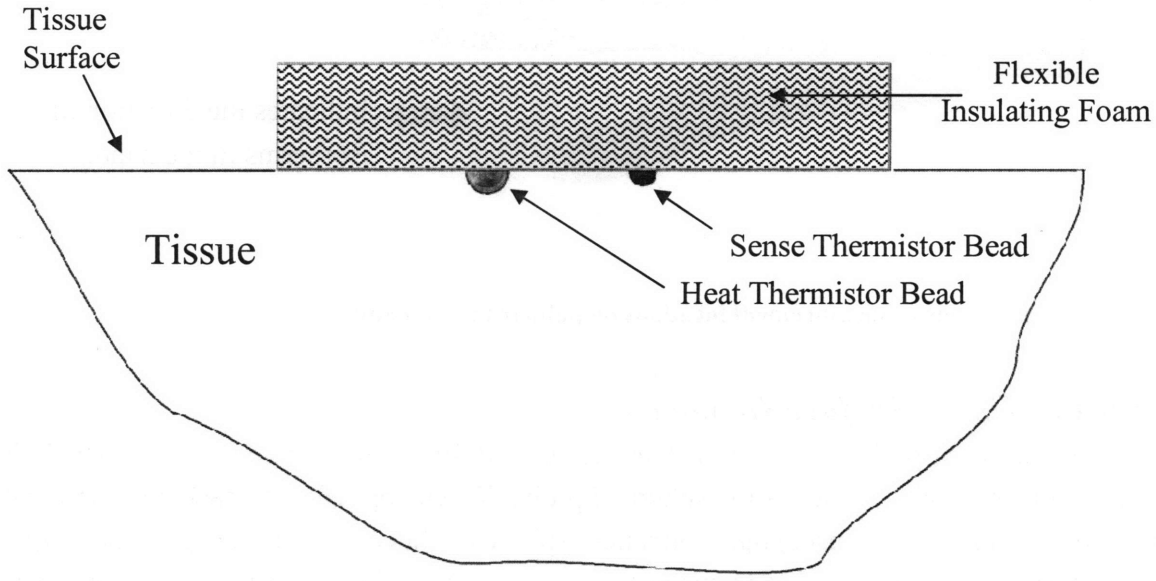

Figure 5.4 Schematic cross-section of exposed thermistors in TDP resting on surface of tissue. The thermistors are insulated from the environment with a thick foam pad adherant to the skin.

5.2.4 Exposed Thermistor Beads

A modification of the invasive TDP construction was made to adapt the sensor for measurement at the skin surface. The thermistor beads are typically contained within a thin flexible catheter to enable simple insertion into soft tissue. However, this is unnecessary for a surface application and adds unnecessary bulk to the sensor, which may affect contact pressure and depth of tissue compression. By exposing the thermistor beads, preliminary measurements can be made to determine the most appropriate method of applying the sensor to the skin (see Figure 5.5). There is also the added advantage of tighter coupling between the sense thermistor and baseline skin temperature, which is much more prone to variation at the skin surface than within soft tissue. Note that the heated thermistor is slightly larger than the sense thermistor in the TDP. The exact dimensions will be discussed in Chapter 6.

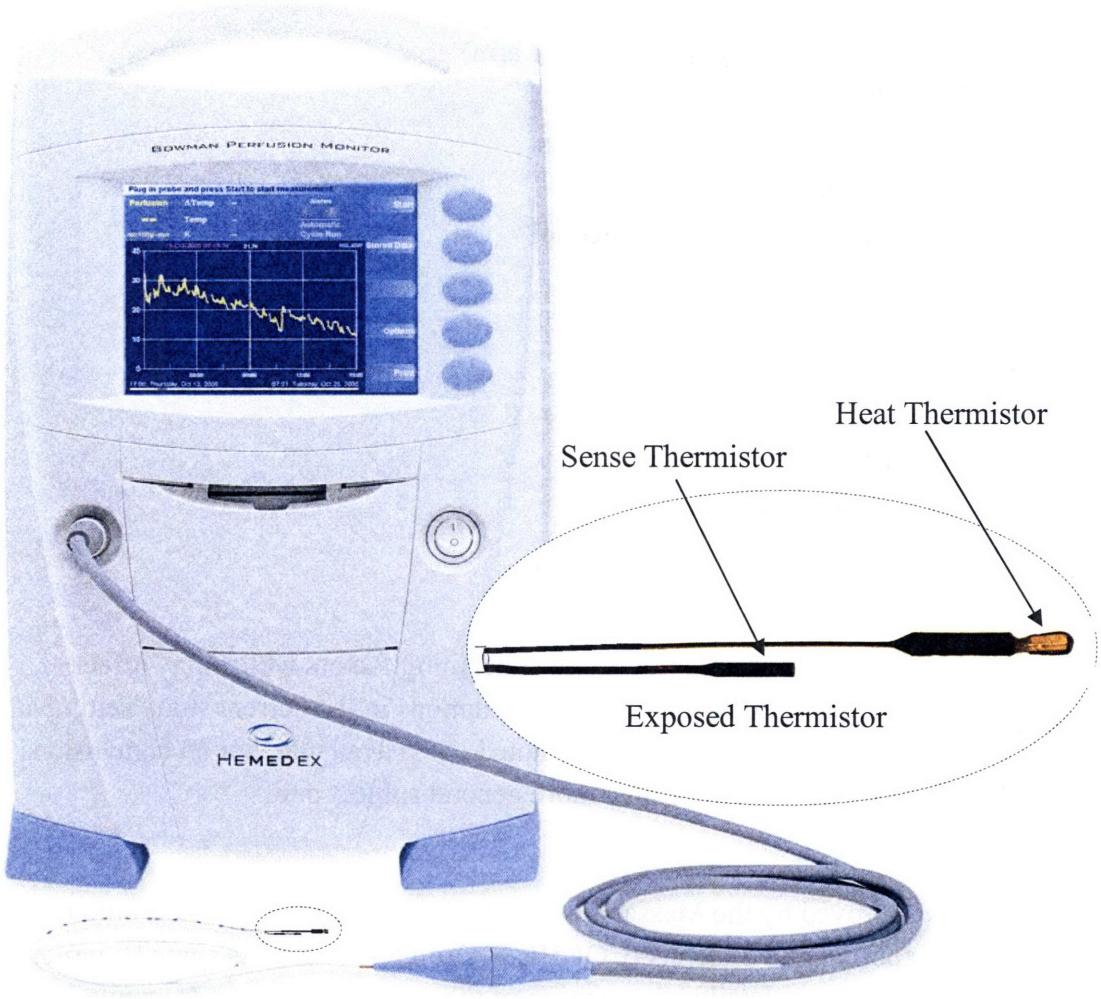

Figure 5.5 Bowman Perfusion Monitor and modified thermal diffusion probe (TDP) for noninvasive application. The thermistors in the TDP are exposed to reveal the heat and sense thermistors. Perfusion and temperature data are processed and stored in the Perfusion Monitor.

5.3 Measurement Protocol: Post-Ischemic Reactive Hyperemia (PORH)

5.3.1 Experimental Considerations

The measurement protocol for post-occlusive reactive hyperemia (PORH) is poorly standardized for measurements of brachial artery diameter during flow-mediated dilatation and even more so for the assessment of skin microvascular reactivity using laser Doppler flowmetry. Individual variables, intra- and inter-individual variation, and environment-related variables can greatly influence vascular measurements. Several conditions have been identified as being important considerations for an experiment employing thermal perfusion measurement [27, 143, 248]. In a clinical study, care should be taken to control for each of these factors and data should be kept regarding any variations:

- Subject age, gender
- Time of the day when testing is performed
- Location of the occlusion cuff (upper vs. lower arm)
- Duration of the occlusion
- Length of withholding vasoactive medications
- Prior food intake (fasting)
- Consumption of nicotine, caffeine, and alcohol
- Phase of menstrual cycle, if appropriate
- Physical and mental activity
- Probe pressure on skin
- Skin temperature
- Ambient temperature, noise, humidity
- Subject position (sitting or supine)
- Anatomical site of measurement
- Length of stabilization period

These are provided to address the current knowledge concerning factors which may affect perfusion response during a test of PORH. Due to the limitations in the current study setting and population, the observed effects of various factors is noted when available, but no conclusions can be drawn regarding their relative impact in a more general subject pool.

5.3.2 Protocol

The study protocol was approved by the Massachusetts Institute of Technology Committee on the Use of Humans as Experimental Subjects (COUHES). Volunteer subjects signed a written informed consent after receiving a detailed description of the study protocol, instrumentation, its benefits and risks. The subjects then completed a questionnaire detailing their cardiovascular risk factors, prior history of cardiovascular and other vascular diseases, and present medications. Relevant health information was noted, including diagnosed coronary artery disease, hypertension, hypercholesterolemia, peripheral arterial disease, or diabetes, as well as history of

myocardial infarction or stroke. As smoking has been identified as one of the factors influencing basal skin perfusion and PORH responses [249], subjects were asked to report if they smoked cigarettes.

Study conditions were standardized to minimize operator and subject variability. All investigations were performed by an experienced research study operator. Subjects refrained from eating, smoking, or drinking alcoholic or caffeinated beverages for the 4 hours prior to the study. They were asked to refrain from ingesting any vasoactive medications for 24 hours before the study, if possible.

All measurements were conducted in a quiet, temperature-controlled room at neutral room temperature (22-24°C). Subjects were asked to lie in a comfortable supine position with their experimental arm resting in a stable position at heart-level. Blood pressure was measured in the contralateral arm after a period of acclimatization. A sphygmomanometer occlusion cuff was placed around the upper arm of the experimental arm at a position 1-2 cm above the antecubital crease, while the modified Thermal Diffusion Probe was placed on the skin of the distal phalanx of the middle finger. In some cases, the thumb, index finger, or thumb pad (thenar eminence) were used and noted (see Figure 5.3). Standard ultrasound gel was applied to the sensor-skin interface to enhance thermal communication. The sensor was then covered with a piece of flexible insulating foam tape (3M, St. Paul, MN) with a non-irritating adhesive that held the sensor comfortably and securely next to the skin. A light cloth was wrapped around the hand and forearm to insulate the hand from air currents or transient temperature changes. The hand was then stabilized to prevent any subject discomfort or movement. Since the sensor is sensitive to changes in position and orientation relative to the skin surface, any finger, hand or arm motions can cause perfusion measurement artifacts and/or corruption of subsequent data.

A typical study sequence was conducted according to the procedure outlined in Figures 5.6 and 5.7. Since the TDP must reach temperature stability before perfusion measurement begins, there is an initial temperature equilibration phase before perfusion calibration. The temperature stability criterion for this study was a temperature change of not more than 0.001°C in 10 seconds. After the subsequent calibration period, a baseline perfusion measurement was recorded for at least 5 minutes. Then, the cuff was then quickly inflated to a suprasystolic pressure (at least 50 mmHg above systolic pressure) to occlude blood flow to the hand. The occlusion pressure was maintained for 4 minutes before rapid cuff deflation. The measurement was continued for approximately 5-15 minutes to allow for perfusion to return to baseline values.

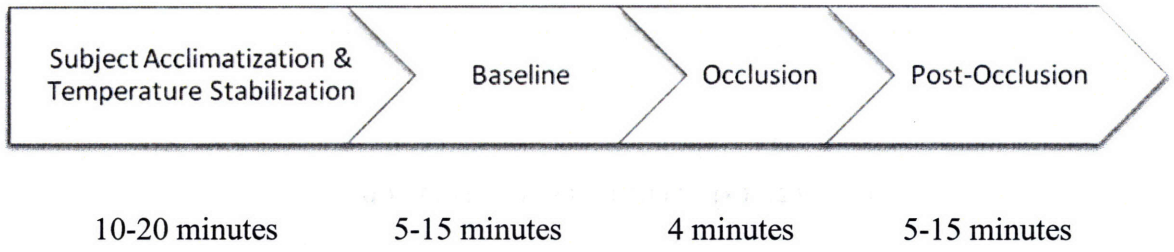

Figure 5.6 Outline of PORH test procedure

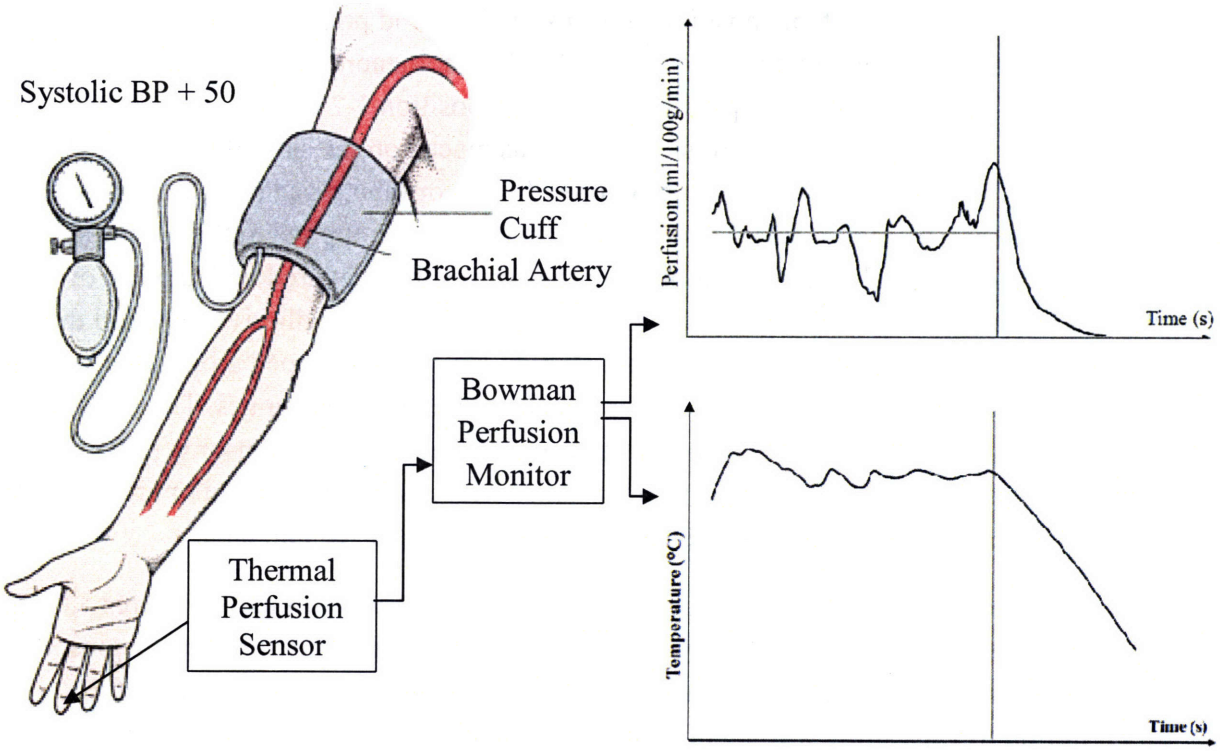

Figure 5.7 Perfusion and temperature are measured during an occlusive challenge to the arm

5.4 Measurement Issues

During data collection, several deviations from an ideal perfusion measurement were apparent. Some could be traced to the shortfalls inherent in the invasive thermal model for surface measurements using these simplified conditions. The major measurement issues were identified as follows:

5.4.1 Motion Artifacts

In operation, the imposition of the temperature step, ΔT, results in the development of a thermal field in the skin tissue around the heated probe tip. If the sensor moves relative to the tissue, the field is no longer fully developed for the new sensor location. This results in a power spike proportional to the distance moved, which creates an artifactual increase in perfusion and non-physiological spikes in the perfusion data (see Figure 5.8).

The invasive probe uses a data processing algorithm to detect motion artifacts and take appropriate action depending on the magnitude of the artifact. If the rate of change of perfusion or power is greater than a specified, physiological threshold, an automatic recalibration to determine the thermal conditions in the new location is conducted *in situ*. For invasive measurements in relatively homogeneous tissue, the perfusion is relatively constant throughout the tissue and the recalibrated perfusion values typically match pre-artifact values. The contact geometry between the probe and the tissue usually remains constant as well for the spherical thermistor embedded in the tissue. However, skin tissue perfusion is often much more heterogeneous across a small surface area. Small perturbations will often lead to a much different post-calibration perfusion measurement, either from relocation of the measurement site or distorted contact geometry.

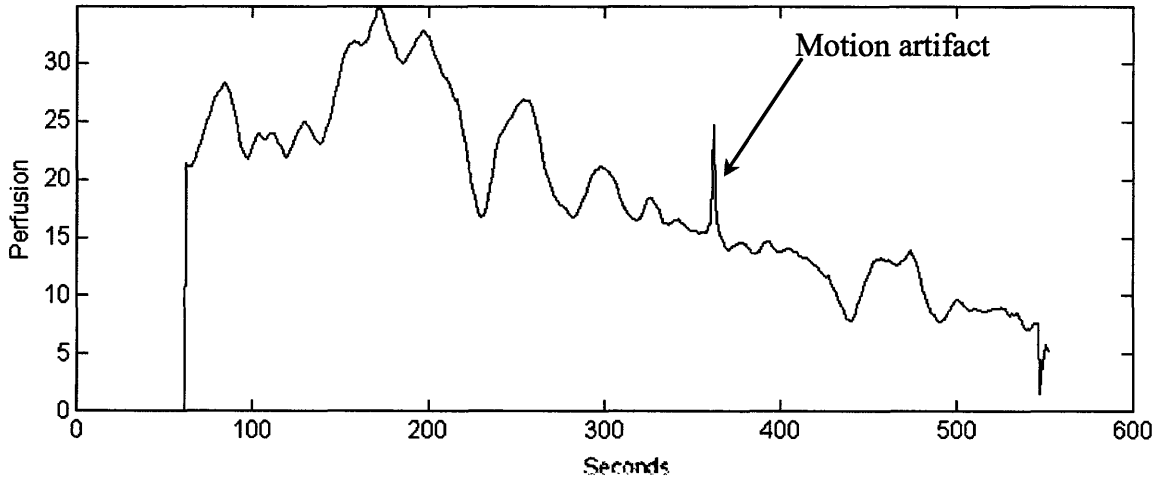

Figure 5.8 Motion artifact during perfusion measurement

5.4.2 Sensor-Surface Tissue Contact

The concept of the TDP technique for measuring thermal conductivity is based on the assumption that a known heat generated within a calibrated probe is transferred to a tissue medium where it is dissipated by conduction and convection effects. the thermal contact between the thermistor and the tissue is assumed to be theoretically perfect (i.e. no thermal contact resistance), which is nearly impossible for skin surface measurements. A spherical thermistor on the skin surface can only interrogate tissue along a hemispherical profile. On fingers, this contact surface is covered with uneven ridges, known as dermal papillae, which comprise a person's fingerprint. Microscopic pockets of air can form in the spaces between the ridges and compromise the effectiveness and reproducibility of heat transfer.

An attempt was made to decrease the effect of skin surface irregularities by wetting the surface of the skin with ultrasound transmission gel, which is routinely used to couple an ultrasound transducer with the skin and provide an acoustic pathway. Just as it is used in ultrasound to eliminate air from the interface and adapt to the contours of the skin, transmission gel was used to increase thermal communication between the sensor and the skin. However, the consistency of contact geometry is still a large source of variability. As will be discussed in Chapter 6, the use of a sensor housing that maintains constant contact pressure and interface geometry could increase the consistency of surface heat transfer.

5.4.3 Undetectable Baseline Perfusion

In some instances, the sensor would measure a perfusion value of zero. Small perturbations of the sensor (pressing on the foam insulator, moving the finger) would cause temporary increases in perfusion, indicating that the sensor was inappropriately applied to the skin or the thermal communication was not optimal (see Figure 5.9). In some of these cases, basal perfusion may have also been low in the subject's skin, such as in people with colder hands.

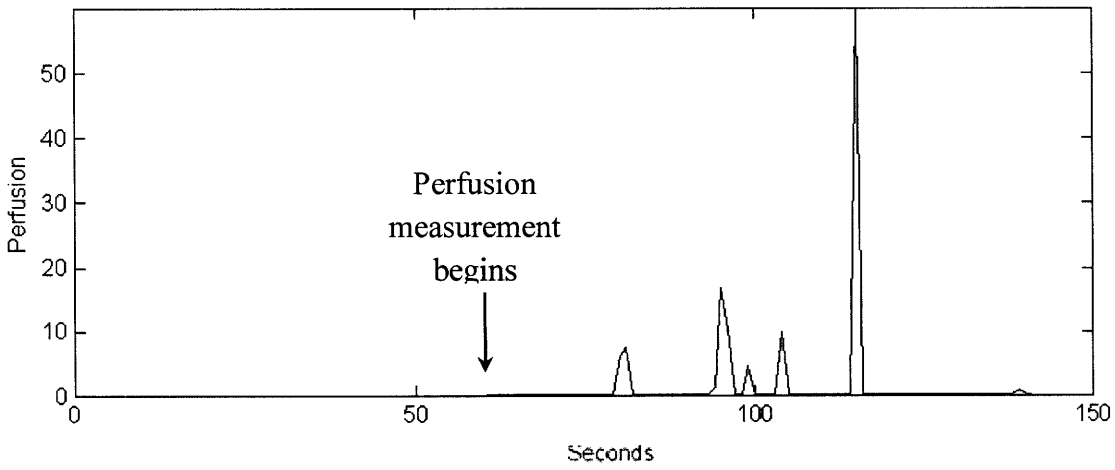

Figure 5.9 Baseline measurement is undetectable. Pressing on the probe causes perfusion spikes.

5.4.4 Non-zero Perfusion During Occlusion

During tests of reactive hyperemia, it is expected that perfusion will decrease to zero during occlusion (see Figure 5.10A). In many cases, this did not occur; instead, perfusion would decrease to a fairly constant non-zero value after blood flow was occluded (see Figure 5.10B). Also, perfusion would sometimes drop to what would seem to be a negative value based on the shape of the temperature cool-down curve at the level of zero perfusion (see Figure 5.10C). The perfusion monitor does not measure perfusion below zero. In any case, the subsequent reactive hyperemia still exceeded baseline perfusion values and it is clear from the sample data that perfusion fluctuations over time are well-tracked by the sensor. Furthermore, the magnitude of measured perfusion is quite close to expected perfusion values, which are statistically on the order of 20 ml/100g·min in a thermoneutral environment. The deviations from expected values can occur from non-ideal contact between the sensor and the skin, such that the actual measurement deviates from the assumed thermal model conditions. The thermal environment of the skin can also change over the course of a measurement (spatially or otherwise), shifting the perfusion values up or down.

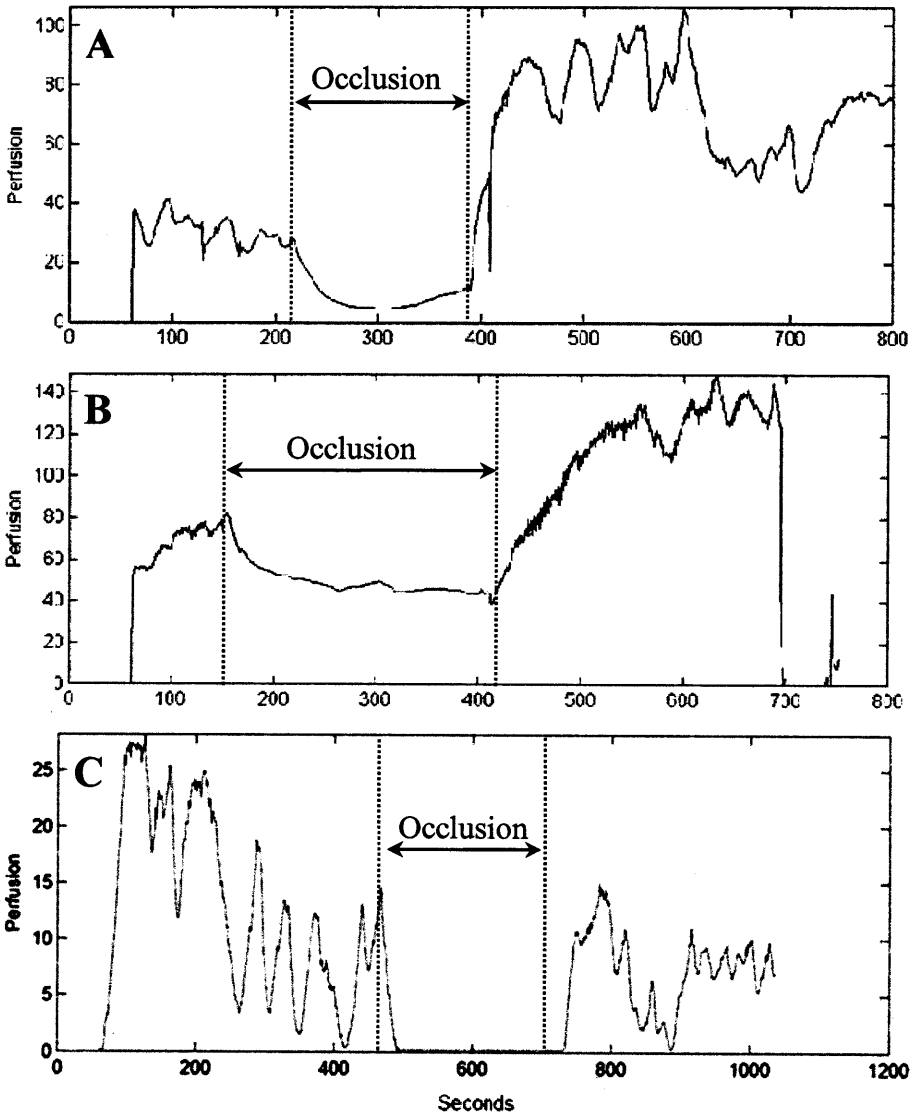

Figure 5.10 Perfusion during occlusion does not reflect absolute zero flow (no flow). Occlusion during PORH should establish a no-flow state. Instead, (A) shows a perfusion measurement with a occluded flow value close to zero. (B) depicts a positive shift in expected value of perfusion during occlusion. A negative value of perfusion is extrapolated from the perfusion measurement in (C).

5.5 Physiological Issues

5.5.1 Baseline Temperature Fluctuations

A major source of measurement uncertainty occurs from wide variations in baseline skin temperature. Unlike environments in which the sensor is completely enclosed in tissue with significant thermal stability, skin temperature undergoes dynamic fluctuations in time due to its role in thermoregulation and is often influenced by a combination of internal and external factors. In addition to heat conduction from underlying subcutaneous structures, blood convection warms the skin by transfer of heat from the core. This heat transfer process is due to perfusion and plays the most influential part in determining overall skin temperature. However, the skin will also constantly lose heat to the environment by radiation, convection, conduction, and evaporative cooling. These changes are most pronounced in the extremities where AVA are present. Therefore, it is critical that the conditions under which skin temperature is measured and used to approximate blood flow are as closely controlled and defined as possible. External influences (e.g. changes in room temperature, contact with other surfaces, air currents) should be kept to a minimum to ensure skin temperature changes reflect physiological phenomena.

Baseline temperature fluctuations occur even in thermally stable environments due to intrinsic oscillations in skin perfusion (see discussion in Section 2.3). Moreover, the heterogeneous nature of skin surface tissue is manifest in both its vascular structure as well as its seemingly random spatial pattern of perfusion. Thus, temperature varies not only with respect to time, but also with respect to location. This poses a considerable challenge for the accurate calculation of perfusion since an experimental value of intrinsic thermal conductivity is determined from the initial propagation of the thermal field based on applied power, P, and the temperature step, ΔT. This temperature step is the difference between the initial baseline tissue temperature, T_i and the volume average temperature of the heat thermistor. Once the ΔT is established, tissue temperature is monitored by the sense bead and the subsequent perfusion signal is calculated based on this value. If the temperature gradient between the heat and the sense thermistors changes such that the baseline temperature (at the sense location) is no longer a true surrogate representation of the basal temperature at the location of the heat thermistor, this change in gradient will lead to a .... in the calculated perfusion value.

Figure 5.11 shows a segment of perfusion and temperature data in which large fluctuations in perfusion are evident in the perfusion signal. When compared with the temperature measurement over the same time window, it is clear that the two are correlated. Temperature is clearly a function of the skin perfusion over time and these changes can be closely monitored by the preliminary noninvasive sensor.

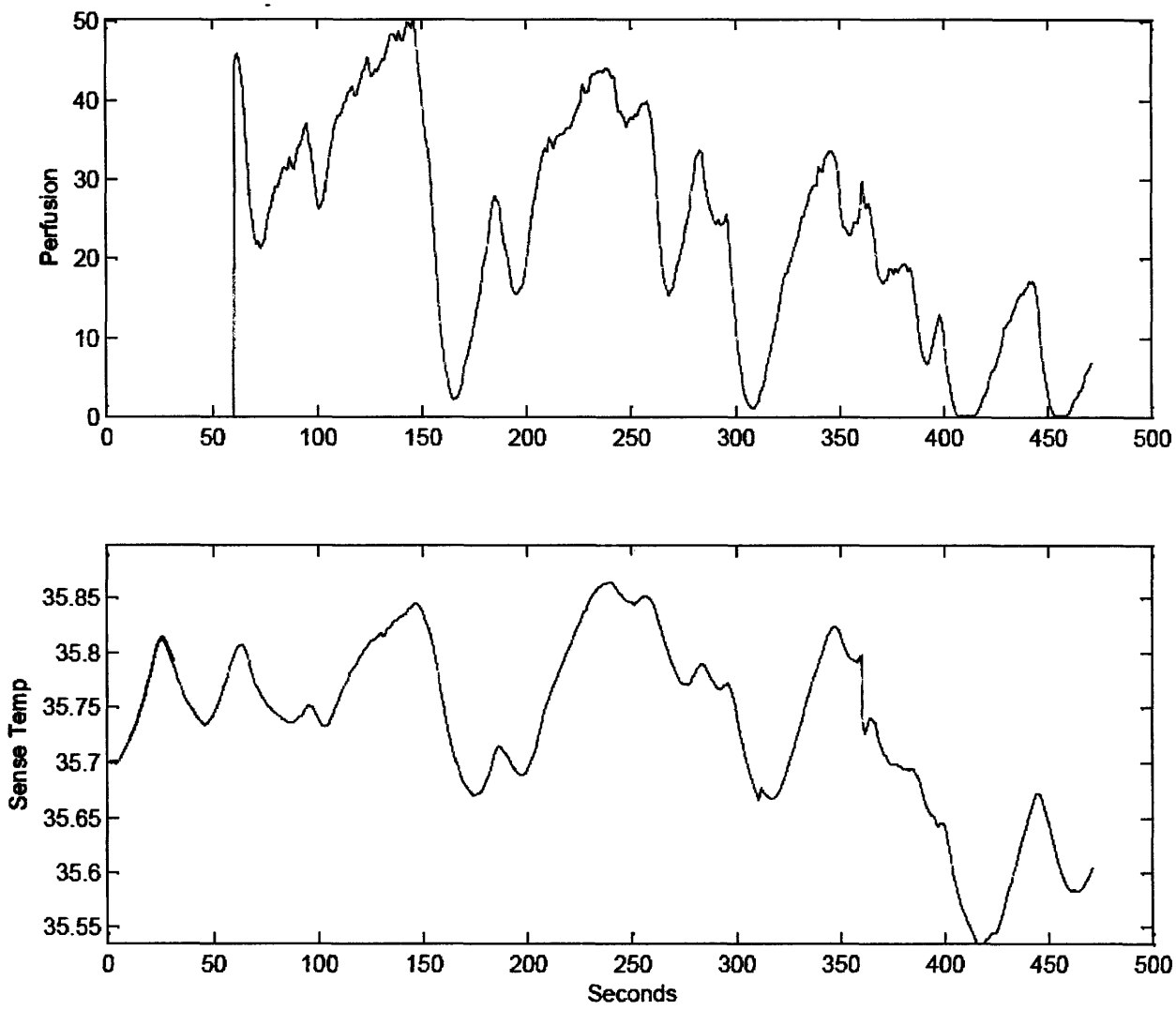

Figure 5.11 Temperature fluctuations in resting skin perfusion and temperature. Large variations in measured perfusion are reflected in temperature changes corresponding in time.

5.5.2 Variability of k_m

Perfusion is calculated at a given tissue point based on an experimentally determined value of k_m (the intrinsic thermal conductivity) at that same point in the tissue. The value of k_m is calculated at the start of every perfusion measurement period and assumed to be constant throughout the period (5-120 minutes). However, multiple repeated measurements taken at least 15 minutes apart show that the calculated skin conductivity changes over time. Many factors have an effect on the value of k_m. Due to the nature of the conductivity algorithm, baseline temperature fluctuations in the skin can affect the calculated value of k_m. Futhermore, perfusion fluctuations and non-ideal contact between the sensor and the tissue can lead to artifact in the perfusion extraction.

One explanation for variability in the value of k_m is that the natural state of skin hydration changes from measurement to measurement. The water content of skin tissue plays a major role in determining its intrinsic thermal conductivity. Moreover, water content is not evenly distributed between the various layers of skin. While the dermis contains about 80% water, the stratum corneum (the most superficial layer of the epidermis) is made up of about 30% water [250]. The degree of surface skin hydration depends primarily on the penetration of water from the dermis, water loss to the environment (e.g. evaporation), and water acquired from ambient humidity [251]. Variation of these factors over the course of a measurement can change skin water content and conductivity, giving rise to inaccurate perfusion values (physiologically induced artifact).

An important function of the capillary bed is fluid exchange with the surrounding tissues. The magnitude and direction of water movement across the capillary walls arise from a balance between the hydrostatic and osmotic pressures across the membrane. Increasing the intracapillary hydrostatic pressure favors movement of fluid from inside the vessel to the surrounding interstitial space, while increasing the concentration of osmotically active particles within the vessel favors the reverse. However, hydrostatic pressure is the principle driving force for capillary filtration (outward movement of water) and exists as a gradient within the capillaries (highest at the arteriolar end). Moreover, changes in venous resistance have a greater effect on capillary hydrostatic pressure than similar changes in arterial resistance. In fact, about 80% of an increase in venous pressure is transmitted back to the capillaries [15]. This is most apparent in cases of edema in which increased venous pressure causes accumulation of excess fluid in the tissues (e.g., congestive heart failure, widespread venous thrombosis, prolonged standing). This becomes an important consideration in a test of reactive hyperemia where an occlusion of the arm vessels causes pressure to increase in the venous network. As a result, capillary filtration increases and there is a net movement of fluid into the tissue. This fluid increase during occlusion can significantly change the intrinsic thermal conductivity of the tissue.

I investigated this effect in the reactive hyperemia data taken from individuals before and after an occlusion. Figure 5.12 presents the pre-occlusion and post-occlusion value of the tissue intrinsic conductivity calculated by the adapted surface thermistor sensor. In all cases, the post-occlusion $k_m$was higher than the pre-occlusion k_m. Furthermore, the data from Subject 8 was taken before and after a 7 minute occlusion, while the others were all occluded for 4 minutes. Correspondingly, k_m increases by 27% whereas the other subjects with shorter occlusion times show k_m gains between 2 and 7%. This is an interesting observation and should be a consideration for future investigations.

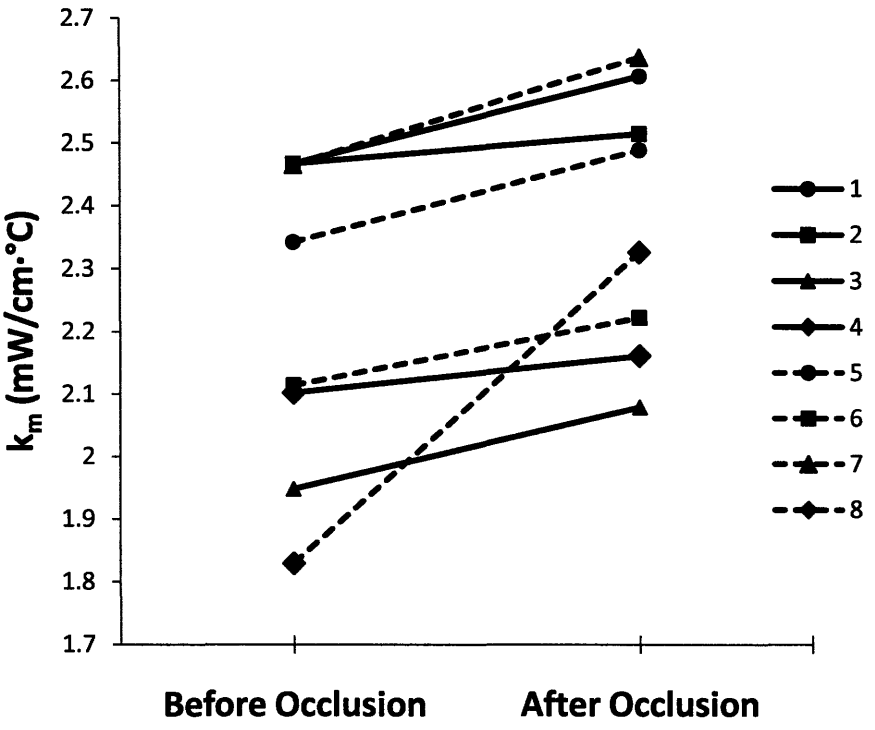

Figure 5.12 Measured intrinsic thermal conductivity of skin (k_m) before and after occlusion in test of PORH. In 8 subjects, k_m was calculated before occlusion and at least 10 minutes after the occlusion was removed. Subjects 1-7 exhibited an increase in measured conductivity between 2% and 7% after 4 minutes of occlusion. Subject 8 exhibited an increase in k_m of 27% following a 7 minute occlusion.

Also note that the value of k_m can be quite variable between individuals, reflecting differences in skin hydration, composition and temperature. Nevertheless, the values obtained from the surface sensor are within the range of previously determined conductivities of skin tissue that past investigators have measured using a variety of methods [185, 227, 252, 253].

5.5.3 Multi-Phasic Perfusion Hyperemia

An observation has been made in multiple measurements of reactive hyperemia. Following the release of the blood pressure cuff after an occlusion, there is often an initial hyperemia response, followed by a return to near baseline values. Soon thereafter (on the order of several seconds to a minute), the perfusion increases to a new peak value. Similar changes are seen in the temperature measurement. The physiological explanation for this observation is not clear, although it may entail vasoactive contributions from multiple local regulatory mechanisms, which operate on different time scales. For example, the initial peak may be mediated by ischemia-induced release of vasodilatory compounds in the microvasculature, while subsequent peaks may result from endogenous, shear-stress-mediated release of nitric oxide. Moreover, there may be competing effects from sympathetic nervous output or thermal regulatory mechanisms which sense rapid changes in temperature. Future studies should investigate the mechanisms that lead to multi-

phasic reactive hyperemia responses as there may be important, additional information therein. For example, it is possible that the relative contributions of distinct vasodilatory responses or the time course of their action may differ between healthy individuals and those with endothelial dysfunction. An example of a biphasic reactive hyperemia is shown in Figure 5.1.3.

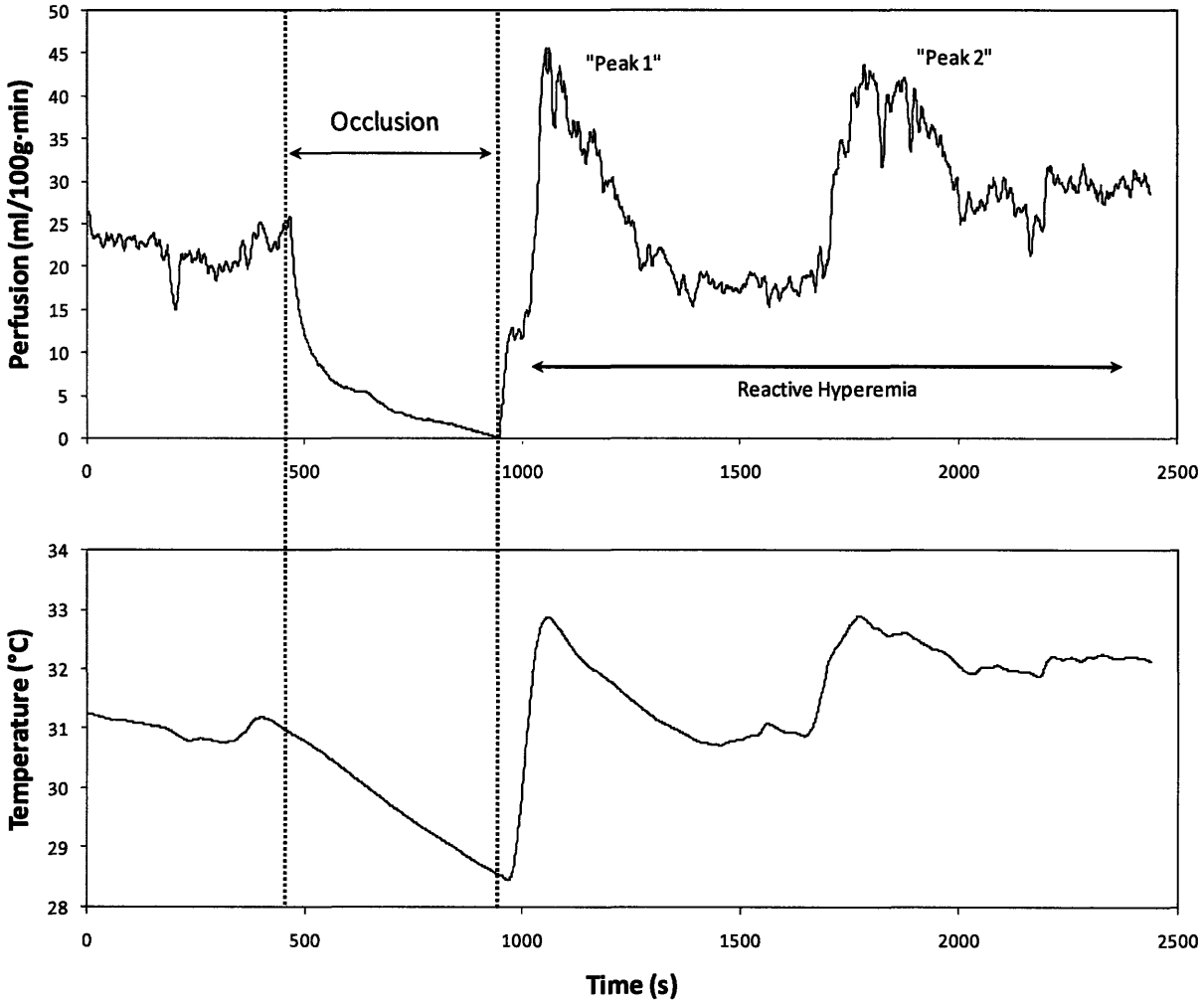

Figure 5.13 Biphasic reactive hyperemia following occlusion

5.6 Methods of Data Analysis

The preliminary experiments involved measuring perfusion and temperature using the modified invasive TDP (see Section 5.2.4). The quality of the data gathered for this thesis from preliminary PORH testing often made it unsuitable for subsequent data analysis. Furthermore, the data that was deemed sufficient for analysis was not obtained in a sample size large enough to permit population comparisons between subject groups with regard to specific characteristics, such as age or CVD risk factors. However, detailing the specific parameters that could be taken from the perfusion and temperature data during a test of PORH establishes a significant foundation upon which to base future testing among larger groups of subjects. In this section, I will present representative data taken from sensors applied noninvasively to the skin of various subjects' fingers with relevant analysis of defined parameters relating to changes in perfusion and temperature following an occlusive blood flow challenge to the arm.

First, we must consider the limitations of a preliminary data analysis:

- The measured perfusion response to an occlusive challenge cannot be correlated with degree of endothelial dysfunction.
- Only representative data is available and any conclusions drawn are speculative.
- The magnitude of the perfusion signal is not a reliable measure of absolute perfusion values due to the model assumption of a 4π geometry.

5.6.1 Filtering

Data obtained from perfusion measurements includes a continuous record regarding the sensor's operational parameters as well as the perfusion and temperature values. As is common for blood flow data, there was a need to isolate the true data from measurement noise, artifacts, and variability encountered during the acquisition procedure. Thus, the data was manually segmented to account for the following information:

a. A written record of events during the measurement that affected perfusion data collection (e.g. motion artifacts, test subject actions, sensor adjustments and/or replacement, etc.)
b. A written record of occlusion start and stop times
c. Knowledge of acceptable physiological limits on baseline and reactivity measurements
d. Automatically generated data regarding sensor operation throughout measurement period (temperature fluctuations, power, k_m, thermistor bead cross-talk, etc.)

Perfusion and temperature were individually analyzed by separating measurement periods corresponding to baseline, occlusion, and post-occlusion reactive hyperemia.

5.6.2 Perfusion Analysis

Post-occlusive reactive hyperemia in skin tissue is an increasingly common model of microvascular reactivity function. The ability to obtain real-time continuous measurements related to changes in microvascular blood perfusion has previously been explored by laser

Doppler flowmetry (Section 3.4.1). Many of those studied parameters can be adapted for perfusion values obtained via the current thermal sensor.

Perfusion data that exhibited non-zero values during occlusion were normalized to reflect zero perfusion at the lowest value reached during the occlusion period. A similar normalization is carried out in laser Doppler flux data, such that biological zero (a non-zero value arising from Brownian motion of macromolecules in the interstitial space) is subtracted from flux values in the raw data [27].

Baseline perfusion was determined by calculating the average value of perfusion for the 1 minute period prior to pressure cuff inflation (occlusion). The occlusion period was 4 minutes long starting from the time of pressure cuff inflation (suprasystolic pressure) to the time of pressure cuff release (subdiastolic pressure). The post-occlusion period was monitored for approximately 10 minutes, depending on the time it took perfusion to return to a baseline value. In cases where perfusion did not return to baseline (no overshoot), post-occlusion data was acquired for 10-20 minutes and a peak was from the highest perfusion value reached within 5 minutes of releasing the blood pressure cuff. Often, it was discovered the post-occlusion perfusion did not match physiological expectations and a recalibration was performed to determine if the sensor measurement had been compromised.

Individual sets of PORH perfusion data were analyzed by examining typical parameters that can be derived from tests of reactive hyperemia (see Figure 5.14). Previous studies using laser Doppler flowmetry have defined both magnitude-based parameters, such as peak amplitude or percentage hyperemic response, as well as temporal-based parameters, such as time-to-peak perfusion [254].

Magnitude-based parameters:

a) ω_{peak}: Amplitude of post-occlusion peak perfusion
b) ω_{max}: Maximum increase of perfusion during reactive hyperemia compared to baseline; defined ω_{peak} - Mean Baseline Perfusion
c) $\omega_{\%}$: Percentage of hyperemic response, defined as $\frac{\omega_{peak} - \text{Mean Baseline Perfusion}}{\text{Mean Baseline Perfusion}} \times 100$
d) ω_{AUC}: Area under the perfusion curve following release

The area under the curve was not calculated in the data presented, as clear definitions have not been established regarding the physiological basis for its use or interpretation.

Temporal-based parameters:

e) TTP_{ω}: Time-to-peak perfusion; time after occlusion cuff release until the post-occlusion peak perfusion (ω_{peak}) is reached
f) V_{mean}: Mean velocity of the post-occlusion hyperemia increase, expressed as $\omega_{peak}/TTP_{\omega}$

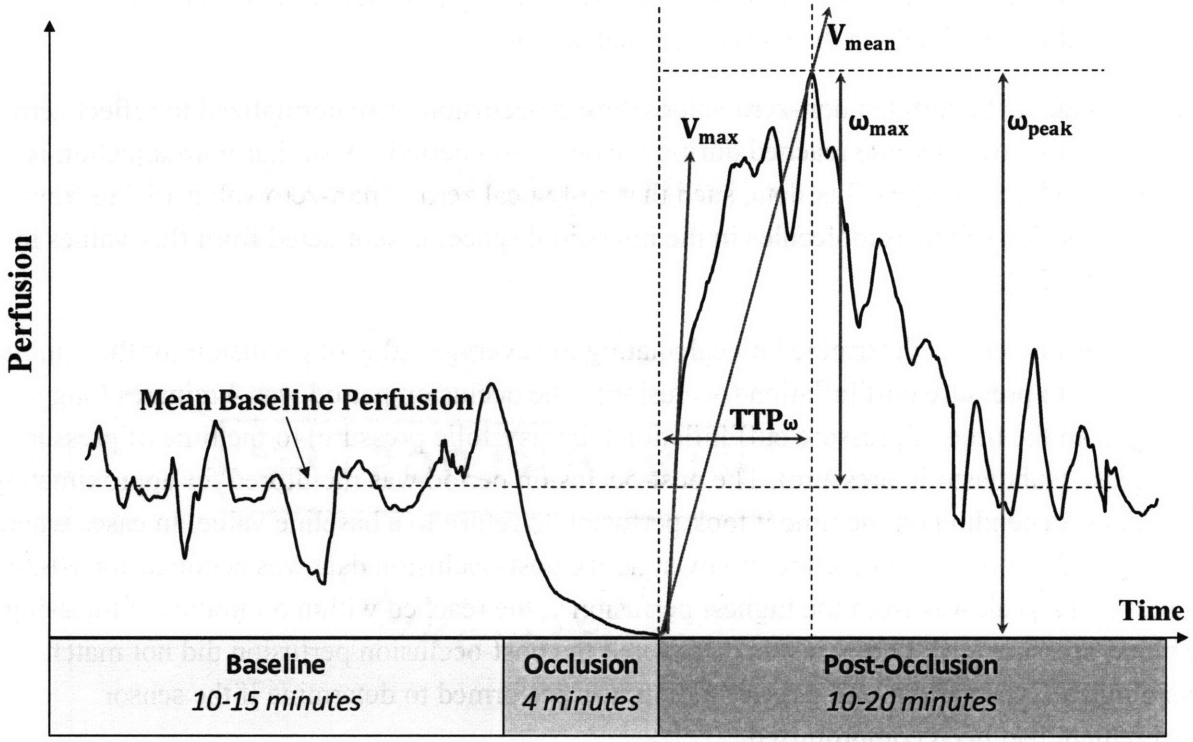

Figure 5.14 Representative PORH perfusion measurement with suggested parameters of reactivity

The most common temporal parameter used in laser Doppler flux data has been the time-to-peak perfusion. Compared to brachial FMD, investigators have determined that a time-to-peak value of greater than 10 seconds is a more specific index for the diagnosis of coronary artery disease [122]. Still, as there is no currently agreed-upon set of parameters which consistently provide reliable information on perfusion changes during PORH, studies have investigated the reproducibility of common laser Doppler flowmetry parameters. In one such study, the parameters corresponding to ω_{max}, TTP_{ω}, ω_{peak}, and V_{mean} were found to be highly reproducible parameters of laser Doppler PORH data (intraday and interday) [122].

5.6.3 Temperature Analysis

The skin is the primary mediator of temperature regulation and is subject to a wide range of thermal influences. However, the role of perfusion is central to the maintenance of temperature in the skin. Some methods have been proposed which place temperature changes during PORH at the center of the investigation into endothelial dysfunction [222]. Therefore, parameters taken from the temperature response following occlusion are important to an overall picture of vascular reactivity in the skin (see Figure 5.15).

Magnitude- and Temporal-based parameters:

a) T_{NP}: Nadir-to-peak temperature change ($T_{peak} - T_{nadir}$)
b) T_R: Temperature recovery, defined as $T_{peak} - T_{initial}$ (initial pre-occlusion temperature)
c) $T_{\%}$: Percent of temperature rebound (compared to the change in temperature during occlusion), defined as $\frac{T_R}{T_{initial} - T_{nadir}} \times 100$
d) T_{AUC}: Area under the temperature curve
e) TTP_T: Time-to-peak temperature

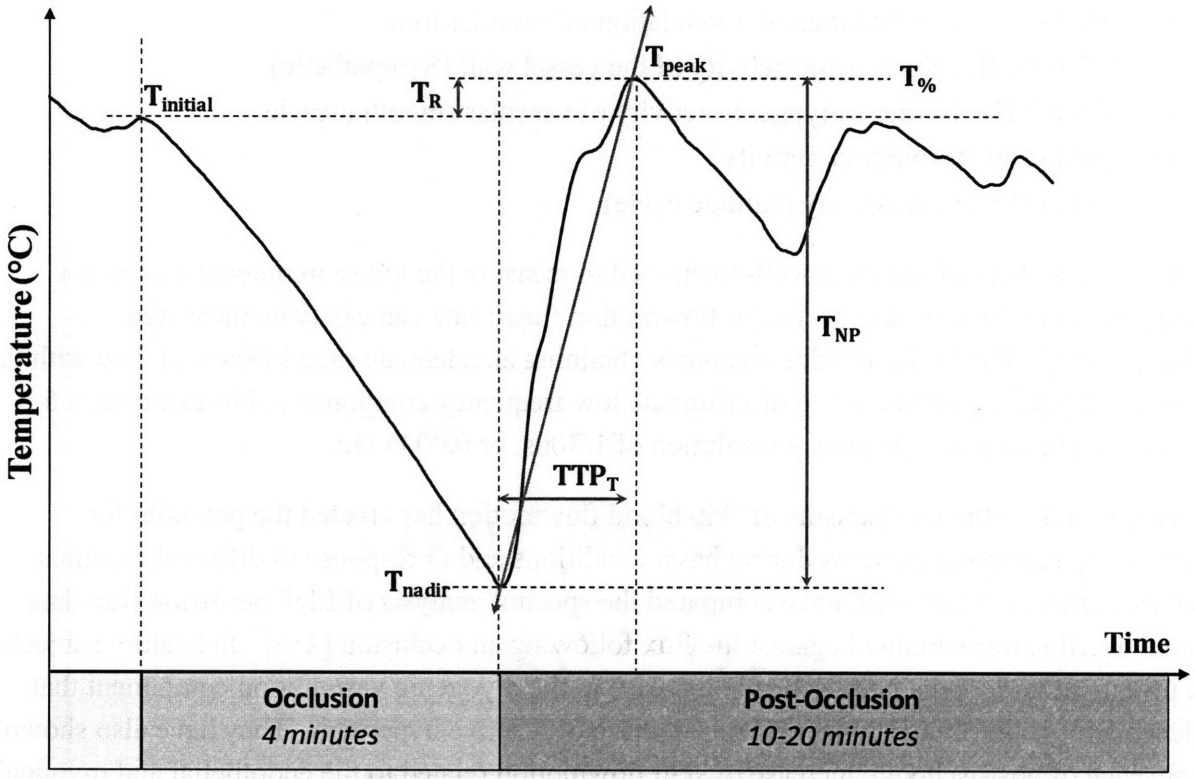

Figure 5.15 Representative PORH temperature measurement with suggested parameters of reactivity

One limitation of the present study could be relatively long cuff inflation and deflation durations that took about 4 to 5 seconds. This relatively long deflation time may cause a minor delay in time-to-peak (TTP_ω and TTP_T). It may also introduce uncertainty into the times of occlusion and initiation of the hyperemic response. Using a rapid cuff inflator that is able to inflate and deflate within 1 second would probably lead to more precise TTP reading and improved reproducibility.

Also, note that in the following analysis, the peak temperature is defined as the maximum temperature that corresponds to the peak hyperemia (normally the first temperature inflection point post-occlusion). This became an important consideration when multiple temperature peaks were apparent.

5.6.4 Frequency Analysis

Clearly, the thermal sensor is capable of discriminating perfusion changes at both high and low biological frequencies. It is also reasonable to assume that the magnitude of changes in perfusion values corresponds with similar fluctuations in skin perfusion over time. These changes can be analyzed in the frequency domain to gather data regarding intrinsic vasomotor regulation of perfusion. With a sampling rate of 1 Hz, it is possible to discriminate frequencies up to 0.5 Hz. In spectral analysis of laser Doppler flowmotion data, which is obtained at sampling frequencies between 30 and 40 Hz, clear oscillations have been identified in the frequency ranges [255]:

- 0.009 – 0.02 Hz: Endothelial modulation of vascular tone
- 0.02-0.06 Hz: Neurogenic activity of the vessel wall (Sympathetic)
- 0.06-0.2 Hz: Intrinsic myogenic activity of vascular smooth muscle
- 0.2-0.6 Hz: Respiratory activity
- 0.6-1.6 Hz: Heart activity (cardiac cycle)

Therefore, the thermal sensor is well-positioned to measure the lower frequency vasomotor components involved in skin perfusion flowmotion (heart rate can easily be measured independently). The limitation thus becomes obtaining an adequate time interval of data with the necessary frequency resolution to discriminate low frequency components. For example, a 5 minute set of data has a frequency resolution of 1/300s, or 0.0033 Hz.

Investigation into the mechanisms of skin blood flowmotion has created the potential for determining regulatory patterns during basal conditions and in response to different stimulus, such as ischemia. Rossi *et al.* have compared the spectral analysis of LDF perfusion flux data from a baseline measurement against the flux following an occlusion [255]. In healthy subjects, the investigators found a post-ischemic increase in the myogenic vasomotion component that independently contributes to the prolonged phase of reactive hyperemia. They have also shown an absence of post-ischemic increase of skin flowmotion related to the endothelial and myogenic activity in chronic smokers, suggesting endothelial and smooth muscle cell dysfunction [182]. It is suggested that vasomotion in the microcirculation contributes to an optimal blood flow distribution in the vascular bed of tissues. Thus, the study of flowmotion has great potential for illuminating specific features of the skin microcirculation in healthy and diseased states.

An example of a simple spectral analysis is provided in Figure 5.16. The analysis was performed on a segment of the resting perfusion signal obtained from the palmar fingertip of a 23 year old female subject (see Figure 5.16A). It is clear that frequencies lower than 0.1 Hz play a large part in the measured perfusion oscillations (by several orders of magnitude) (see Figure 5.16B). The frequencies that are most identified in the perfusion signal seem to result from endothelial activity and sympathetic activity, which are local perfusion control mechanisms (see Figure 5.16 C). However, there is undoubtedly the need for selective filtering as it is clear that a simple spectral analysis does not fully describe the oscillatory patterns of skin blood flow. Indeed, the magnitude of oscillation at a specific frequency does not imply a higher proportion of control.

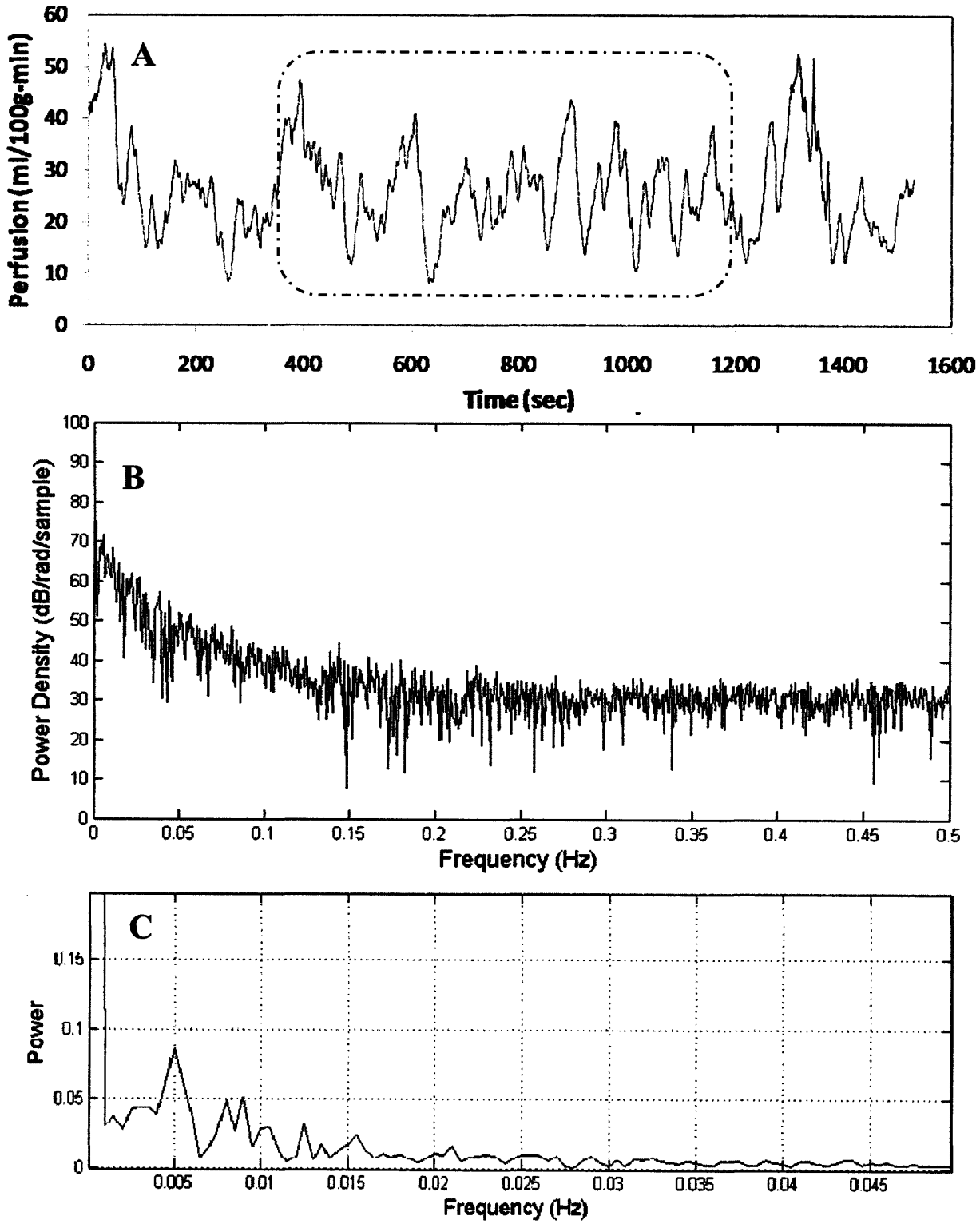

Figure 5.16 Spectral analysis of perfusion signal measured by thermal sensor. (A) Basal perfusion signal measured from fingertip of 23 year old female subject. The indicated time window is analyzed in the frequency domain in (B), power spectral density (note log scale) and (C), simple spectral analysis zoomed in on low frequency components.

5.7.1 24 year old Male, Healthy

The perfusion and temperature data during a test of PORH is presented for a healthy, 24 year old male with no family history of heart disease, diabetes, or atherosclerosis in Figure 5.17. Baseline perfusion was calculated as the average perfusion 1 minute prior to inflation of the arm blood pressure cuff. Following the occlusion period, there is a rapid increase in perfusion and temperature, followed by a substantial drop in both values. Another rise in perfusion and temperature is seen shortly thereafter. This is an example of the multi-phasic phenomenon mentioned in Section 5.5.3. The relevant parameters are displayed on the perfusion and temperature plots as examples of possible data analysis (ref. Sections 5.6.2 and 5.6.3).

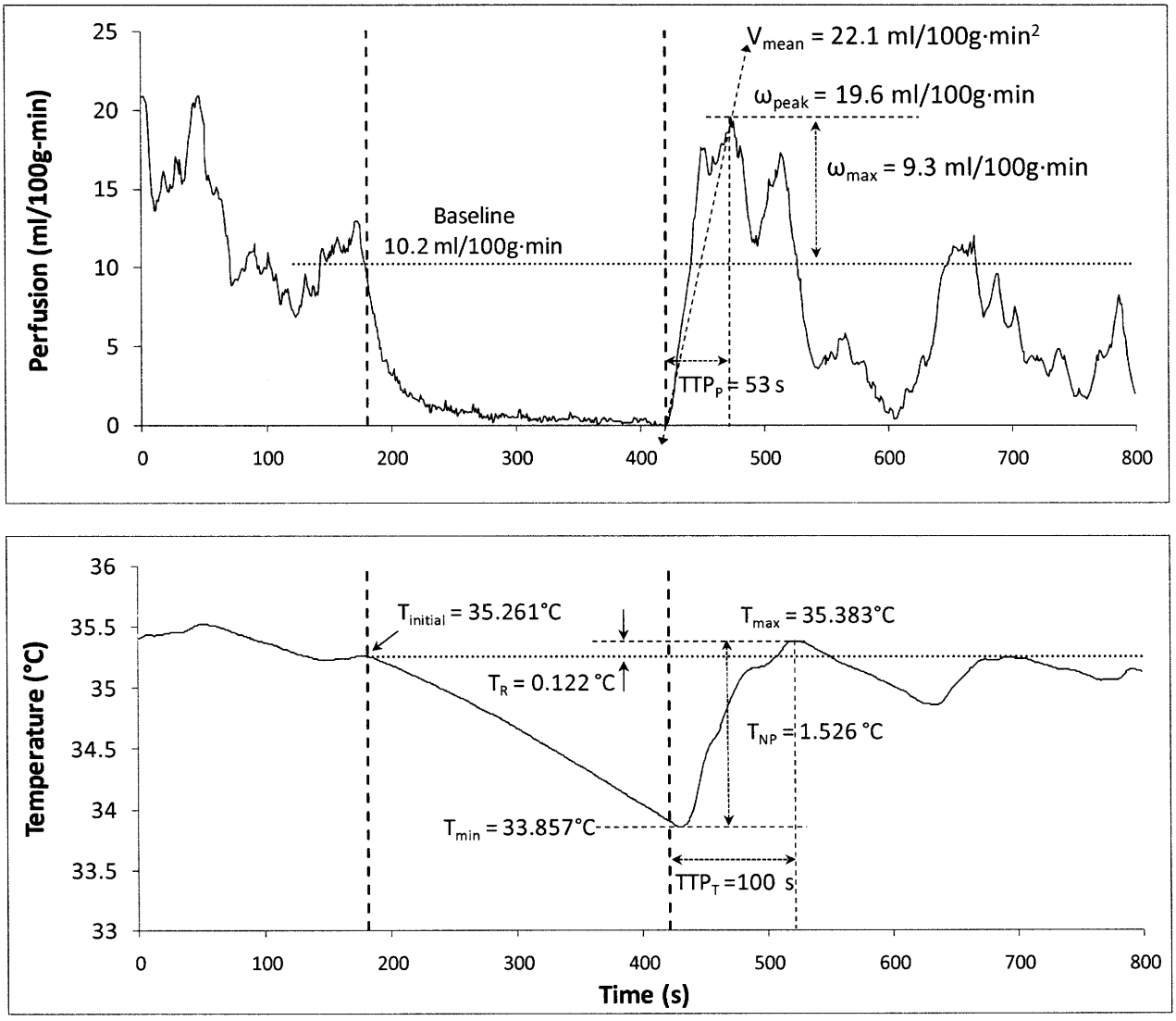

Figure 5.17 Perfusion and Temperature during test of PORH in 24 year old, healthy male. The relevant parameters are calculated as described in Section 5.6.2 and 5.6.3)

5.7.2 30 year old Male, Cigarette Smoker

Another example of data taken during a test of PORH is shown in Figure 5.18. The subject was an active 30 year old male who reported smoking cigarettes. Similar parameters of reactivity to the previous analysis of Figure 5.17 are displayed. It is clear that the peak reactive hyperemia has a much lower magnitude compared to the previous subject, although both had similar baseline perfusion. Moreover, the post-occlusion perfusion returns to pre-occlusion levels immediately following reactive hyperemia, with no indication of the sustained, elevated perfusion that would be expected following a substantial period of ischemia. The temperature response also contrasts with the previous subject. Rather than exhibiting a temperature rebound exceeding the initial pre-occlusion temperature, the temperature increases to a peak value 0.304°C less than the initial temperature. A new baseline temperature seems to be established as a result, since the subsequent temperature data remains relatively constant around this new value.

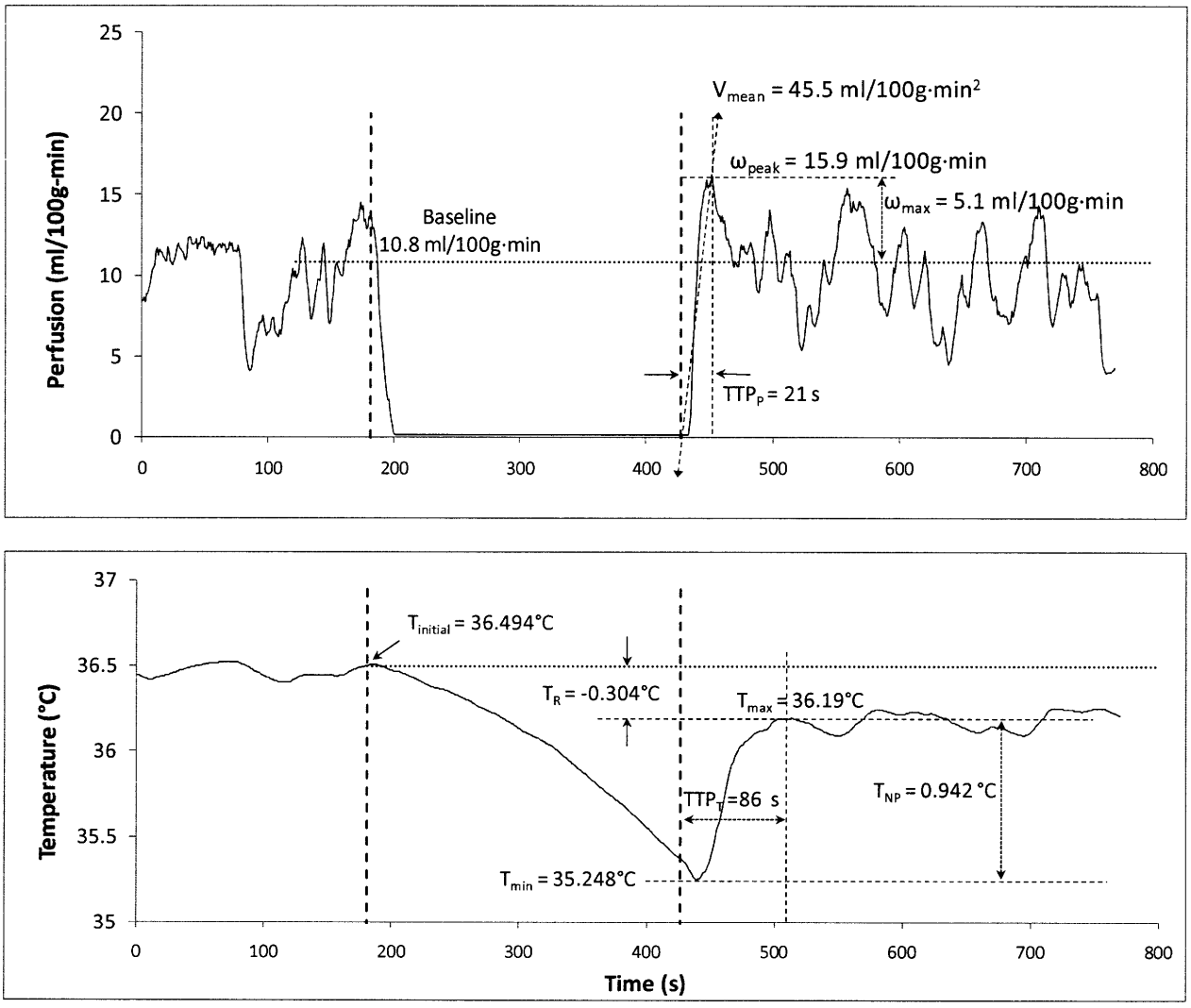

Figure 5.18 Perfusion and Temperature during test of PORH in 30 year old, male, smoker. The relevant parameters are calculated as described in Section 5.6.2 and 5.6.3)

Chapter 6. Design of the Noninvasive Sensor

6.1 Design Issues to Address

The design of the non-invasive sensor must satisfy the following specifications:

- The sensor must be in good thermal communication with the tissue surface.
- The sensor should be applied to the tissue without causing capillary collapse or distorted regional blood flow.
- The sensor should be insulated from environmental changes on all sides except the sensor-tissue interface to maximize the signal and simplify the analysis.
- The sensor must be applied in a suitable configuration that promotes the analytical extraction and interpretation of perfusion values from the resulting thermal field.
- The sensor should be low cost and easy to apply in a reproducible fashion.

The preliminary data shows that noninvasive perfusion measurements can be obtained using the invasive thermal model. This is reasonable based on previous work with the invasive sensor and its data extraction algorithm in which the fundamental heat transfer processes are modeled at the capillary level for a variety of soft tissues, including brain, liver, kidney, muscle and skin.

A significant effort has been made towards optimization of a sensor contact pressure by designing appropriate sensor housing that controls the sensor protrusion depth into the tissue. To permit accurate measurement of perfusion in the skin, the contact pressure between the sensor and skin tissue, as well as the sensor protrusion depth, must not exceed values that may alter local perfusion. At the same time, the contact pressure should be high enough to ensure consistent thermal communication between the sensor and skin, as it is essential for extracting accurate perfusion values. Multiple housing designs have been investigated for reproducibly mounting and applying the noninvasive thermistor sensors to skin. Design criteria include:

- Contact pressure such that sensor displacement into the compressed tissue is both highly reproducible and less than 1 mm (~0.6 mm) to avoid significant capillary collapse
- Minimal thermal conduction paths from the perfusion sensor to any sensor encasement to the environment thus rendering perfusion extraction less complex
- Thermal isolation of the sensor from environmental temperature variations
- Sensor adhesion to skin in manner that does not alter regional blood flow
- Compatibility with wetting agents that consistently enhance sensor-skin thermal communication
- Noninvasive sensor configuration that is simple in concept and can be readily fabricated reproducibly at low component and labor cost

- Configuration is in a shape that facilitates the calibration procedures necessary to determine those sensor thermal characteristics, which in turn are necessary to permit accurate measurement of temperature, tissue thermal properties and the accurate extraction of perfusion

6.2 Geometry

The sensor shape governs its interface with the tissue as well as the thermal field generated during a measurement of perfusion. Therefore, an appropriate geometry will minimize contact-induced perfusion artifacts and simplify the thermal model from which tissue thermal properties and perfusion are determined.

6.2.1 Disk

Two disk-shaped surface thermistors were proposed by Steven Charles in 2004 [247]. One consists of a flat, circular disk thermistor that rests flush against the tissue surface and is insulated on all other exposed surfaces. The other consists of an inner heated disk and an outer ring. The two are thermally isolated from each other by a thin insulating ring and the temperature is controlled in the disk while the power required to maintain this temperature is used to calculate perfusion. Both were modeled as one-dimensional infinite slabs (see Figure 6.1). The disk was also modeled as a one-dimensional hemispherical shape as the isotherms in tissue heated by a disk approach those of a hemispherical solution at large distances. A finite difference analysis allowed him to determine that a disk design with a hemispherical model was sufficient for measurement of perfusion within clinically acceptable error limits. However, disk models suffered from edge effects and errors were quite large. Charles concluded that generally, errors caused by approximating two-dimensional geometries by a one-dimensional model were too large for clinical acceptance.

6.2.2 Hemisphere

As in the invasive TDP, a nearly spherical thermistor surrounded by tissue allows for simplification of the governing heat equations to a one-dimensional model in spherical coordinates. Both transient and steady-state solutions exist for a spherical thermistor embedded in perfused, infinite tissue. Due to spherical symmetry, the spherical solution is valid for a hemispherical probe embedded in a semi-infinite solid, where the free surfaces of the probe and tissue are insulated.

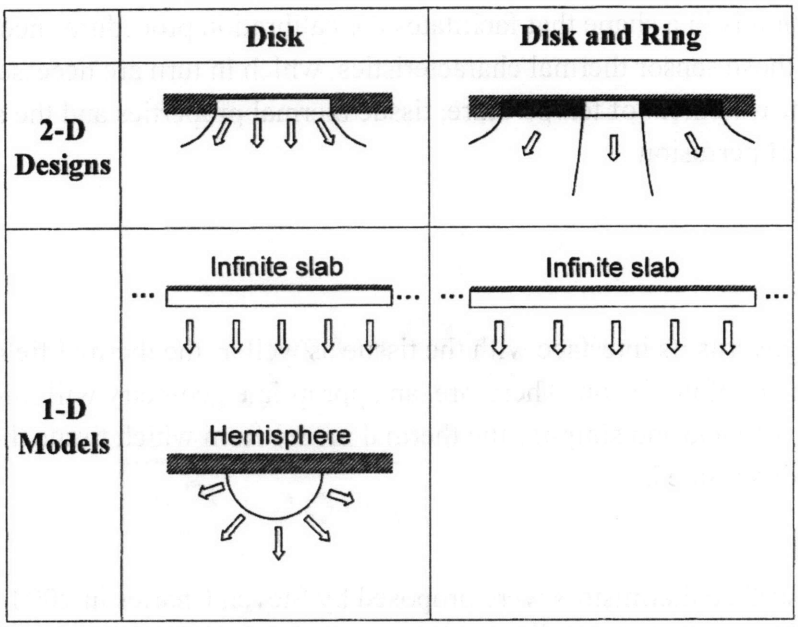

Figure 6.1 Two-dimensional noninvasive designs with corresponding one-dimensional models considered by Charles, 2004. [247]

6.3 Tissue-Sensor Interface

A suitable wetting agent that increases the thermal communication between the sensor and the skin may aid in obtaining reliable, repeated perfusion measurements. Ultrasound gel has been used with some success and no negative effects. However, it is possible to use liquids and gels of different types to determine which are most appropriate. One potential substance is thermally conductive grease, which has the ability to provide a highly conductive interface with minimal contact resistance.

6.4 Sensor Fixation and Placement

The thermistors must mate with the housing in a reproducible manner to achieve consistent measurements. The currently available thermistors have specific dimensions, which dictate the internal dimensions of the sensor housing. For the sensor I am proposing, the heat thermistor has a bead diameter of 0.028 inches (0.71 mm) and the sense thermistor has a diameter of 0.017 inches (0.43 mm). The thermistor leads are contained in a flexible catheter tubing with the thermistor beads extending from the end. The beads must be fit into a housing which thermally insulates the thermistor beads on all surfaces except for the tissue interface. Furthermore, the sensor must be applied with the appropriate contact pressure, which preliminary testing as shown to be 0.5 mmHg.

6.5 Initial Designs and Rapid Prototyping

Many different sensor and thermophobic sensor housing configurations have been considered. The sensor housing addresses many of the issues related to skin surface perfusion measurements:

- By fixing the thermistors at a defined location relative to the skin tissue, the depth of displacement can be precisely controlled to avoid altering local perfusion through capillary collapse.
- The insulating material and thermistor configuration serves to thermally isolate the sensor so that the dissipated heat is directed into the tissue and is consistent with the thermal model governing perfusion extraction.
- Mounting the sensor within the housing provides additional structural strength and is able to mate the sensor, the fragile internal lead wires and the insulating material.
- Fabrication of the housing can be accomplished inexpensively and with controlled reproducibility.

6.5.1 Molded Design

One design was proposed by Chris Savage, an undergraduate in Mechanical Engineering [256]. The "bead holder" consisted of an interface that held the thermistors in a reproducible orientation with respect to the tissue upon which it would be placed. Small, sharp projections reduce the area of contact with the thermistor and are able to thermally isolate the sensor. A CAD model (SolidWorks) is shown in Figure 6.2 detailing the internal geometries. The design was initially realized through rapid prototyping, followed by testing the effectiveness of the interface. Rapid prototyping of the various designs was carried out on a ZCorporation Spectrum 510 high-definition, full-color 3-D composite prototyping printer at the MIT Media Lab. The 3-D printer receives a solid model file as an input and builds prototypes layer-by-layer with a plastic and resin composite. These prototypes give accurate geometries and the process allows production of tens and hundreds of parts in a batch with different designs within the batch.

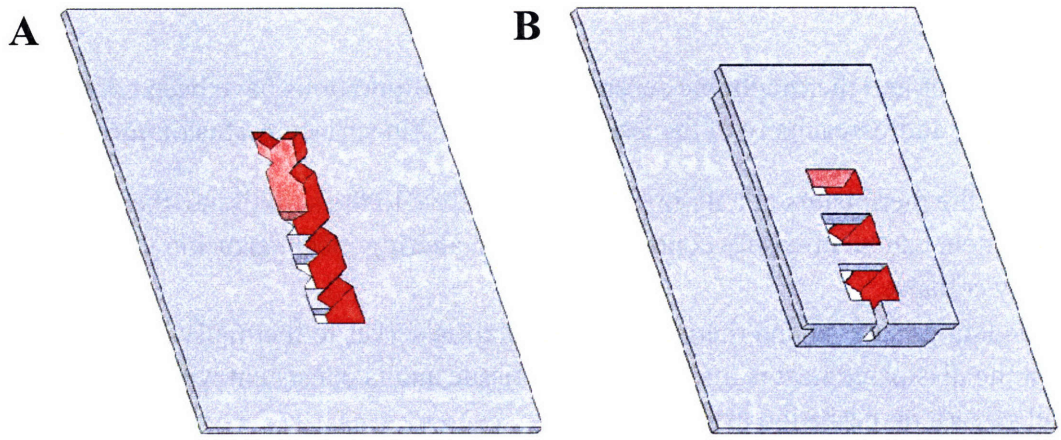

Figure 6.2 Solid model of proposed thermistor bead holder, designed by Savage, 2007 [256]. (A) Bottom face of thermistor holder displaying internal geometries designed to thermally isolate thermistor during measurement. (B) Opposite face of thermistor holder showing relative size of bottom flange for anchoring to skin tissue (by adhesive).

For still greater fidelity and to gain an understanding for the physical interface of the holder with the sensor, the part was made on another rapid prototyping system, the inVision si^2 3-D modeler (3D Systems), which thermally deposits cross sections of acrylic plastic layer-by-layer. This 3-D printer is capable of printing with a z-axis resolution of 800 dots per inch (dpi) and 656 dpi in the x- and y-axes. A part is supported by wax that encases the acrylic so that the final part is revealed after melting away the wax. After experimenting with the interface between the sensor and cradle, certain adjustments were made to the dimensions to ensure proper fit and placement of the sensor bead. Subsequent iterations called for the fabrication of different cradles exhibiting a variety of depths of bead protrusion between 0.01" and 0.015." Figure 6.3 shows magnified photographs of an acrylic prototype thermistor holder made in this way.

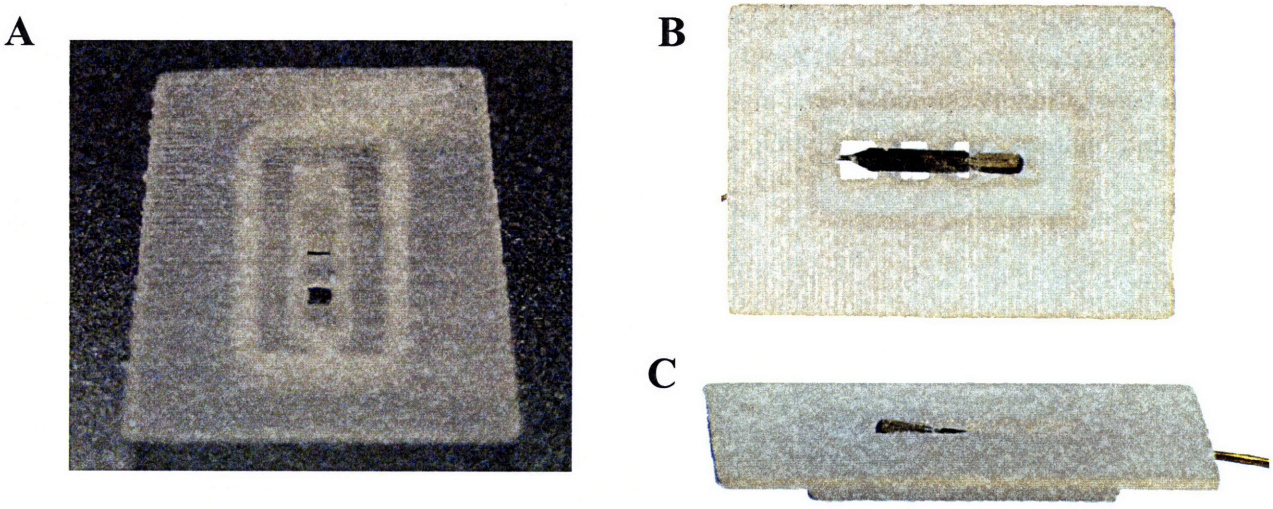

Figure 6.3 Three-dimensional printed acrylic prototype thermistor bead holder. (A) Bottom (skin-side) view of holder revealing internal geometries. (B) Bottom view of holder with sensor in position. (C) Side view of holder shown with protruding sensor thermistor bead.

The final realization of this design would be most appropriately produced by injection molding, which is cost effective for manufacturing small parts in large quantities. However, the process is limited by the internal contours of the injection mold and is not customizable for the most appropriate thermistor fit. Furthermore, the complex internal geometries of the holder would introduce similar complexities in the corresponding mold, which must be manufactured to specification. This aspect is limited by the machine limits in milling the mold. Another concern in manufacturing the part was supplying enough pressure during injection molding to introduce molten thermoplastic material into the small crevices and projections of the small mold. These limitations made it unrealistic to pursue injection molding as a method of manufacturing this part.

6.5.2 Extruded Design

An alternative method of forming the sensor housing was suggested by Robert Poirier of Dunn Industries, Inc. (Manchester, NH). His experience with the medical device industry, particularly in tubing design, aided in the conception of an extrusion from flexible tubing material with a suitable cross-section to accommodate sensor thermistors in the required orientation.

Thermoplastic Extrusion

Plastic extrusion is a steady state and high-volume manufacturing process that forms raw thermoplastic polymers into a long, continuous profile. The process involves feeding small beads of the desired material, called resin, into an extruder barrel with a rotating screw, where molten polymer is produced through a combination of appropriate melt heat, pressure, and friction (see Figure 6.4). The molten polymer then flows through the barrel to a breaker plate, which removes contaminants and creates back pressure in the barrel. The shape of the tubing is defined by a die located at the end of an extruder barrel. The die creates tubing with a specific profile and can be designed to take on a variety of contours. Hollow sections within the tubing are extruded by placing a pin or mandrel inside of the die to create the lumens within the extruded shape. The extrudate from the die is cooled and wound onto a spool. One limiting element of extrusion is the linear nature of the process, which requires that the cross-section of the part remain constant throughout the entire length. Injection molding, on the other hand, is a cyclic process which produces discrete products with varying cross sections in each axis.

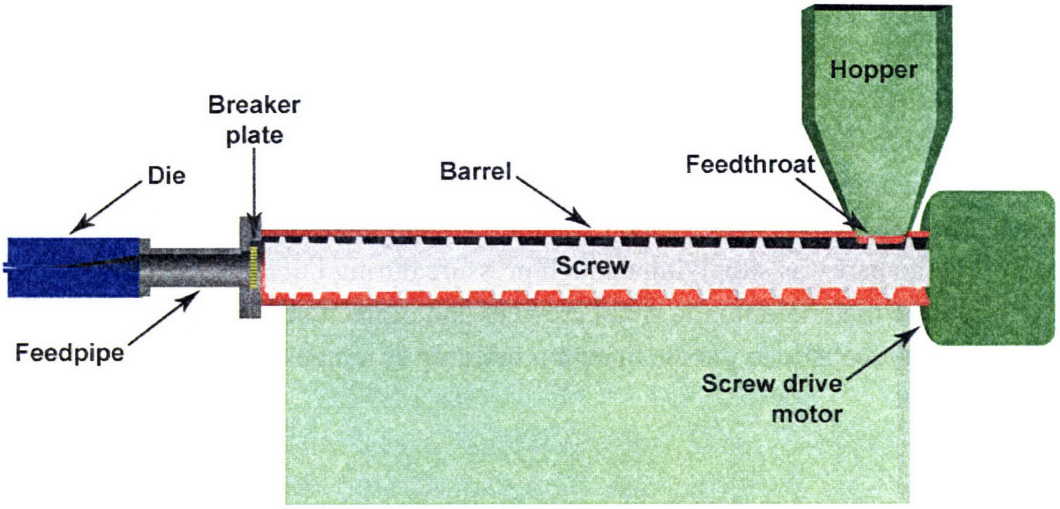

Figure 6.4 Plastic extruder cut away to reveal operating components

It was concluded that the intricate internal geometries for precise placement of the thermistors could be formed during the extrusion process and the tubing would provide both versatility and flexibility for the sensor design. These extrusions could be manufactured from medical-grade tubing material in large quantities at a low cost. This design allows the discrete housing necessary for an individual sensor to simply be taken from a linear tubing of a fixed cross-sectional profile.

Design and Prototyping

However, initial testing of the physical interface was necessary before an extrusion die with fixed geometries was fabricated. Figure 6.5 shows one such design that holds the heat and sense thermistor beads of the sensor in extruded channels, isolated by three sharp projections that reduce the area of contact between the thermistor beads and the extruded channels. These projections reduce the natural heat conduction paths into the housing. The sensor is also naturally insulated from environmental temperature variations by an appropriate thermally insulating tubing material and the air contained within that tubing. The sensor configuration would be placed on top of the tissue surface, where the individual thermistors maintain a fixed depth that would not allow for significant perfusion disturbances.

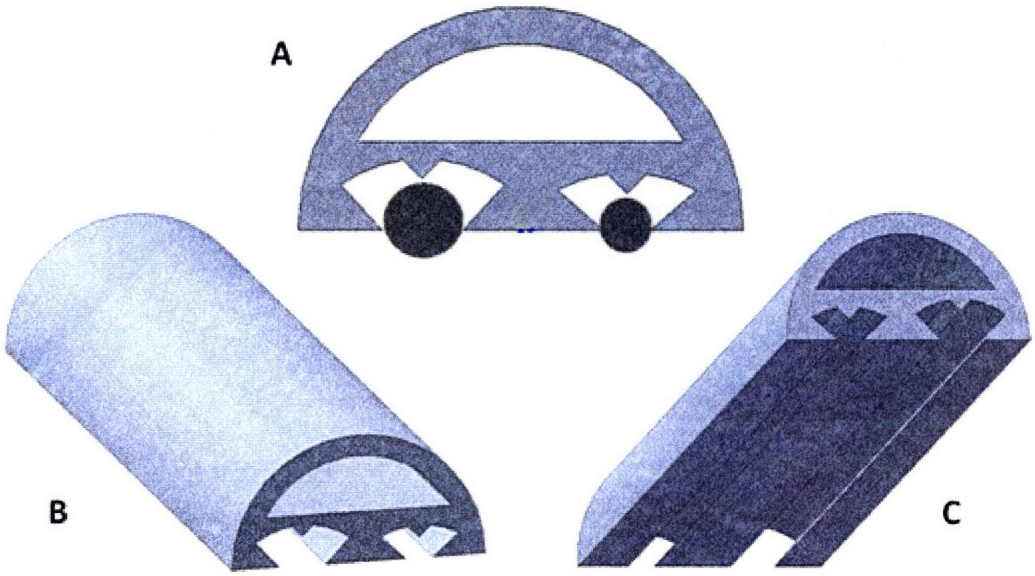

Figure 6.5 Extruded tubing with channels designed for thermistor beads fixed at specified depths relative to the skin surface. (A) Cross-section of extrusion shown with mock thermistor beads showing degree of contact between sensor beads and extrusion. (B) and (C) show different angle views of a 0.5 inch extrusion of (A).

To gain an understanding of the interface between the extruded design and the sensor, multiple iterations of extruded cross-sections were printed in acrylic on the rapid-prototyping machine in four-inch long pieces. We varied the sensor protrusion depth, channel shape, tubing shape, and the profile of the extrusion channels for thermistors of various size and number. The acrylic prototypes lack the thermal material characteristics necessary for a final prototype. However, the geometry of the interface between the extrusion channels and the sensor allowed for preliminary data to be taken on the skin of the hand indicating that relative perfusion could be measured using the suggested sensor configuration. Furthermore, vascular responsiveness and endogenous vasomotor activity were readily obtained from the perfusion data.

Figure 6.6 shows a configured sensor that incorporates the extruded housing design. Computer-drawn solid models of the sensor are displayed with magnified photos of an acrylic prototype sensor. As shown, the housing holds the thermistors within the channels at a fixed depth and is enclosed in a circular foam pad that has an adhesive coat for fixation to the skin surface. The protrusion of the thermistors determines the depth that the noninvasive sensor will project into the skin and is the most critical parameter to make reproducible. A rapid prototype of the extrusion was made and placed in the anticipated configuration with one heat and two sense beads (a slight modification from the original design).

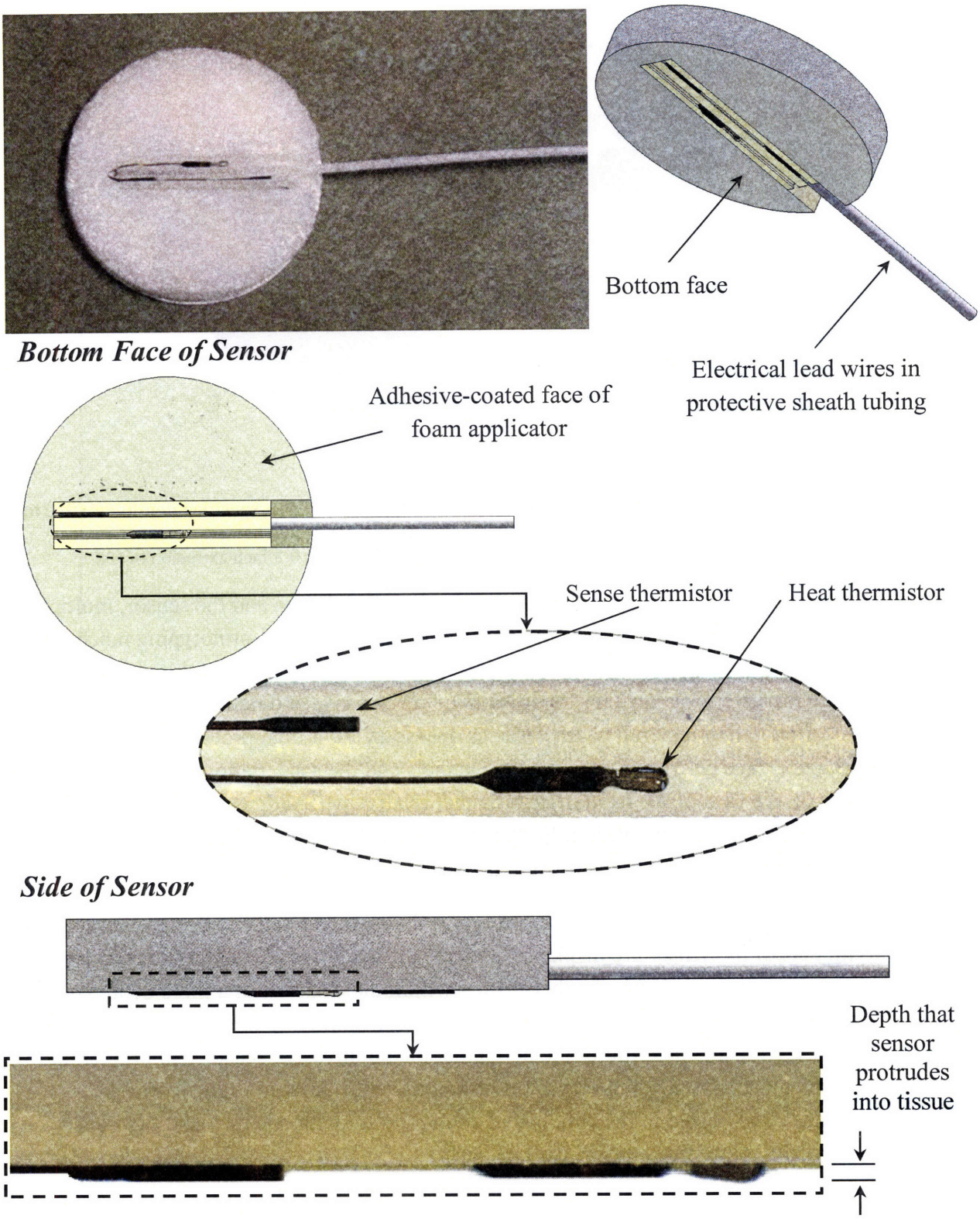

Figure 6.6 Multiple perspectives of solid model and prototype of alternative extruded housing design. (A) is a photograph of an actual prototype senseor. (B)-(D) show th conceptual solid model displaying a central heating thermistor and two passive sense thermistors connected in series to adjust for baseline temperature. Magnified selections of (C) and (D) are provided by (c) and (d), which are high-magnification photos of the actual prototype.

Our next generation noninvasive sensor will likely utilize commercially extruded sensor housing produced by Dunn Industries (Manchester, NH), a leader in medical plastics. The tubing material will be made of Santoprene™, a thermoplastic elastomer (TPE) that consists of a mixture of ethylene-propylene-diene monomer (EDPM) copolymer and polypropylene. It combines the characteristics of vulcanized rubber (heat resistance, low compression set) and the processing ease of thermoplastics.

6.6 Proposed Sensor Design

Considering all the relevant design criteria and collective experimental experiences to date, I propose the sensor design shown in Figures 6.8-6.10 as a candidate design for an ideal thermal-based noninvasive perfusion sensor.

This design incorporates the following features which permit a simple, reproducible, and reliable method of measuring surface perfusion:

- Commercially available and inexpensive spherical thermistors are mounted in the extrusion in a hemispherical geometry. This is an ideal geometry with respect to the thermal models, thus allowing perfusion to be determined from an analytical solution.
- An extruded sensor housing thermally isolates (and insulates) the thermistors in order to approximate ideal adiabatic conditions. The nature of the extrusion process produces the housing in a linear fashion, enabling large quantity production at low cost.
- A flexible foam pad made of thermally insulating material and coated with a skin-compatible adhesive. The foam pad insulates the sensor from unstable environmental conditions and provides the adhesion necessary to maintain adequate contact pressure relative to the skin.

To assemble the sensor, the self-heated thermistor (perfusion sensor) and the baseline tracking sense thermistor are mounted in the extruded sensor housing shown in Figures 6.7-6.10. Proper contact between the skin and sensor is ensured by the set protrusion depth of the sensor (see Figure 6.9). This value is much smaller than the depth at which perfusion is altered by capillary collapse and is still adequate for maintaining appropriate thermal communication between the sensor and the tissue. Sensor thermal insulation is established by the three small contact points in the housing, which minimize thermal conduction paths away from the sensor. The housing is in turn contained within the body of a flexible, adhesive foam pad, which lends additional insulation from the effects of environmental temperature variations. Electrical leads from the two

thermistors are thermally anchored to the housing to minimize heat leakage. Furthermore, the catheter containing the leads is contained within the housing to minimize damage to the lead wires which might result in current leakage. The complete assembly of the sensor is shown in Figure 6.10C. To apply the sensor, the adhesive face containing the exposed sensor is simply affixed to the skin surface.

The final extrusion profile iteration had to account for a number of design specifications:

- There are constraints on the inclusion of sharp projections in an extrusion. Within the slots, there are sharp edges which hold the thermistor beads in place, while minimizing contact surface area to reduce heat conduction paths. These sharp projections in the slots were given a slight curvature to balance the manufacturing constraints and the thermal model constraints.
- Further efforts to reduce heat conduction from the thermistor to the extrusion led to the addition of lumens within the extrusion (0.01" in diameter), which minimize conduction paths near the lateral sensor/extrusion interfaces.

6.6.1 Design and Manufacture of Sensor Housing

The final housing design is presented in Figure 6.7 with the relevant dimensions custom-fit to the currently available thermistor sensors (units in inches as required by toolmaker). A model of the anticipated extrusion is shown in Figure 6.8. The housing specifications were provided to Dunn Industries for manufacture of the extrusion. However, the first step in the manufacturing process involved contracting an outside source for the necessary tooling (extrusion die). The difficulties in manufacturing such a small part with specific geometries led to a tremendous delay in the actual manufacture of the part (e.g. crushed tooling, unacceptable products). Furthermore, the extrusion process was hampered by machine malfunctions that damaged both the tooling and the extruded product. Several repetitions of these problems prevented completion of the part in the time necessary to test the sensor for inclusion in this thesis. However, the proposed sensor design and assembly is presented for use in the future.

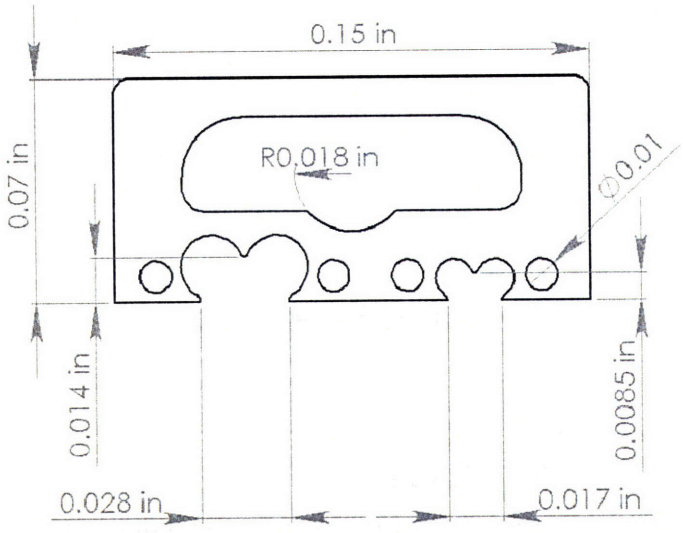

Figure 6.7 Dimensioned cross-section of sensor housing for extrusion die manufacture

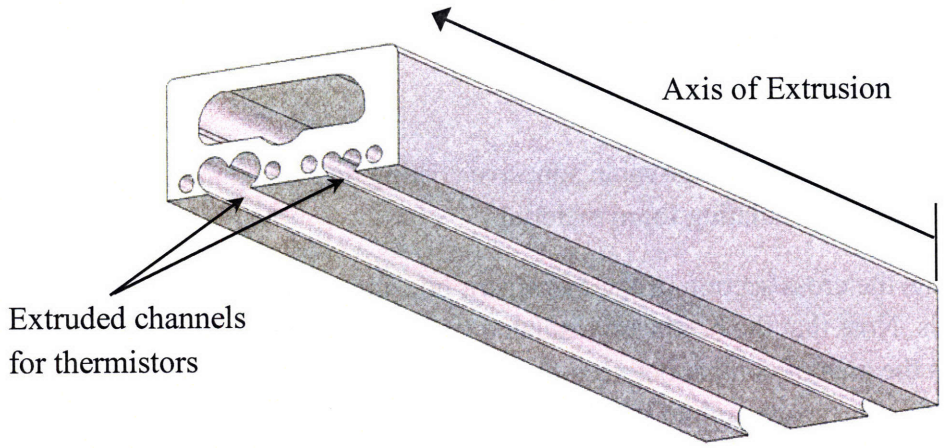

Figure 6.8 Three-dimensional model of a small length of sensor housing extrusion

6.7 Calibration

The calibration of the invasive TDP is accomplished by inserting an assembled probe into different media of known thermal conductivities, achieving a 4π geometry with respect to the surrounding medium. In this case, all of the heat that leaves the thermistor enters the tissue medium. A similar situation would be desirable for the noninvasive sensor, as this would allow for the sensor to be calibrated in the same way as the invasive TDP.

As was discussed in Section 5.1.2, the TDP is calibrated by first establishing a resistance-temperature relationship for each thermistor. Then, the conductivity of the bead and the effective

bead radius, which define the heat transfer properties of the thermistor, are determined. This procedure allows for rapid calibration of probes in bulk. Assuming that the noninvasive sensor housing provides sufficient insulation to direct the bulk of heat transfer into the tissue, the same calibration procedure would be adequate. This assumption can be tested by performing the standard calibration in a 4π geometry and comparing data taken from its use in a 2π geometry (surface application).

6.8 Sensor Assembly

The final sensor will be assembled from its component parts:

- Thermistors :
  - Heat thermistor bead: 0.028" diameter
  - Sense thermistor: 0.017" diameter
  - Positioned 8 to 10 mm apart, extending from medical grade catheter tubing (see Figure 6.10A)
- Extruded Housing
  - Flexible medical-grade Santoprene thermoplastic
  - Extruded with given cross-sectional design
  - Channels along length of extrusion designed to hold thermistors with hemispherical bead protrusion
- Foam pad
  - Skin-compatible, removable adhesive coating on side applied to the skin
  - Thermally insulating foam material

Figure 6.9 presents the cross section of the thermistor housing with thermistors placed in the extruded channels. Note that the beads are insulated from the environment by the housing design, which minimizes the area of contact between the projections from the housing and incorporates pockets of air within the space around the thermistors. The interface with the skin on the bottom face of the housing allows a hemispherical portion of the thermistors to protrude a maximum distance of 0.35 mm into the skin, which is a much smaller depth than that at which perfusion would be affected (1.5 mm).

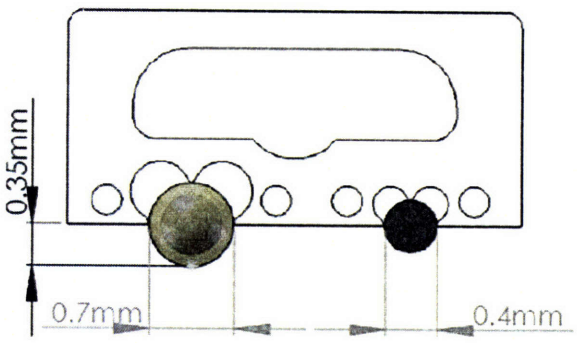

Figure 6.9 Cross-section of thermistor beads placed in sensor housing

The final assembly of the sensor is shown in Figure 6.10. First, the thermistors are incorporated into the extruded housing such that the lead wires wrap around the end of the housing and into the catheter tubing, which is contained in the upper portion of the housing (Figure 6.10B). The extrusion is then laid into the adhesive face of a foam pad such that the bottom of the extrusion is flush with the adhesive face of the foam (Figure 6.10C).

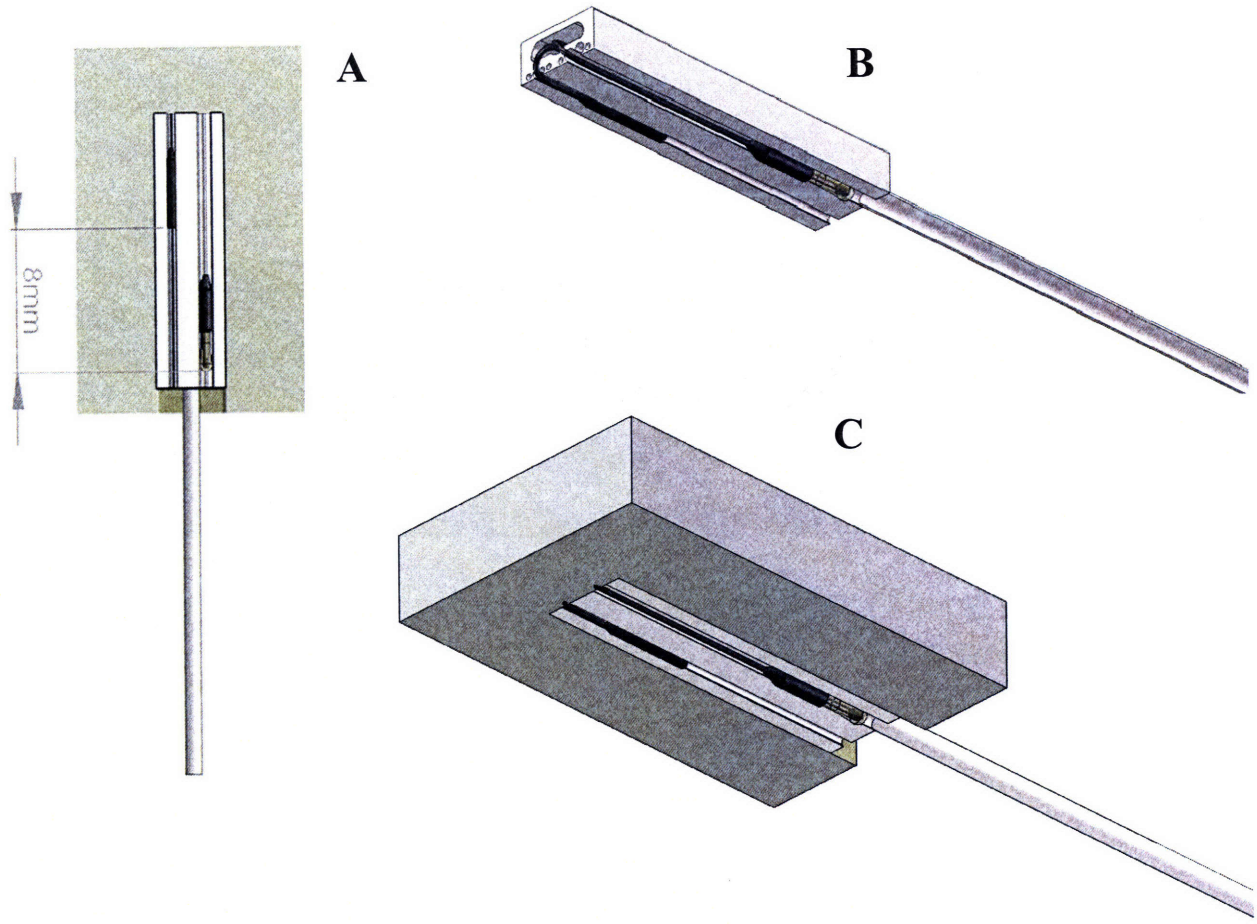

Figure 6.10 Complete assembly of proposed noninvasive surface perfusion sensor. (A) Bottom face of proposed sensor indicating relative distance from heat thermistor to sense thermistor. (B) Housing with thermistors placed in extruded channels and electrical leads fed into tubing within the housing. (C) Final assembly showing placement in adhesive foam pad.

An assembled sensor will be applied to the surface of skin tissue where contact pressure is maintained by the adhesive on bottom face of the enclosing foam insulator. A suitable wetting agent can be used to enhance thermal communication and reduce contact resistance.

Figure 6.11 provides a schematic cross-section of the final sensor assembly on the surface of a tissue.

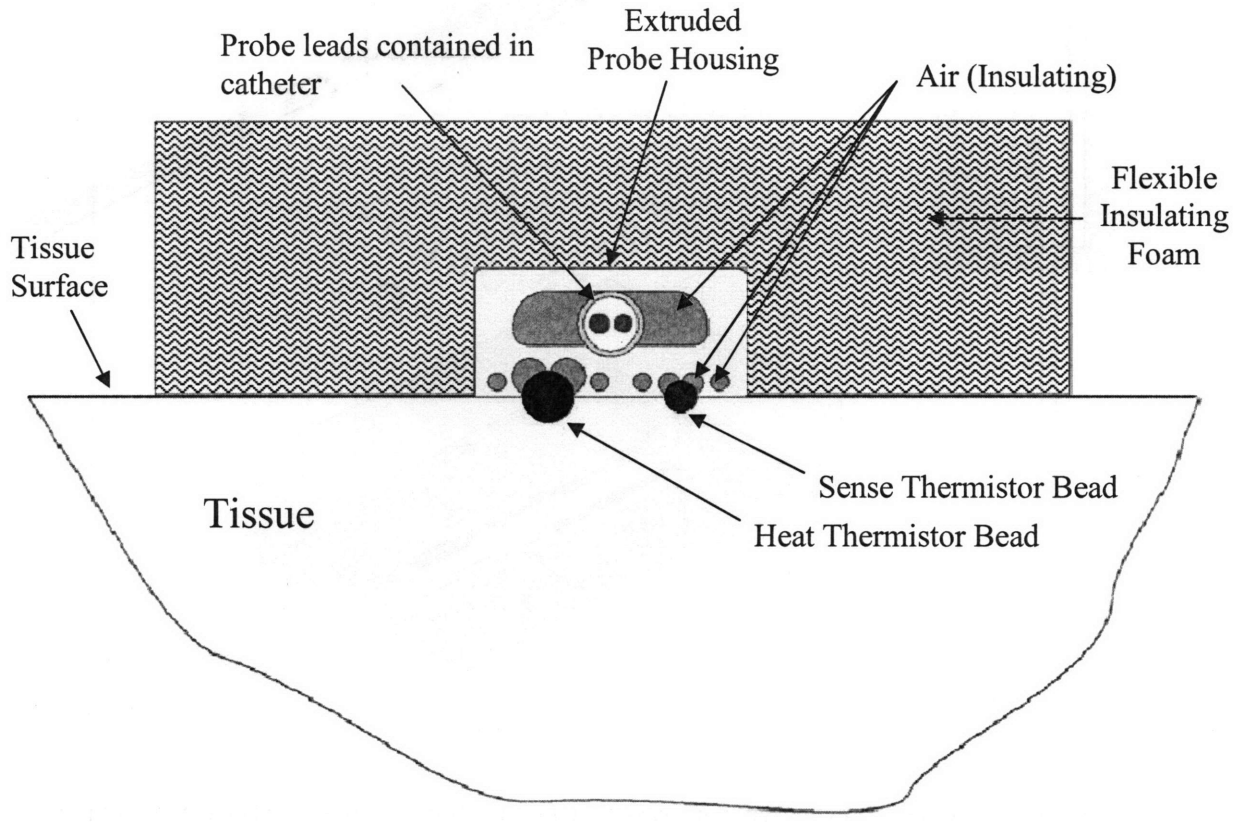

Figure 6.11 Schematic cross-section of assembled noninvasive sensor resting on surface of tissue

Chapter 7. Conclusion and Recommendations

The goal of this research was to investigate the use of a noninvasive thermal perfusion sensor in tests of post-occlusive reactive hyperemia for the determination of endothelial dysfunction as detected in the digital skin tissue. To do this, several steps were taken that reflect the breadth and potential in this field of research.

I explored the physiological mechanisms of skin tissue perfusion and reactive hyperemia and considered how endothelial dysfunction may deregulate such mechanisms. The current research suggests that skin microcirculation is an appropriate vascular bed for independent assessment of endothelial dysfunction, although the fundamental mechanisms of reactive hyperemia may not be the same as for conduit artery reactivity. Furthermore, there are regulatory components in the time course of skin perfusion which may be differentially affected by disease states. Therefore, absolute and continuous measurement of skin perfusion can reveal both temporal as well as functional indices of global cardiovascular health.

I established the current clinical need for noninvasive perfusion measurement technologies and for reliable tests of endothelial dysfunction by reviewing currently available noninvasive methods which hold the greatest promise. Each method has distinct advantages and disadvantages, and it is possible that a combination of these technologies can offer a greater depth of understanding. The gap in cardiovascular risk detection occurs in people who have no clinical symptoms of disease. Therefore, it is vital to develop new technologies which are safe, reliable, noninvasive, inexpensive, and standardized between operators. As I have shown, thermal perfusion monitoring has the potential to meet all these needs and can also reflect the dynamic biology of the endothelium throughout the progression of atherosclerotic disease by offering absolute parameters of functional health. It is possible that, with further development and clinical studies, these parameters could provide prognostic information for patients and encourage individuals to improve their overall state of health, as endothelial dysfunction has been shown to be reversible. In addition to noninvasive applications, such a device could provide quantitative analysis of the microcirculation during surgery (transplant, cardiac, vascular, neurological, plastic, etc.), wound healing, tumor therapy and intensive care medicine.

I have performed an extensive review of the scientific literature regarding the systemic impact of endothelial dysfunction and its manifestations in the coronary, conduit, and microvascular circulations. These interrelations are necessary to establish validity for a technique which measures endothelial dysfunction in the peripheral circulation as a surrogate for the coronary circulation, where most cardiac complications occur. I discovered a clear need for a simple, noninvasive diagnostic tool for endothelial dysfunction in both experimental and clinical settings to evaluate and monitor the microvascular consequence of conditions such as heart disease, peripheral arterial disease, hypertension, shock, or diabetes.

I have also summarized the technological innovations that have led to the development of the minimally invasive Thermal Diffusion Probe (TDP), which measures absolute tissue perfusion in small volumes of tissue. This technology forms the foundation for the thermal method that I propose to use to measure skin blood flow. Its validation in minimally invasive applications has positioned it for a natural step toward research in noninvasive applications.

The final part of my thesis consisted of investigating the feasibility of a noninvasive thermal sensor by performing preliminary tests of PORH on the digital skin of volunteers using a modified TDP. Although no conclusions could be drawn due to the small set of subject data, I have taken significant steps to establish a protocol for reproducible measurement techniques. Moreover, it is clear from the acquired data that surface perfusion can be accurately tracked in real-time with a simple surface application of the exposed thermistor beads when care is taken to insulate the surrounding environment. A presentation of representative data analysis further establishes the potential parameters that can be used to gauge microvascular reactivity in the skin using a thermal method.

Finally, I have presented the steps taken to design and manufacture a truly noninvasive perfusion sensor based on the thermal requirements of a tissue surface perfusion measurement. Extensive computer-assisted modeling was carried out to arrive at a suitable sensor design, while communication with industrial manufacturers has further refined the feasible specifications of such a design.

Further investigations should apply the design contained herein to establish the feasibility of measuring surface perfusion using a sensor calibrated for invasive applications. While the design of the sensor housing is a key step in facilitating this simplification of the thermal model, it is necessary to test this hypothesis. Steps may also be taken toward establishing a dedicated method of calibrating sensors noninvasively. The measurement issues discussed in Chapter 5 should serve as guidelines for improving the measurement technique and enhancing reproducibility. Once a sensor has been shown to measure perfusion in skin tissue in a reproducible and reliable way (measuring temporal variations and absolute magnitude of perfusion), a more extensive clinical study needs to be carried out to establish a link between thermal sensor-derived parameters of reactive hyperemia and cardiovascular risk.

Chapter 8. Bibliography

1. Anderson, T.J., *Assessment and treatment of endothelial dysfunction in humans.* J Am Coll Cardiol, 1999. **34**(3): p. 631-638.
2. Reddy, K.G., Nair, R.N., Sheehan, H.M., and Hodgson, J.M., *Evidence that selective endothelial dysfunction may occur in the absence of angiographic or ultrasound atherosclerosis in patients with risk factors for atherosclerosis.* J Am Coll Cardiol, 1994. **23**(4): p. 833-843.
3. Munzel, T., Sinning, C., Post, F., Warnholtz, A., and Schulz, E., *Pathophysiology, diagnosis and prognostic implications of endothelial dysfunction.* Ann Med, 2008. **40**(3): p. 180-196.
4. Furnas, H. and Rosen, J.M., *Monitoring in microvascular surgery.* Ann Plast Surg, 1991. **26**(3): p. 265-272.
5. Maitz, P.K., Khot, M.B., Mayer, H.F., Martin, G.T., Pribaz, J.J., Bowman, H.F., and Orgill, D.P., *Continuous and real-time blood perfusion monitoring in prefabricated flaps.* J Reconstr Microsurg, 2004. **20**(1): p. 35-41.
6. Bowman, H., *Estimation of tissue blood flow*, in *Heat Transfer in Medicine and Biology*, A.S.a.R.C. Eberhart, Editor. 1985, Plenum: New York. p. 193-230.
7. Klar, E., Kraus, T., Bredt, M., Osswald, B., Senninger, N., Herfarth, C., and Otto, G., *First clinical realization of continuous monitoring of liver microcirculation after transplantation by thermodiffusion.* Transpl Int, 1996. **9 Suppl 1**: p. S140-143.
8. Vajkoczy, P., Roth, H., Horn, P., Lucke, T., Thome, C., Hubner, U., Martin, G.T., Zappletal, C., Klar, E., Schilling, L., and Schmiedek, P., *Continuous monitoring of regional cerebral blood flow: experimental and clinical validation of a novel thermal diffusion microprobe.* J Neurosurg, 2000. **93**(2): p. 265-274.
9. Mayrovitz, H.N., *Assessment of Human Microvascular Function*, in *Analysis of Cardiovascular Function*, G. Drzewiecki, Editor. 1998. p. 248.
10. Braverman, I.M., *The cutaneous microcirculation: ultrastructure and microanatomical organization.* Microcirculation, 1997. **4**(3): p. 329-340.
11. Midttun, M. and Sejrsen, P., *Blood flow rate in arteriovenous anastomoses and capillaries in thumb, first toe, ear lobe, and nose.* Clin Physiol, 1996. **16**(3): p. 275-289.
12. Grant, R.T. and Bland, E.F., *Observations on arteriovenous anastomoses in human skin and in the bird's foot with special reference to the reaction to cold.* . Heart, 1931. **15**: p. 385-407.
13. Swain, I.D. and Grant, L.J., *Methods of measuring skin blood flow.* Phys Med Biol, 1989. **34**(2): p. 151-175.
14. Singh, S. and Swerlick, R.A., *Structure and function of the cutaneous vasculature*, in *The Biology of the Skin*, R.K. Freinkel and D. Woodley, Editors. 2001, Parthenon: New York, NY. p. 177-189.
15. Berne, R.M., Levy, M.N., Koeppen, B.M., and Stanton, B.A., eds. *Physiology*. 5 ed. 2004, Elsevier Mosby: St. Louis, MO.
16. Furchgott, R.F. and Zawadzki, J.V., *The obligatory role of endothelial cells in the relaxation of arterial smooth muscle by acetylcholine.* Nature, 1980. **288**(5789): p. 373-376.
17. Palmer, R.M., Ferrige, A.G., and Moncada, S., *Nitric oxide release accounts for the biological activity of endothelium-derived relaxing factor.* Nature, 1987. **327**(6122): p. 524-526.

18. Palmer, R.M., Ashton, D.S., and Moncada, S., *Vascular endothelial cells synthesize nitric oxide from L-arginine.* Nature, 1988. **333**(6174): p. 664-666.

19. Verma, S., Buchanan, M.R., and Anderson, T.J., *Endothelial function testing as a biomarker of vascular disease.* Circulation, 2003. **108**(17): p. 2054-2059.

20. Luscher, T.F. and Noll, G., *The pathogenesis of cardiovascular disease: role of the endothelium as a target and mediator.* Atherosclerosis, 1995. **118 Suppl**: p. S81-90.

21. Charkoudian, N., *Skin blood flow in adult human thermoregulation: how it works, when it does not, and why.* Mayo Clin Proc, 2003. **78**(5): p. 603-612.

22. Clough, G.F. and Church, M.K., *Vascular responses in the skin: an accessible model of inflammation.* News Physiol Sci, 2002. **17**: p. 170-174.

23. Savage, M.V. and Brengelmann, G.L., *Control of skin blood flow in the neutral zone of human body temperature regulation.* J Appl Physiol, 1996. **80**(4): p. 1249-1257.

24. Rossi, M., Carpi, A., Galetta, F., Franzoni, F., and Santoro, G., *The investigation of skin blood flowmotion: a new approach to study the microcirculatory impairment in vascular diseases?* Biomed Pharmacother, 2006. **60**(8): p. 437-442.

25. Stefanovska, A., Bracic, M., and Kvernmo, H.D., *Wavelet analysis of oscillations in the peripheral blood circulation measured by laser Doppler technique.* IEEE Trans Biomed Eng, 1999. **46**(10): p. 1230-1239.

26. Kvandal, P., Stefanovska, A., Veber, M., Kvernmo, H.D., and Kirkeboen, K.A., *Regulation of human cutaneous circulation evaluated by laser Doppler flowmetry, iontophoresis, and spectral analysis: importance of nitric oxide and prostaglandines.* Microvasc Res, 2003. **65**(3): p. 160-171.

27. Cracowski, J.L., Minson, C.T., Salvat-Melis, M., and Halliwill, J.R., *Methodological issues in the assessment of skin microvascular endothelial function in humans.* Trends Pharmacol Sci, 2006. **27**(9): p. 503-508.

28. Loscalzo, J. and Vita, J.A., *Ischemia, hyperemia, exercise, and nitric oxide. Complex physiology and complex molecular adaptations.* Circulation, 1994. **90**(5): p. 2556-2559.

29. Higashi, Y., Sasaki, S., Nakagawa, K., Matsuura, H., Kajiyama, G., and Oshima, T., *A noninvasive measurement of reactive hyperemia that can be used to assess resistance artery endothelial function in humans.* Am J Cardiol, 2001. **87**(1): p. 121-125, A129.

30. Meredith, I.T., Currie, K.E., Anderson, T.J., Roddy, M.A., Ganz, P., and Creager, M.A., *Postischemic vasodilation in human forearm is dependent on endothelium-derived nitric oxide.* Am J Physiol, 1996. **270**(4 Pt 2): p. H1435-1440.

31. Khan, F., Elhadd, T.A., Greene, S.A., and Belch, J.J., *Impaired skin microvascular function in children, adolescents, and young adults with type 1 diabetes.* Diabetes Care, 2000. **23**(2): p. 215-220.

32. Bonetti, P.O., Lerman, L.O., and Lerman, A., *Endothelial dysfunction: a marker of atherosclerotic risk.* Arterioscler Thromb Vasc Biol, 2003. **23**(2): p. 168-175.

33. Esper, R.J., Nordaby, R.A., Vilarino, J.O., Paragano, A., Cacharron, J.L., and Machado, R.A., *Endothelial dysfunction: a comprehensive appraisal.* Cardiovasc Diabetol, 2006. **5**: p. 4.

34. Cai, H. and Harrison, D.G., *Endothelial dysfunction in cardiovascular diseases: the role of oxidant stress.* Circ Res, 2000. **87**(10): p. 840-844.

35. Quyyumi, A.A., *Prognostic value of endothelial function.* Am J Cardiol, 2003. **91**(12A): p. 19H-24H.

36. Lerman, A. and Burnett, J.C., Jr., *Intact and altered endothelium in regulation of vasomotion.* Circulation, 1992. **86**(6 Suppl): p. III12-19.

37. Vogel, R.A., *Cholesterol lowering and endothelial function.* Am J Med, 1999. **107**(5): p. 479-487.

38. Taddei, S., Virdis, A., Ghiadoni, L., Sudano, I., and Salvetti, A., *Effects of antihypertensive drugs on endothelial dysfunction: clinical implications.* Drugs, 2002. **62**(2): p. 265-284.

39. Celermajer, D.S., Sorensen, K.E., Georgakopoulos, D., Bull, C., Thomas, O., Robinson, J., and Deanfield, J.E., *Cigarette smoking is associated with dose-related and potentially reversible impairment of endothelium-dependent dilation in healthy young adults.* Circulation, 1993. **88**(5 Pt 1): p. 2149-2155.

40. Vita, J.A. and Keaney, J.F., Jr., *Hormone replacement therapy and endothelial function: the exception that proves the rule?* Arterioscler Thromb Vasc Biol, 2001. **21**(12): p. 1867-1869.

41. Doshi, S.N., McDowell, I.F., Moat, S.J., Lang, D., Newcombe, R.G., Kredan, M.B., Lewis, M.J., and Goodfellow, J., *Folate improves endothelial function in coronary artery disease: an effect mediated by reduction of intracellular superoxide?* Arterioscler Thromb Vasc Biol, 2001. **21**(7): p. 1196-1202.

42. Hambrecht, R., Fiehn, E., Weigl, C., Gielen, S., Hamann, C., Kaiser, R., Yu, J., Adams, V., Niebauer, J., and Schuler, G., *Regular physical exercise corrects endothelial dysfunction and improves exercise capacity in patients with chronic heart failure.* Circulation, 1998. **98**(24): p. 2709-2715.

43. Celermajer, D.S., Sorensen, K.E., Spiegelhalter, D.J., Georgakopoulos, D., Robinson, J., and Deanfield, J.E., *Aging is associated with endothelial dysfunction in healthy men years before the age-related decline in women.* J Am Coll Cardiol, 1994. **24**(2): p. 471-476.

44. Taddei, S., Virdis, A., Mattei, P., Ghiadoni, L., Gennari, A., Fasolo, C.B., Sudano, I., and Salvetti, A., *Aging and endothelial function in normotensive subjects and patients with essential hypertension.* Circulation, 1995. **91**(7): p. 1981-1987.

45. Tao, J., Jin, Y.F., Yang, Z., Wang, L.C., Gao, X.R., Lui, L., and Ma, H., *Reduced arterial elasticity is associated with endothelial dysfunction in persons of advancing age: comparative study of noninvasive pulse wave analysis and laser Doppler blood flow measurement.* Am J Hypertens, 2004. **17**(8): p. 654-659.

46. Gerhard, M., Roddy, M.A., Creager, S.J., and Creager, M.A., *Aging progressively impairs endothelium-dependent vasodilation in forearm resistance vessels of humans.* Hypertension, 1996. **27**(4): p. 849-853.

47. Mancini, G.B., Henry, G.C., Macaya, C., O'Neill, B.J., Pucillo, A.L., Carere, R.G., Wargovich, T.J., Mudra, H., Luscher, T.F., Klibaner, M.I., Haber, H.E., Uprichard, A.C., Pepine, C.J., and Pitt, B., *Angiotensin-converting enzyme inhibition with quinapril improves endothelial vasomotor dysfunction in patients with coronary artery disease. The TREND (Trial on Reversing ENdothelial Dysfunction) Study.* Circulation, 1996. **94**(3): p. 258-265.

48. Higashi, Y., Sasaki, S., Nakagawa, K., Ueda, T., Yoshimizu, A., Kurisu, S., Matsuura, H., Kajiyama, G., and Oshima, T., *A comparison of angiotensin-converting enzyme inhibitors, calcium antagonists, beta-blockers and diuretic agents on reactive hyperemia in patients with essential hypertension: a multicenter study.* J Am Coll Cardiol, 2000. **35**(2): p. 284-291.

49. Bush, D.E., Jones, C.E., Bass, K.M., Walters, G.K., Bruza, J.M., and Ouyang, P., *Estrogen replacement reverses endothelial dysfunction in postmenopausal women.* Am J Med, 1998. **104**(6): p. 552-558.

50. Gerhard, M., Walsh, B.W., Tawakol, A., Haley, E.A., Creager, S.J., Seely, E.W., Ganz, P., and Creager, M.A., *Estradiol therapy combined with progesterone and endothelium-dependent vasodilation in postmenopausal women.* Circulation, 1998. **98**(12): p. 1158-1163.

51. Antoniades, C., Tousoulis, D., Vasiliadou, C., Marinou, K., Tentolouris, C., Ntarladimas, I., and Stefanadis, C., *Combined effects of smoking and hypercholesterolemia on inflammatory process, thrombosis/fibrinolysis system, and forearm hyperemic response.* Am J Cardiol, 2004. **94**(9): p. 1181-1184.

52. Kullo, I.J., Malik, A.R., Santos, S., Ehrsam, J.E., and Turner, S.T., *Association of cardiovascular risk factors with microvascular and conduit artery function in hypertensive subjects.* Am J Hypertens, 2007. **20**(7): p. 735-742.

53. Lerman, A., Burnett, J.C., Jr., Higano, S.T., McKinley, L.J., and Holmes, D.R., Jr., *Long-term L-arginine supplementation improves small-vessel coronary endothelial function in humans.* Circulation, 1998. **97**(21): p. 2123-2128.

54. Celermajer, D.S., Adams, M.R., Clarkson, P., Robinson, J., McCredie, R., Donald, A., and Deanfield, J.E., *Passive smoking and impaired endothelium-dependent arterial dilatation in healthy young adults.* N Engl J Med, 1996. **334**(3): p. 150-154.

55. Hung, J., Lam, J.Y., Lacoste, L., and Letchacovski, G., *Cigarette smoking acutely increases platelet thrombus formation in patients with coronary artery disease taking aspirin.* Circulation, 1995. **92**(9): p. 2432-2436.

56. Clarkson, P., Montgomery, H.E., Mullen, M.J., Donald, A.E., Powe, A.J., Bull, T., Jubb, M., World, M., and Deanfield, J.E., *Exercise training enhances endothelial function in young men.* J Am Coll Cardiol, 1999. **33**(5): p. 1379-1385.

57. DeSouza, C.A., Shapiro, L.F., Clevenger, C.M., Dinenno, F.A., Monahan, K.D., Tanaka, H., and Seals, D.R., *Regular aerobic exercise prevents and restores age-related declines in endothelium-dependent vasodilation in healthy men.* Circulation, 2000. **102**(12): p. 1351-1357.

58. Wang, J.S., Lan, C., Chen, S.Y., and Wong, M.K., *Tai Chi Chuan training is associated with enhanced endothelium-dependent dilation in skin vasculature of healthy older men.* J Am Geriatr Soc, 2002. **50**(6): p. 1024-1030.

59. Clarkson, P., Celermajer, D.S., Donald, A.E., Sampson, M., Sorensen, K.E., Adams, M., Yue, D.K., Betteridge, D.J., and Deanfield, J.E., *Impaired vascular reactivity in insulin-dependent diabetes mellitus is related to disease duration and low density lipoprotein cholesterol levels.* J Am Coll Cardiol, 1996. **28**(3): p. 573-579.

60. Golster, H., Hyllienmark, L., Ledin, T., Ludvigsson, J., and Sjoberg, F., *Impaired microvascular function related to poor metabolic control in young patients with diabetes.* Clin Physiol Funct Imaging, 2005. **25**(2): p. 100-105.

61. Ishibashi, Y., Takahashi, N., Shimada, T., Sugamori, T., Sakane, T., Umeno, T., Hirano, Y., Oyake, N., and Murakami, Y., *Short duration of reactive hyperemia in the forearm of subjects with multiple cardiovascular risk factors.* Circ J, 2006. **70**(1): p. 115-123.

62. Calles-Escandon, J. and Cipolla, M., *Diabetes and endothelial dysfunction: a clinical perspective.* Endocr Rev, 2001. **22**(1): p. 36-52.

63. Clarkson, P., Adams, M.R., Powe, A.J., Donald, A.E., McCredie, R., Robinson, J., McCarthy, S.N., Keech, A., Celermajer, D.S., and Deanfield, J.E., *Oral L-arginine improves endothelium-dependent dilation in hypercholesterolemic young adults.* J Clin Invest, 1996. **97**(8): p. 1989-1994.

64. Cosentino, F., Hishikawa, K., Katusic, Z.S., and Luscher, T.F., *High glucose increases nitric oxide synthase expression and superoxide anion generation in human aortic endothelial cells.* Circulation, 1997. **96**(1): p. 25-28.

65. Verhaar, M.C., Honing, M.L., van Dam, T., Zwart, M., Koomans, H.A., Kastelein, J.J., and Rabelink, T.J., *Nifedipine improves endothelial function in hypercholesterolemia, independently of an effect on blood pressure or plasma lipids.* Cardiovasc Res, 1999. **42**(3): p. 752-760.

66. *Effect of nifedipine and cerivastatin on coronary endothelial function in patients with coronary artery disease: the ENCORE I Study (Evaluation of Nifedipine and Cerivastatin On Recovery of coronary Endothelial function).* Circulation, 2003. **107**(3): p. 422-428.

67. Celermajer, D.S., Sorensen, K.E., Gooch, V.M., Spiegelhalter, D.J., Miller, O.I., Sullivan, I.D., Lloyd, J.K., and Deanfield, J.E., *Non-invasive detection of endothelial dysfunction in children and adults at risk of atherosclerosis.* Lancet, 1992. **340**(8828): p. 1111-1115.

68. Celermajer, D.S., Sorensen, K.E., Bull, C., Robinson, J., and Deanfield, J.E., *Endothelium-dependent dilation in the systemic arteries of asymptomatic subjects relates to coronary risk factors and their interaction.* J Am Coll Cardiol, 1994. **24**(6): p. 1468-1474.

69. Stroes, E.S., Koomans, H.A., de Bruin, T.W., and Rabelink, T.J., *Vascular function in the forearm of hypercholesterolaemic patients off and on lipid-lowering medication.* Lancet, 1995. **346**(8973): p. 467-471.

70. Haak, E., Abletshauser, C., Weber, S., Goedicke, C., Martin, N., Hermanns, N., Lackner, K., Kusterer, K., Usadel, K.H., and Haak, T., *Fluvastatin therapy improves microcirculation in patients with hyperlipidaemia.* Atherosclerosis, 2001. **155**(2): p. 395-401.

71. Binggeli, C., Spieker, L.E., Corti, R., Sudano, I., Stojanovic, V., Hayoz, D., Luscher, T.F., and Noll, G., *Statins enhance postischemic hyperemia in the skin circulation of hypercholesterolemic patients: a monitoring test of endothelial dysfunction for clinical practice?* J Am Coll Cardiol, 2003. **42**(1): p. 71-77.

72. Egashira, K., Hirooka, Y., Kai, H., Sugimachi, M., Suzuki, S., Inou, T., and Takeshita, A., *Reduction in serum cholesterol with pravastatin improves endothelium-dependent coronary vasomotion in patients with hypercholesterolemia.* Circulation, 1994. **89**(6): p. 2519-2524.

73. Laufs, U., Wassmann, S., Hilgers, S., Ribaudo, N., Bohm, M., and Nickenig, G., *Rapid effects on vascular function after initiation and withdrawal of atorvastatin in healthy, normocholesterolemic men.* Am J Cardiol, 2001. **88**(11): p. 1306-1307.

74. Treasure, C.B., Klein, J.L., Weintraub, W.S., Talley, J.D., Stillabower, M.E., Kosinski, A.S., Zhang, J., Boccuzzi, S.J., Cedarholm, J.C., and Alexander, R.W., *Beneficial effects of cholesterol-lowering therapy on the coronary endothelium in patients with coronary artery disease.* N Engl J Med, 1995. **332**(8): p. 481-487.

75. Panza, J.A., Quyyumi, A.A., Brush, J.E., Jr., and Epstein, S.E., *Abnormal endothelium-dependent vascular relaxation in patients with essential hypertension.* N Engl J Med, 1990. **323**(1): p. 22-27.

76. Panza, J.A., Casino, P.R., Kilcoyne, C.M., and Quyyumi, A.A., *Role of endothelium-derived nitric oxide in the abnormal endothelium-dependent vascular relaxation of patients with essential hypertension.* Circulation, 1993. **87**(5): p. 1468-1474.

77. Perticone, F., Ceravolo, R., Pujia, A., Ventura, G., Iacopino, S., Scozzafava, A., Ferraro, A., Chello, M., Mastroroberto, P., Verdecchia, P., and Schillaci, G., *Prognostic significance of endothelial dysfunction in hypertensive patients.* Circulation, 2001. **104**(2): p. 191-196.

78. Tamai, O., Matsuoka, H., Itabe, H., Wada, Y., Kohno, K., and Imaizumi, T., *Single LDL apheresis improves endothelium-dependent vasodilatation in hypercholesterolemic humans.* Circulation, 1997. **95**(1): p. 76-82.

79. Sorensen, K.E., Celermajer, D.S., Georgakopoulos, D., Hatcher, G., Betteridge, D.J., and Deanfield, J.E., *Impairment of endothelium-dependent dilation is an early event in children with familial hypercholesterolemia and is related to the lipoprotein(a) level.* J Clin Invest, 1994. **93**(1): p. 50-55.

80. Mullen, M.J., Kharbanda, R.K., Cross, J., Donald, A.E., Taylor, M., Vallance, P., Deanfield, J.E., and MacAllister, R.J., *Heterogenous nature of flow-mediated dilatation in human conduit arteries in vivo: relevance to endothelial dysfunction in hypercholesterolemia.* Circ Res, 2001. **88**(2): p. 145-151.

81. Casino, P.R., Kilcoyne, C.M., Quyyumi, A.A., Hoeg, J.M., and Panza, J.A., *The role of nitric oxide in endothelium-dependent vasodilation of hypercholesterolemic patients.* Circulation, 1993. **88**(6): p. 2541-2547.

82. Creager, M.A., Cooke, J.P., Mendelsohn, M.E., Gallagher, S.J., Coleman, S.M., Loscalzo, J., and Dzau, V.J., *Impaired vasodilation of forearm resistance vessels in hypercholesterolemic humans.* J Clin Invest, 1990. **86**(1): p. 228-234.

83. Kaufmann, P.A., Gnecchi-Ruscone, T., di Terlizzi, M., Schafers, K.P., Luscher, T.F., and Camici, P.G., *Coronary heart disease in smokers: vitamin C restores coronary microcirculatory function.* Circulation, 2000. **102**(11): p. 1233-1238.

84. Skyrme-Jones, R.A., O'Brien, R.C., Berry, K.L., and Meredith, I.T., *Vitamin E supplementation improves endothelial function in type I diabetes mellitus: a randomized, placebo-controlled study.* J Am Coll Cardiol, 2000. **36**(1): p. 94-102.

85. Skyrme-Jones, R.A., O'Brien, R.C., Luo, M., and Meredith, I.T., *Endothelial vasodilator function is related to low-density lipoprotein particle size and low-density lipoprotein vitamin E content in type 1 diabetes.* J Am Coll Cardiol, 2000. **35**(2): p. 292-299.

86. Barretto, S., Ballman, K.V., Rooke, T.W., and Kullo, I.J., *Early-onset peripheral arterial occlusive disease: clinical features and determinants of disease severity and location.* Vasc Med, 2003. **8**(2): p. 95-100.

87. Verhaar, M.C., Stroes, E., and Rabelink, T.J., *Folates and cardiovascular disease.* Arterioscler Thromb Vasc Biol, 2002. **22**(1): p. 6-13.

88. Doshi, S.N., McDowell, I.F., Moat, S.J., Payne, N., Durrant, H.J., Lewis, M.J., and Goodfellow, J., *Folic acid improves endothelial function in coronary artery disease via mechanisms largely independent of homocysteine lowering.* Circulation, 2002. **105**(1): p. 22-26.

89. Higashi, Y., Sasaki, S., Nakagawa, K., Matsuura, H., Chayama, K., and Oshima, T., *Effect of obesity on endothelium-dependent, nitric oxide-mediated vasodilation in normotensive individuals and patients with essential hypertension.* Am J Hypertens, 2001. **14**(10): p. 1038-1045.

90. Al Suwaidi, J., Higano, S.T., Holmes, D.R., Jr., Lennon, R., and Lerman, A., *Obesity is independently associated with coronary endothelial dysfunction in patients with normal or mildly diseased coronary arteries.* J Am Coll Cardiol, 2001. **37**(6): p. 1523-1528.

91. Ziccardi, P., Nappo, F., Giugliano, G., Esposito, K., Marfella, R., Cioffi, M., D'Andrea, F., Molinari, A.M., and Giugliano, D., *Reduction of inflammatory cytokine concentrations and improvement of endothelial functions in obese women after weight loss over one year.* Circulation, 2002. **105**(7): p. 804-809.

92. Kubo, S.H., Rector, T.S., Bank, A.J., Williams, R.E., and Heifetz, S.M., *Endothelium-dependent vasodilation is attenuated in patients with heart failure.* Circulation, 1991. **84**(4): p. 1589-1596.

93. Fischer, D., Rossa, S., Landmesser, U., Spiekermann, S., Engberding, N., Hornig, B., and Drexler, H., *Endothelial dysfunction in patients with chronic heart failure is independently associated with increased incidence of hospitalization, cardiac transplantation, or death.* Eur Heart J, 2005. **26**(1): p. 65-69.

94. Hadi, H.A., Carr, C.S., and Al Suwaidi, J., *Endothelial dysfunction: cardiovascular risk factors, therapy, and outcome.* Vasc Health Risk Manag, 2005. **1**(3): p. 183-198.

95. Goodfellow, J., Bellamy, M.F., Ramsey, M.W., Jones, C.J., and Lewis, M.J., *Dietary supplementation with marine omega-3 fatty acids improve systemic large artery endothelial function in subjects with hypercholesterolemia.* J Am Coll Cardiol, 2000. **35**(2): p. 265-270.

96. Chambers, J.C., McGregor, A., Jean-Marie, J., Obeid, O.A., and Kooner, J.S., *Demonstration of rapid onset vascular endothelial dysfunction after hyperhomocysteinemia: an effect reversible with vitamin C therapy.* Circulation, 1999. **99**(9): p. 1156-1160.

97. Chambers, J.C., Obeid, O.A., and Kooner, J.S., *Physiological increments in plasma homocysteine induce vascular endothelial dysfunction in normal human subjects.* Arterioscler Thromb Vasc Biol, 1999. **19**(12): p. 2922-2927.

98. Husain, S., Andrews, N.P., Mulcahy, D., Panza, J.A., and Quyyumi, A.A., *Aspirin improves endothelial dysfunction in atherosclerosis.* Circulation, 1998. **97**(8): p. 716-720.

99. Stewart, J., Kohen, A., Brouder, D., Rahim, F., Adler, S., Garrick, R., and Goligorsky, M.S., *Noninvasive interrogation of microvasculature for signs of endothelial dysfunction in patients with chronic renal failure.* Am J Physiol Heart Circ Physiol, 2004. **287**(6): p. H2687-2696.

100. Annuk, M., Lind, L., Linde, T., and Fellstrom, B., *Impaired endothelium-dependent vasodilatation in renal failure in humans.* Nephrol Dial Transplant, 2001. **16**(2): p. 302-306.

101. Fichtlscherer, S., Rosenberger, G., Walter, D.H., Breuer, S., Dimmeler, S., and Zeiher, A.M., *Elevated C-reactive protein levels and impaired endothelial vasoreactivity in patients with coronary artery disease.* Circulation, 2000. **102**(9): p. 1000-1006.

102. Prasad, A., Zhu, J., Halcox, J.P., Waclawiw, M.A., Epstein, S.E., and Quyyumi, A.A., *Predisposition to atherosclerosis by infections: role of endothelial dysfunction.* Circulation, 2002. **106**(2): p. 184-190.

103. Kasprzak, J.D., Klosinska, M., and Drozdz, J., *Clinical aspects of assessment of endothelial function.* Pharmacol Rep, 2006. **58 Suppl**: p. 33-40.

104. Kannel, W.B., Sorlie, P., and McNamara, P.M., *Prognosis after initial myocardial infarction: the Framingham study.* Am J Cardiol, 1979. **44**(1): p. 53-59.

105. Anderson, T.J., Gerhard, M.D., Meredith, I.T., Charbonneau, F., Delagrange, D., Creager, M.A., Selwyn, A.P., and Ganz, P., *Systemic nature of endothelial dysfunction in atherosclerosis.* Am J Cardiol, 1995. **75**(6): p. 71B-74B.

106. Anderson, T.J., Uehata, A., Gerhard, M.D., Meredith, I.T., Knab, S., Delagrange, D., Lieberman, E.H., Ganz, P., Creager, M.A., Yeung, A.C., and et al., *Close relation of endothelial function in the human coronary and peripheral circulations.* J Am Coll Cardiol, 1995. **26**(5): p. 1235-1241.

107. Takase, B., Uehata, A., Akima, T., Nagai, T., Nishioka, T., Hamabe, A., Satomura, K., Ohsuzu, F., and Kurita, A., *Endothelium-dependent flow-mediated vasodilation in coronary and brachial arteries in suspected coronary artery disease.* Am J Cardiol, 1998. **82**(12): p. 1535-1539, A1537-1538.

108. Marcus, M.L., Chilian, W.M., Kanatsuka, H., Dellsperger, K.C., Eastham, C.L., and Lamping, K.G., *Understanding the coronary circulation through studies at the microvascular level.* Circulation, 1990. **82**(1): p. 1-7.

109. Chilian, W.M., *Coronary microcirculation in health and disease. Summary of an NHLBI workshop.* Circulation, 1997. **95**(2): p. 522-528.

110. Kaufmann, P.A., Gnecchi-Ruscone, T., Schafers, K.P., Luscher, T.F., and Camici, P.G., *Low density lipoprotein cholesterol and coronary microvascular dysfunction in hypercholesterolemia.* J Am Coll Cardiol, 2000. **36**(1): p. 103-109.

111. Antonios, T.F., Kaski, J.C., Hasan, K.M., Brown, S.J., and Singer, D.R., *Rarefaction of skin capillaries in patients with anginal chest pain and normal coronary arteriograms.* Eur Heart J, 2001. **22**(13): p. 1144-1148.

112. Ijzerman, R.G., de Jongh, R.T., Beijk, M.A., van Weissenbruch, M.M., Delemarre-van de Waal, H.A., Serne, E.H., and Stehouwer, C.D., *Individuals at increased coronary heart disease risk are characterized by an impaired microvascular function in skin.* Eur J Clin Invest, 2003. **33**(7): p. 536-542.

113. Serne, E.H., RG, I.J., Gans, R.O., Nijveldt, R., De Vries, G., Evertz, R., Donker, A.J., and Stehouwer, C.D., *Direct evidence for insulin-induced capillary recruitment in skin of healthy subjects during physiological hyperinsulinemia.* Diabetes, 2002. **51**(5): p. 1515-1522.

114. Tooke, J.E., Lins, P.E., Ostergren, J., Adamson, U., and Fagrell, B., *The effects of intravenous insulin infusion on skin microcirculatory flow in Type 1 diabetes.* Int J Microcirc Clin Exp, 1985. **4**(1): p. 69-83.

115. Caballero, A.E., Arora, S., Saouaf, R., Lim, S.C., Smakowski, P., Park, J.Y., King, G.L., LoGerfo, F.W., Horton, E.S., and Veves, A., *Microvascular and macrovascular reactivity is reduced in subjects at risk for type 2 diabetes.* Diabetes, 1999. **48**(9): p. 1856-1862.

116. Irving, R.J., Walker, B.R., Noon, J.P., Watt, G.C., Webb, D.J., and Shore, A.C., *Microvascular correlates of blood pressure, plasma glucose, and insulin resistance in health.* Cardiovasc Res, 2002. **53**(1): p. 271-276.

117. Serne, E.H., Gans, R.O., ter Maaten, J.C., Tangelder, G.J., Donker, A.J., and Stehouwer, C.D., *Impaired skin capillary recruitment in essential hypertension is caused by both functional and structural capillary rarefaction.* Hypertension, 2001. **38**(2): p. 238-242.

118. Serne, E.H., Gans, R.O., ter Maaten, J.C., ter Wee, P.M., Donker, A.J., and Stehouwer, C.D., *Capillary recruitment is impaired in essential hypertension and relates to insulin's metabolic and vascular actions.* Cardiovasc Res, 2001. **49**(1): p. 161-168.

119. Vuilleumier, P., Decosterd, D., Maillard, M., Burnier, M., and Hayoz, D., *Postischemic forearm skin reactive hyperemia is related to cardovascular risk factors in a healthy female population.* J Hypertens, 2002. **20**(9): p. 1753-1757.

120. Khan, F., Litchfield, S.J., and Belch, J.J., *Cutaneous microvascular responses are improved after cholesterol-lowering in patients with peripheral vascular disease and hypercholesterolaemia.* Adv Exp Med Biol, 1997. **428**: p. 49-54.

121. Rauch, U., Osende, J.I., Chesebro, J.H., Fuster, V., Vorchheimer, D.A., Harris, K., Harris, P., Sandler, D.A., Fallon, J.T., Jayaraman, S., and Badimon, J.J., *Statins and cardiovascular diseases: the multiple effects of lipid-lowering therapy by statins.* Atherosclerosis, 2000. **153**(1): p. 181-189.

122. Shamim-Uzzaman, Q.A., Pfenninger, D., Kehrer, C., Chakrabarti, A., Kacirotti, N., Rubenfire, M., Brook, R., and Rajagopalan, S., *Altered cutaneous microvascular responses to reactive hyperaemia in coronary artery disease: a comparative study with conduit vessel responses.* Clin Sci (Lond), 2002. **103**(3): p. 267-273.

123. Hansell, J., Henareh, L., Agewall, S., and Norman, M., *Non-invasive assessment of endothelial function - relation between vasodilatory responses in skin microcirculation and brachial artery.* Clin Physiol Funct Imaging, 2004. **24**(6): p. 317-322.

124. Nakamura, T., Saito, Y., Kato, T., Sumino, H., Hoshino, J., Ono, Z., Sakamaki, T., and Nagai, R., *Flow-mediated vasodilation of a conduit artery in relation to downstream peripheral tissue blood flow during reactive hyperemia in humans.* Jpn Circ J, 1997. **61**(9): p. 772-780.

125. Gori, T., Di Stolfo, G., Sicuro, S., Dragoni, S., Lisi, M., Parker, J.D., and Forconi, S., *Correlation analysis between different parameters of conduit artery and microvascular vasodilation.* Clin Hemorheol Microcirc, 2006. **35**(4): p. 509-515.

126. Joannides, R., Haefeli, W.E., Linder, L., Richard, V., Bakkali, E.H., Thuillez, C., and Luscher, T.F., *Nitric oxide is responsible for flow-dependent dilatation of human peripheral conduit arteries in vivo.* Circulation, 1995. **91**(5): p. 1314-1319.

127. Wong, B.J., Wilkins, B.W., Holowatz, L.A., and Minson, C.T., *Nitric oxide synthase inhibition does not alter the reactive hyperemic response in the cutaneous circulation.* J Appl Physiol, 2003. **95**(2): p. 504-510.

128. Huang, A.L., Silver, A.E., Shvenke, E., Schopfer, D.W., Jahangir, E., Titas, M.A., Shpilman, A., Menzoian, J.O., Watkins, M.T., Raffetto, J.D., Gibbons, G., Woodson, J., Shaw, P.M., Dhadly, M., Eberhardt, R.T., Keaney, J.F., Jr., Gokce, N., and Vita, J.A., *Predictive value of reactive hyperemia for cardiovascular events in patients with peripheral arterial disease undergoing vascular surgery.* Arterioscler Thromb Vasc Biol, 2007. **27**(10): p. 2113-2119.

129. Ludmer, P.L., Selwyn, A.P., Shook, T.L., Wayne, R.R., Mudge, G.H., Alexander, R.W., and Ganz, P., *Paradoxical vasoconstriction induced by acetylcholine in atherosclerotic coronary arteries.* N Engl J Med, 1986. **315**(17): p. 1046-1051.

130. Vita, J.A., Treasure, C.B., Nabel, E.G., McLenachan, J.M., Fish, R.D., Yeung, A.C., Vekshtein, V.I., Selwyn, A.P., and Ganz, P., *Coronary vasomotor response to acetylcholine relates to risk factors for coronary artery disease.* Circulation, 1990. **81**(2): p. 491-497.

131. Linder, L., Kiowski, W., Buhler, F.R., and Luscher, T.F., *Indirect evidence for release of endothelium-derived relaxing factor in human forearm circulation in vivo. Blunted response in essential hypertension.* Circulation, 1990. **81**(6): p. 1762-1767.

132. Panza, J.A., Quyyumi, A.A., Callahan, T.S., and Epstein, S.E., *Effect of antihypertensive treatment on endothelium-dependent vascular relaxation in patients with essential hypertension.* J Am Coll Cardiol, 1993. **21**(5): p. 1145-1151.

133. Cardillo, C., Campia, U., Bryant, M.B., and Panza, J.A., *Increased activity of endogenous endothelin in patients with type II diabetes mellitus.* Circulation, 2002. **106**(14): p. 1783-1787.

134. Drexler, H., Hayoz, D., Munzel, T., Hornig, B., Just, H., Brunner, H.R., and Zelis, R., *Endothelial function in chronic congestive heart failure.* Am J Cardiol, 1992. **69**(19): p. 1596-1601.

135. Heitzer, T., Baldus, S., von Kodolitsch, Y., Rudolph, V., and Meinertz, T., *Systemic endothelial dysfunction as an early predictor of adverse outcome in heart failure.* Arterioscler Thromb Vasc Biol, 2005. **25**(6): p. 1174-1179.

136. Heitzer, T., Schlinzig, T., Krohn, K., Meinertz, T., and Munzel, T., *Endothelial dysfunction, oxidative stress, and risk of cardiovascular events in patients with coronary artery disease.* Circulation, 2001. **104**(22): p. 2673-2678.

137. Noma, K., Higashi, Y., Jitsuiki, D., Hara, K., Kimura, M., Nakagawa, K., Goto, C., Oshima, T., Yoshizumi, M., and Chayama, K., *Smoking activates rho-kinase in smooth muscle cells of forearm vasculature in humans.* Hypertension, 2003. **41**(5): p. 1102-1105.

138. Wilkinson, I.B. and Webb, D.J., *Venous occlusion plethysmography in cardiovascular research: methodology and clinical applications.* Br J Clin Pharmacol, 2001. **52**(6): p. 631-646.

139. Yvonne-Tee, G.B., Rasool, A.H., Halim, A.S., and Rahman, A.R., *Noninvasive assessment of cutaneous vascular function in vivo using capillaroscopy, plethysmography and laser-Doppler instruments: its strengths and weaknesses.* Clin Hemorheol Microcirc, 2006. **34**(4): p. 457-473.

140. Pedrinelli, R., Spessot, M., and Salvetti, A., *Reactive hyperemia during short-term blood flow and pressure changes in the hypertensive forearm.* J Hypertens, 1990. **8**(5): p. 467-471.

141. Joannides, R., Bellien, J., and Thuillez, C., *Clinical methods for the evaluation of endothelial function-- a focus on resistance arteries.* Fundam Clin Pharmacol, 2006. **20**(3): p. 311-320.

142. Cooke, J.P. and Dzau, V.J., *Nitric oxide synthase: role in the genesis of vascular disease.* Annu Rev Med, 1997. **48**: p. 489-509.

143. Corretti, M.C., Anderson, T.J., Benjamin, E.J., Celermajer, D., Charbonneau, F., Creager, M.A., Deanfield, J., Drexler, H., Gerhard-Herman, M., Herrington, D., Vallance, P., Vita, J., and Vogel, R., *Guidelines for the ultrasound assessment of endothelial-dependent flow-mediated vasodilation of the brachial artery: a report of the International Brachial Artery Reactivity Task Force.* J Am Coll Cardiol, 2002. **39**(2): p. 257-265.

144. Betik, A.C., Luckham, V.B., and Hughson, R.L., *Flow-mediated dilation in human brachial artery after different circulatory occlusion conditions.* Am J Physiol Heart Circ Physiol, 2004. **286**(1): p. H442-448.

145. Peretz, A., Leotta, D.F., Sullivan, J.H., Trenga, C.A., Sands, F.N., Aulet, M.R., Paun, M., Gill, E.A., and Kaufman, J.D., *Flow mediated dilation of the brachial artery: an investigation of methods requiring further standardization.* BMC Cardiovasc Disord, 2007. **7**: p. 11.

146. Berardesca, E., Leveque, J.L., and Masson, P., *EEMCO guidance for the measurement of skin microcirculation.* Skin Pharmacol Appl Skin Physiol, 2002. **15**(6): p. 442-456.

147. Fagrell, B., *Advances in microcirculation network evaluation: an update.* Int J Microcirc Clin Exp, 1995. **15 Suppl 1**: p. 34-40.

148. Rendell, M., Saxena, S., and Shah, D., *Cutaneous Blood Flow and Peripheral Resistance in Type II Diabetes as Compared to Intermittent Claudication Patients.* International Journal of Angiology, 2003. **12**(3): p. 166.

149. Catalano, M., Schioppa, S., Sampietro, G., Contini, P., and Ninno, D., *Skin blood flow during vasoconstrictive and vasodilative stimuli in essential hypertension patients: a laser Doppler flowmetry study.* Int J Microcirc Clin Exp, 1997. **17**(2): p. 80-85.

150. Farkas, K., Kolossvary, E., Jarai, Z., Nemcsik, J., and Farsang, C., *Non-invasive assessment of microvascular endothelial function by laser Doppler flowmetry in patients with essential hypertension.* Atherosclerosis, 2004. **173**(1): p. 97-102.

151. Kvernebo, K., Slasgsvold, C.E., and Stranden, E., *Laser Doppler flowmetry in evaluation of skin post-ischaemic reactive hyperaemia. A study in healthy volunteers and atherosclerotic patients.* J Cardiovasc Surg (Torino), 1989. **30**(1): p. 70-75.

152. Young, J.D. and Cameron, E.M., *Dynamics of skin blood flow in human sepsis.* Intensive Care Med, 1995. **21**(8): p. 669-674.

153. Kvandal, P., Landsverk, S.A., Bernjak, A., Stefanovska, A., Kvernmo, H.D., and Kirkeboen, K.A., *Low-frequency oscillations of the laser Doppler perfusion signal in human skin.* Microvasc Res, 2006. **72**(3): p. 120-127.

154. Colantuoni, A., Bertuglia, S., and Intaglietta, M., *Microvascular vasomotion: origin of laser Doppler flux motion.* Int J Microcirc Clin Exp, 1994. **14**(3): p. 151-158.

155. Struijker-Boudier, H.A., Rosei, A.E., Bruneval, P., Camici, P.G., Christ, F., Henrion, D., Levy, B.I., Pries, A., and Vanoverschelde, J.L., *Evaluation of the microcirculation in hypertension and cardiovascular disease.* Eur Heart J, 2007. **28**(23): p. 2834-2840.

156. Groner, W., Winkelman, J.W., Harris, A.G., Ince, C., Bouma, G.J., Messmer, K., and Nadeau, R.G., *Orthogonal polarization spectral imaging: a new method for study of the microcirculation.* Nat Med, 1999. **5**(10): p. 1209-1212.

157. Spronk, P.E., Ince, C., Gardien, M.J., Mathura, K.R., Oudemans-van Straaten, H.M., and Zandstra, D.F., *Nitroglycerin in septic shock after intravascular volume resuscitation.* Lancet, 2002. **360**(9343): p. 1395-1396.

158. De Backer, D., Creteur, J., Dubois, M.J., Sakr, Y., and Vincent, J.L., *Microvascular alterations in patients with acute severe heart failure and cardiogenic shock.* Am Heart J, 2004. **147**(1): p. 91-99.

159. Knotzer, H. and Hasibeder, W.R., *Microcirculatory function monitoring at the bedside--a view from the intensive care.* Physiol Meas, 2007. **28**(9): p. R65-86.

160. Verdant, C. and De Backer, D., *How monitoring of the microcirculation may help us at the bedside.* Curr Opin Crit Care, 2005. **11**(3): p. 240-244.

161. Lupi, O., Semenovitch, I., Treu, C., and Bouskela, E., *Orthogonal polarization technique in the assessment of human skin microcirculation.* Int J Dermatol, 2008. **47**(5): p. 425-431.

162. Langer, S., Born, F., Hatz, R., Biberthaler, P., and Messmer, K., *Orthogonal polarization spectral imaging versus intravital fluorescent microscopy for microvascular studies in wounds.* Ann Plast Surg, 2002. **48**(6): p. 646-653.

163. Harris, A.G., Sinitsina, I., and Messmer, K., *The Cytoscan Model E-II, a new reflectance microscope for intravital microscopy: comparison with the standard fluorescence method.* J Vasc Res, 2000. **37**(6): p. 469-476.

164. Hayward, C.S., Kraidly, M., Webb, C.M., and Collins, P., *Assessment of endothelial function using peripheral waveform analysis: a clinical application.* J Am Coll Cardiol, 2002. **40**(3): p. 521-528.

165. Kuvin, J.T., Patel, A.R., Sliney, K.A., Pandian, N.G., Sheffy, J., Schnall, R.P., Karas, R.H., and Udelson, J.E., *Assessment of peripheral vascular endothelial function with finger arterial pulse wave amplitude.* Am Heart J, 2003. **146**(1): p. 168-174.

166. Lavie, P., Schnall, R.P., Sheffy, J., and Shlitner, A., *Peripheral vasoconstriction during REM sleep detected by a new plethysmographic method.* Nat Med, 2000. **6**(6): p. 606.

167. Bonetti, P.O., Pumper, G.M., Higano, S.T., Holmes, D.R., Jr., Kuvin, J.T., and Lerman, A., *Noninvasive identification of patients with early coronary atherosclerosis by assessment of digital reactive hyperemia.* J Am Coll Cardiol, 2004. **44**(11): p. 2137-2141.

168. Coffman, J.D., *Effects of endothelium-derived nitric oxide on skin and digital blood flow in humans.* Am J Physiol, 1994. **267**(6 Pt 2): p. H2087-2090.

169. Noon, J.P., Haynes, W.G., Webb, D.J., and Shore, A.C., *Local inhibition of nitric oxide generation in man reduces blood flow in finger pulp but not in hand dorsum skin.* J Physiol, 1996. **490 (Pt 2)**: p. 501-508.

170. Nohria, A., Gerhard-Herman, M., Creager, M.A., Hurley, S., Mitra, D., and Ganz, P., *Role of nitric oxide in the regulation of digital pulse volume amplitude in humans.* J Appl Physiol, 2006. **101**(2): p. 545-548.

171. Itamar Medical, Ltd., *Endothelial Function Assessment with Endo-PAT2000.* [Web Page] 2008 [cited May 1, 2008]; Available from: <http://www.itamar-medical.com/Product.asp?pid=3005>.

172. Bowman, H.F., Cravalho, E.G., and Woods, M., *Theory, measurement, and application of thermal properties of biomaterials.* Annu Rev Biophys Bioeng, 1975. **4**(00): p. 43-80.

173. Eberhart, R.C., Shitzer, A., and Hernandez, E.J., *Thermal dilution methods: estimation of tissue blood flow and metabolism.* Ann N Y Acad Sci, 1980. **335**: p. 107-132.

174. Bowman, H.F., *Estimation of tissue blood flow*, in *Heat Transfer in Medicine and Biology: Analysis and Application*, A. Shitzer and R.C. Eberhart, Editors. 1985, Plenum Press: New York, NY. p. 193-230.

175. Chato, J.C., *Measurement of thermal properties of biological materials*, in *Heat Transfer in Medicine and Biology*, A. Shitzer and R.C. Eberhart, Editors. 1985, Plenum Press: New York. p. 167-192.

176. Joly, H.R. and Weil, M.H., *Temperature of the great toe as an indication of the severity of shock.* Circulation, 1969. **39**(1): p. 131-138.

177. Murdoch, I.A., Qureshi, S.A., Mitchell, A., and Huggon, I.C., *Core-peripheral temperature gradient in children: does it reflect clinically important changes in circulatory haemodynamics?* Acta Paediatr, 1993. **82**(9): p. 773-776.

178. Muravchick, S., Conrad, D.P., and Vargas, A., *Peripheral temperature monitoring during cardiopulmonary bypass operation.* Ann Thorac Surg, 1980. **29**(1): p. 36-41.

179. Kurz, A., Sessler, D.I., Birnbauer, F., Illievich, U.M., and Spiss, C.K., *Thermoregulatory vasoconstriction impairs active core cooling.* Anesthesiology, 1995. **82**(4): p. 870-876.

180. Lima, A. and Bakker, J., *Noninvasive monitoring of peripheral perfusion.* Intensive Care Med, 2005. **31**(10): p. 1316-1326.

181. Akata, T., Kanna, T., Yoshino, J., Higashi, M., Fukui, K., and Takahashi, S., *Reliability of fingertip skin-surface temperature and its related thermal measures as indices of peripheral perfusion in the clinical setting of the operating theatre.* Anaesth Intensive Care, 2004. **32**(4): p. 519-529.

182. Rubinstein, E.H. and Sessler, D.I., *Skin-surface temperature gradients correlate with fingertip blood flow in humans.* Anesthesiology, 1990. **73**(3): p. 541-545.

183. House, J.R. and Tipton, M.J., *Using skin temperature gradients or skin heat flux measurements to determine thresholds of vasoconstriction and vasodilatation.* Eur J Appl Physiol, 2002. **88**(1-2): p. 141-145.

184. Gibbs, F.A., *A thermoelectric blood flow recorder in the form of a needle.* Proc. Soc. Exp. Biol. Med., 1933. **31**: p. 141-146.

185. Bender, F. and Hensel, H., *Fortlaufende Bestimmung der Hautdurchblutung am Menschen mit einem elektrischen Warmeleitmesser.*

[Continuous determination of blood flow in human skin by a heat conductivity measuring device.]. Pflugers Arch, 1956. **263**(5): p. 603-614.

186. Kuiper, J.B. and van de Staak, W.J.B.M., *Experiences with the combined use of three methods for measuring peripheral circulation.* Curr Probl Dermatol, 1970. **3**: p. 164-193.

187. Tamura, T., Togawa, T., and Yokoyama, K., *Comparison of laser Doppler fluxmetry and the thermal diffusion method of measuring skin blood flow with hydrogen clearance.* Int J Microcirc Clin Exp, 1992. **11**(1): p. 95-107.

188. Dittmar, A., Arnaud, F., Delhomme, G., Girard, P., Newman, W.H., and Martelet, C., *Non invasive characterization of skin using micro thermal diffusion sensor*, in *Engineering in Medicine and Biology Society, 1995., IEEE 17th Annual Conference.* 1995. p. 1569-1570.

189. Nitzan, M., Anteby, S.O., and Mahler, Y., *Transient heat clearance method for regional blood flow measurements.* Phys Med Biol, 1985. **30**(6): p. 557-563.

190. Challoner, A.V., *Accurate measurement of skin blood flow by a thermal conductance method.* Med Biol Eng, 1975. **13**(2): p. 196-201.

191. Holti, G. and Mitchell, K.W., *Estimation of the nutrient skin blood flow using a segmented thermal clearance probe.* Clin Exp Dermatol, 1978. **3**(2): p. 189-198.

192. Thalayasingam, S. and Delpy, D.T., *Thermal clearance blood flow sensor--sensitivity, linearity and flow depth discrimination.* Med Biol Eng Comput, 1989. **27**(4): p. 394-398.

193. Raamat, R., Kudimov, B., and Jagomagi, K., *Similarity of fingertip skin blood flow patterns recorded by the model-based thermal clearance and large area laser Doppler probes.* Med Eng Phys, 2001. **23**(9): p. 665-671.

194. Saumet, J.L., Dittmar, A., and Leftheriotis, G., *Non-invasive measurement of skin blood flow: comparison between plethysmography, laser-Doppler flowmeter and heat thermal clearance method.* Int J Microcirc Clin Exp, 1986. **5**(1): p. 73-83.

195. Wright, H.M., *Measurement of the cutaneous circulation.* J Appl Physiol, 1965. **20**(4): p. 696-702.

196. Dittmar, A., Marichy, J., Grippari, J.L., Delhomme, G., and Roussel, B., *Measurement by heat clearance of skin blood flow of healthy, burned, and grafted skin.* Prog Clin Biol Res, 1982. **107**: p. 413-419.

197. Roussel, B., Dittmar, A., Delhomme, C., Grippari, J.L., and Schmitt, M., *Normal and pathologic aspects of skin blood flow measured by a thermal clearance method.* Prog Clin Biol Res, 1982. **107**: p. 421-429.

198. Brown, B.H., Bygrave, C., Robinson, P., and Henderson, H.P., *A critique of the use of a thermal clearance probe for the measurement of skin blood flow.* Clinical Physics and Physiological Measurement, 1980(3): p. 237.

199. Corcoran, J.S., Owens, C.W., and Yudkin, J.S., *Measurement of fingertip blood flow using thermal clearance reflects anastomotic rather than nutrient blood flow.* Clin Sci (Lond), 1987. **72**(2): p. 225-232.

200. Jaszczak, P. and Sejrsen, P., *Determination of skin blood flow by 133Xe washout and by heat flux from a heated tc-PO2 electrode.* Acta Anaesthesiol Scand, 1984. **28**(5): p. 482-489.

201. Midttun, M., Sejrsen, P., and Colding-Jorgensen, M., *Heat-washout: a new method for measuring cutaneous blood flow rate in areas with and without arteriovenous anastomoses.* Clin Physiol, 1996. **16**(3): p. 259-274.

202. Kety, S.S., *Measurement of regional circulation by the local clearance of radioactive sodium.* Am Heart J, 1949. **38**(3): p. 321-328.

203. Patera, A.T., Eden, G., Mikic, B.B., and Bowman, H.F., *Prediction of tissue perfusion from measurement of the phase shift between heat flux and temperature.* Proc. Advances in Bioengineering, Winter Annu. Meeting ASME, 1979: p. 187-191.

204. Anderson, G.T. and Burnside, G. *A Focused Ultrasound Heating Technique To Measure Perfusion.* in *Engineering in Medicine and Biology Society, 1990., Proceedings of the Twelfth Annual International Conference of the IEEE.* 1990.

205. Liu, J., Zhou, Y.X., and Deng, Z.S., *Sinusoidal heating method to noninvasively measure tissue perfusion.* IEEE Trans Biomed Eng, 2002. **49**(8): p. 867-877.

206. Castellana, F.S., Skalak, R., Cho, J.M., and Case, R.B., *Steady-state analysis and evaluation of a new thermal sensor for surface measurements of tissue perfusion.* Ann Biomed Eng, 1983. **11**(2): p. 101-115.

207. Walsh, J.T. and Massachusetts Institute of Technology. Dept. of Electrical Engineering and Computer Science., *A noninvasive thermal method for the quantification of tissue perfusion.* 1984. p. 188 leaves.

208. Patel, P.A., Valvano, J.W., Pearce, J.A., Prahl, S.A., and Denham, C.R., *A self-heated thermistor technique to measure effective thermal properties from the tissue surface.* J Biomech Eng, 1987. **109**(4): p. 330-335.

209. Michener, M., Hager, J.M., Terrell, J.P., Veit, H., and Diller, T.E., *Noninvasive blood perfusion measurement with a heat flux microsensor.*, in *Advances in Biological Heat and Mass Transfer. HTD-Vol. 189/BED-Vol. 18* 1991: ASME, New York. p. 9-14.

210. Fouquet, Y., Hager, J., Terrell, J., and Diller, T., *Blood perfusion estimation from noninvasive heat flux measurements*, in *Advances in Bioheat and Mass Transfer - 1993: Microscale Analysis of Thermal Injury Processes, Instrumentation, Modeling, and Clinical Applications*, R.B. Roener, Editor. 1993, New York: ASME. p. 53-60.

211. O'Reilly, T., Gonzales, T., and Diller, T., *Development of a noninvasive blood perfusion probe*, in *Advances in Biological Heat and Mass Transfer. HTD-Vol. 337/BED-Vol. 34.*, L.J. Hayes and S. Clegg, Editors. 1996, ASME. p. 67-73.

212. Robinson, P.S., *Development of Methodologies for the Noninvasive Estimation of Blood Perfusion.* Master of Science in Mechanical Engineering Thesis. Virginia Polytechnic Institute and State University, Blacksburg, VA, 1998.

213. Scott, E.P., Robinson, P.S., and Diller, T.E., *Development of methodologies for the estimation of blood perfusion using a minimally invasive thermal probe.* Measurement Science and Technology, 1998. **9**: p. 888-897.

214. Cardinali, A.V., *Validation of a Noninvasive Blood Perfusion Measurement Sensor.* Master of Science in Mechanical Engineering Thesis. Virginia Polytechnic Institute and State University, Blacksburg, VA, 2002.

215. Mudalier, A.V., *Development of a Phantom Tissue for Blood Perfusion Measurements and Noninvasive Blood Perfusion Estimation in Living Tissue. PhD Dissertation.* Virginia Polytechnic Institute and State University, Blacksburg, VA, 2007.

216. Kharalkar, N., Valvano, J.W., Naghavi, M., and Chia Ling, W., *Novel temperature based technique for measurement of endothelial dysfunction*, in *Engineering in Medicine and Biology Society, 2003. Proceedings of the 25th Annual International Conference of the IEEE.* 2003. p. 308-311.

217. Kharalkar, N. and Valvano, J.W., *Analysis of a thermal method for assessing endothelial dysfunction.* Biomed Sci Instrum, 2004. **40**: p. 86-92.

218. Endothelix, Inc. *Publications.* [Web Page] 2008 [cited 2008 May 6]; Available from: <http://endothelix.com/publications.html>.

219. Carlier, S.G., Jamieson, M., Gul, K., Wang, Z., Jamieson, C., Naghavi, M., *Conference Poster P3006: Digital thermal monitoring : the clinical utility of a new non-invasive, non-imaging device for cardiovascular risk assessment*, in *European Society of Cardiology Congress.* 2006: Barcelona, Spain.

220. Ahmadi, N., Gul, K., Hajsadeghi, F., Jamieson, C., Gopal, A., Metcalfe, R.., Hartley, C., Kakadiaris, I., Naghavi, M., Budoff, M.J., *Poster: Digital Thermal Monitoring of Reactive Hyperemia Predicts Coronary Calcium and Framingham Risk Score*, in *2nd Annual Scientific Meeting of the Society of Cardiovascular Computed Tomography.* 2007: Washington, D.C.

221. Ahmadi, N., Hajsadeghi, F., Akhtar, M., Kleis, S., Jamieson, C., Hecht, H., Naghavi, M., Mehran, R., Budoff, M., *Poster TCT No. 388: Vascular Function Measured by Fingertip Thermal Reactivity is Impaired in Patients with Metabolic Syndrome and Diabetes* in *Transcatheter Cardiovascular Therapeutics 2007.* 2007: Washington, D.C.

222. Budoff, M., Ahmadi, N., Hartley, C., Khurram, N., Tanaka, H., Metcalfe, R., Hecht, H., Kleis, S., Gul, K., Akhtar, W., Jamieson, C., Mehran, R., Rumberger, J., Carlier, S., Berman, D., and Naghavi, M., *Digital (Fingertip) Thermal Monitoring of Vascular Reactivity and Endothelial Function Improves Cardiovascular Risk Assessment: A comprehensive report by the Endothelix Scientific Advisory Board.* 2008, Endothelix White Paper.

223. Kinlay, S. and Ganz, P., *Relation between endothelial dysfunction and the acute coronary syndrome: implications for therapy.* Am J Cardiol, 2000. **86**(8B): p. 10J-13J; discussion 13J-14J.

224. Rosamond, W., Flegal, K., Furie, K., Go, A., Greenlund, K., Haase, N., Hailpern, S.M., Ho, M., Howard, V., Kissela, B., Kittner, S., Lloyd-Jones, D., McDermott, M., Meigs, J., Moy, C., Nichol, G., O'Donnell, C., Roger, V., Sorlie, P., Steinberger, J., Thom, T., Wilson, M., and Hong, Y., *Heart disease and stroke statistics--2008 update: a report from the American Heart Association Statistics Committee and Stroke Statistics Subcommittee.* Circulation, 2008. **117**(4): p. e25-e146.

225. Wilson, P.W., Smith, S.C., Jr., Blumenthal, R.S., Burke, G.L., and Wong, N.D., *34th Bethesda Conference: Task force #4--How do we select patients for atherosclerosis imaging?* J Am Coll Cardiol, 2003. **41**(11): p. 1898-1906.

226. Spence, J.D., Eliasziw, M., DiCicco, M., Hackam, D.G., Galil, R., and Lohmann, T., *Carotid plaque area: a tool for targeting and evaluating vascular preventive therapy.* Stroke, 2002. **33**(12): p. 2916-2922.

227. Bowman, H.F., *Heat transfer mechanisms and thermal dosimetry.* Natl Cancer Inst Monogr, 1982. **61**: p. 437-445.

228. Poppendiek, H.F., Randall, R., Breeden, J.A., Chambers, J.E., and Murphy, J.R., *Thermal conductivity measurements and predictions for biological fluids and tissues.* Cryobiology, 1967. **3**(4): p. 318-327.

229. Pennes, H.H., *Analysis of tissue and arterial blood temperatures in the resting human forearm.* J Appl Physiol, 1948. **1**(2): p. 93-122.

230. Chen, M.M. and Holmes, K.R., *Microvascular contributions in tissue heat transfer.* Ann N Y Acad Sci, 1980. **335**: p. 137-150.

231. Chato, J.C., *Heat transfer to blood vessels.* J Biomech Eng, 1980. **102**(2): p. 110-118.

232. Charney, C.K., *Mathematical Models of Bioheat Transfer.* Advances in Heat Transfer, 1992. **22**: p. 110-118.

233. Grayson, J., *Internal calorimetry.* J Physiol, 1951. **115**(1): p. 29-30 P.

234. Grayson, J., *The measurement of intestinal blood flow in man.* J Physiol, 1951. **114**(4): p. 419-434.

235. Grayson, J., *Internal calorimetry in the determination of thermal conductivity and blood flow.* J Physiol, 1952. **118**(1): p. 54-72.

236. Grayson, J., Coulson, R.L., and Winchester, B., *Internal calorimetry--assessment of myocardial blood flow and heat production.* J Appl Physiol, 1971. **30**(2): p. 251-257.

237. Balasubramaniam, T.A. and Bowman, H.F., *Thermal Conductivity and thermal diffusivity of biomaterials: A simultaneous measurement technique.* Journal of Biomechanical Engineering, 1977. **99**: p. 148-154.

238. Chato, J.C., *A method for the measurement of thermal properties of biological materials*, in *ASME Symposium on Thermal Problems in Biotechnology*. 1968, ASME: New York. p. 16-25.

239. Valvano, J.W., Allen, J.T., and Bowman, H.F., *The simultaneous measurement of thermal conductivity, thermal diffusivity, and perfusion in small volumes of tissue.* J Biomech Eng, 1984. **106**(3): p. 192-197.

240. Bowman, H.F., Balasubramaniam, T.A., and Woods, M., *Determination of tissue perfusion from "in vivo" thermal conductivity measurements.* Heat Transfer in Biotechnology, ASME, 1977. **77-WA/HT-40**.

241. Martin, G.T. and Bowman, H.F., *Validation of real-time continuous perfusion measurement.* Med Biol Eng Comput, 2000. **38**(3): p. 319-325.

242. Klar, E., Kraus, T., Bleyl, J., Newman, W.H., Bowman, H.F., Hofmann, W.J., Kummer, R., Bredt, M., and Herfarth, C., *Thermodiffusion for continuous quantification of hepatic microcirculation--validation and potential in liver transplantation.* Microvasc Res, 1999. **58**(2): p. 156-166.

243. Valvano, J.W., Allen, J.T., Walsh, J.T., Hnatowich, D.J., Tomera, J.F., Brunengraber, H., and Bowman, H.F., *An isolated rat liver model for the evaluation of thermal techniques to quantify perfusion.* J Biomech Eng, 1984. **106**(3): p. 187-191.

244. Chen, M.M. and Holmes, K.R., *Thermal Pulse-Decay Method for Simultaneous Measurement of Thermal Conductivity and Local Blood Perfusion Rate of Living Tissues.* 1980 Advances in Bioengineering, ASME, 1980: p. 113-115.

245. Arkin, H., Holmes, K.R., Chen, M.M., and Bottje, W.G., *Thermal pulse decay method for simultaneous measurement of local thermal conductivity and blood perfusion: a theoretical analysis.* J Biomech Eng, 1986. **108**(3): p. 208-214.

246. Hemedex, Inc. *Product Info.* [Web Page] 2002 [cited 2008 May 1]; Available from: <http://www.hemedex.com>.

247. Charles, S.K. and Massachusetts Institute of Technology. Dept. of Mechanical Engineering., *Design and thermal modeling of a non-invasive probe for measuring perfusion by thermodiffusion.* 2004. p. 1-111.

248. Bircher, A., de Boer, E.M., Agner, T., Wahlberg, J.E., and Serup, J., *Guidelines for measurement of cutaneous blood flow by laser Doppler flowmetry. A report from the Standardization Group of the European Society of Contact Dermatitis.* Contact Dermatitis, 1994. **30**(2): p. 65-72.

249. Rossi, M., Carpi, A., Di Maria, C., Galetta, F., and Santoro, G., *Absent post-ischemic increase of blood flowmotion in the cutaneous microcirculation of healthy chronic cigarette smokers.* Clin Hemorheol Microcirc, 2007. **36**(2): p. 163-171.

250. Silva, C.L., Topgaard, D., Kocherbitov, V., Sousa, J.J., Pais, A.A., and Sparr, E., *Stratum corneum hydration: phase transformations and mobility in stratum corneum, extracted lipids and isolated corneocytes.* Biochim Biophys Acta, 2007. **1768**(11): p. 2647-2659.

251. Rawlings, A.V. and Harding, C.R., *Moisturization and skin barrier function.* Dermatol Ther, 2004. **17 Suppl 1**: p. 43-48.

252. Aschoff, J. and Kaempffer, F., *Warmedurchgang durch die Haut und seine Anderung bei Vasokonstriktion.* Pflugers Arch, 1947. **129**: p. 112-124.

253. Buettner, R., *The influence of blood circulation on the transport of heat in the skin.* Strahlentherapie, 1936. **55**: p. 333.

254. Yvonne-Tee, G.B., Rasool, A.H., Halim, A.S., and Rahman, A.R., *Reproducibility of different laser Doppler fluximetry parameters of postocclusive reactive hyperemia in human forearm skin.* J Pharmacol Toxicol Methods, 2005. **52**(2): p. 286-292.

255. Rossi, M., Carpi, A., Di Maria, C., Franzoni, F., Galetta, F., and Santoro, G., *Post-ischaemic peak flow and myogenic flowmotion component are independent variables for skin post-ischaemic reactive hyperaemia in healthy subjects.* Microvasc Res, 2007. **74**(1): p. 9-14.

256. Savage, C.R. and Massachusetts Institute of Technology. Dept. of Mechanical Engineering., *Design of a bead holder for thermal atherosclerosis sensor.* 2007, Massachusetts Institute of Technology: Cambridge, MA. p. 1-22.